Eruptive stars spectroscopy
Cataclysmics, Symbiotics, Novae

Eruptive Stars
Information Letter n° 50 #2022-01 12-05-2023
Observations of Jan. - Jun. 2022

Contents

Novae p. 2
Three novae during the semester:
Nova Vel 2022, Nova Mus 2022, Nova Cir 2022
Recurrent nova event of U Sco
Monitoring of Nova Cas 2021 and Nova Per 2020 in nebular phase

Symbiotics p. 28
Continuous monitoring
BX Mon: egress of eclipse

Notes

Transcients band Spectroscopy Analysis: p. 81
The intermediate luminosity optical transcients (ILOT) & stellar mergers
Steve Shore

An emission line from Earth's atmosphere p. 89
Paolo Berardi

PlotSpectra:a data visualization utility for amateur astronomical spectroscopy p. 90
Tim Lester

Editors:

F. Teyssier, D. Boyd, F. Sims, C. Boussin

Authors :

F. Teyssier, D. Boyd, F. Sims, C. Boussin, S. Shore, T. Lester, P. Berardi, J.P. Nougayrede, K. Shank, P. A. Dubovsky, J. Guarro, Y. Markus, S. Curry, I. Diabassoura, V. Bouttard, J. F. Coliac, C. Laulhère, C. Eldridge, P. Velez, R. Ehlert, F. Boubault, H. Barker, P. Luckas, T. Bohlsen, B. Buccheim, P. Somogyi, U. Sollecchia, M. Le Lain, V. Lecocq, G. Bertrand,J. Hinnefeld, J. Michelet, D. Cujedo, J.Coffin, T. Love, L.Franco, P.Cazzato, H.Allen, T.Love, T.Bohlsen, T.Medulka, 2SPOT(O.Garde;L.Mulato;P.LeDu;S.Charbonnel; T. Petit)

"We acknowledge with thanks the variable star observations from the AAVSO International Database contributed by observers worldwide and used in this letter."
Kafka, S., 2020, Observations from the AAVSO International Database, http://www.aavso.org

Many thanks to Matthieu Lelain and Vincent Lecoq for their fruiful support for Python coding

Eruptive stars spectroscopy
Cataclysmics, Symbiotics, Novae

Novae
Information Letter n° 50 #2022-01 14-05-2023
Observations of Jan. - Jun. 2022

Spectroscopic observations of novae in 2022-S1

Stars: Nova Cir 2022, FQ Cir, TCP J15244460-6059200 , V415 Mus, Nova Mus 2022, U Sco, Nova Vel 2022, AT 2022bpq, Nova Per 2020, V1112 Per, Nova Cas 2021, V1405 Cas, Nova Vul 2021, V606 Vul

Authors :

F. Teyssier, D. Boyd, F. Sims, C. Boussin, P. A. Dubovsky, J. Guarro, 2SPOT (O. Garde;L.Mulato;P. LeDu; S. Charbonnel;T. Petit), A. Leduc, P. Velez, K. Shank, H. Barker, U. Sollecchia, V. Lecocq, P. Cazzato, H. Allen, T. Love, T. Bohlsen, T. Medulka

Novae observed during 2022-S1

Name	RA	DE	GCVS	nb	first	last
CN Cha	10 59 57.62	-79 57 01.1	CN Cha	39	2020-12-08	2022-06-04
Nova Cas 2021	23 24 47.73	+61 11 14.8	V1405 Cas	507	2021-03-19	2022-09-22
Nova Per 2020	04 29 18.80	+43 54 23.2	V1112 Per	319	2020-07-26	2022-03-19
Nova Vul 2021	20 21 07.70	+29 14 09 3		73	2021-07-16	2022-08-29
Nova Vel 2022	09 29 53.06	-56 17 25.94		8	2022-05-01	2022-05-10
U Sco	16 22 30.78	-17 52 43.16	RN 2022	67	2022-06-06	2022-06-29
Nova Mus 2022	13 24 31.30	-72 10 30.3	V415 Mus	20	2022-06-10	2022-07-01
Nova Cir 2022	15 24 47.63	-60 59 47.3	FQ Cir	4	2022-06-26	2022-07-03

Abstract:

Three novae outbursts were observed during the semester:

Nova Vel 2022 : classical nova
Nova Mus 2022 : fast classical nova showing He I and NII/NII lines soon after the peak of luminosity
Nova Cir 2022 : very fast nova with He I and NII lines and very high velocity (around 5000 km.s^{-1} from Balmer lines profiles). The spectrum at maximum luminosity shows peculiar shapes of the emission lines. The nature of this object is doutfull.

The recurrent nova U Sco was detected in outburst on 2022 June, 7th.

A series of spectra shows the nova Per 2020 in nebular phase.

Nova Cas 2021 (slow nova with strong oscillations during a plateau at maximum luminosity) was observed during the semester with 55 spectra.

Continuous monitoring of the symbiotic nova CN Cha

Nova Cir 2022

RA (2000)	15 24 47.63
DE (2000)	-60 59 47.3
Mag max V	11.3
JD max	2459756

Andrew Pearce (AU) discovered Nova Cir 2022 on June 25.487 UT at C = 10.7.
Tom Love (NZ) identified the nova with an Alpy (R = 600) on June 26.946 UT
This transcient is peculiar: very high velocity

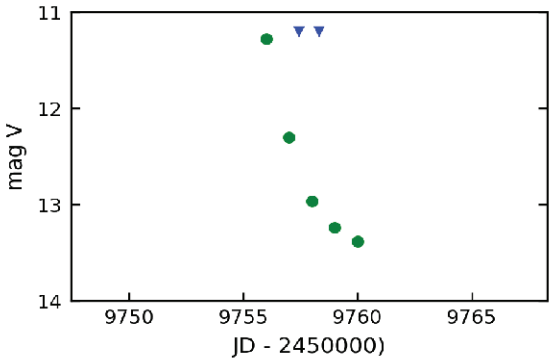

AAVSO V band lightcurve
ARAS Spectra: blue triangles

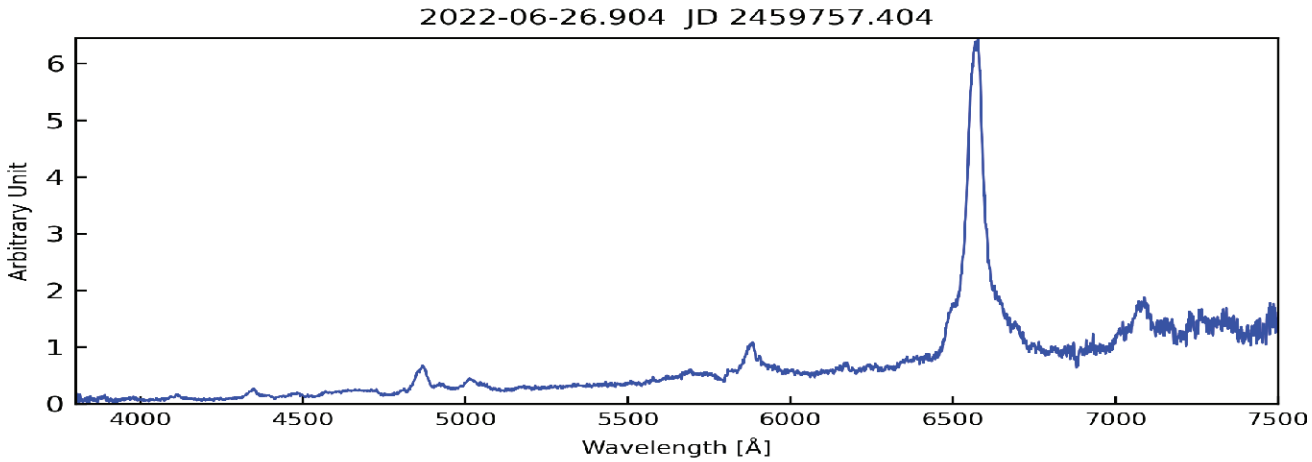

Observer: LTOC
Site: Saesteorra Instrument: RC12AF6-Alpy-ASI1600MM Resolution: 614

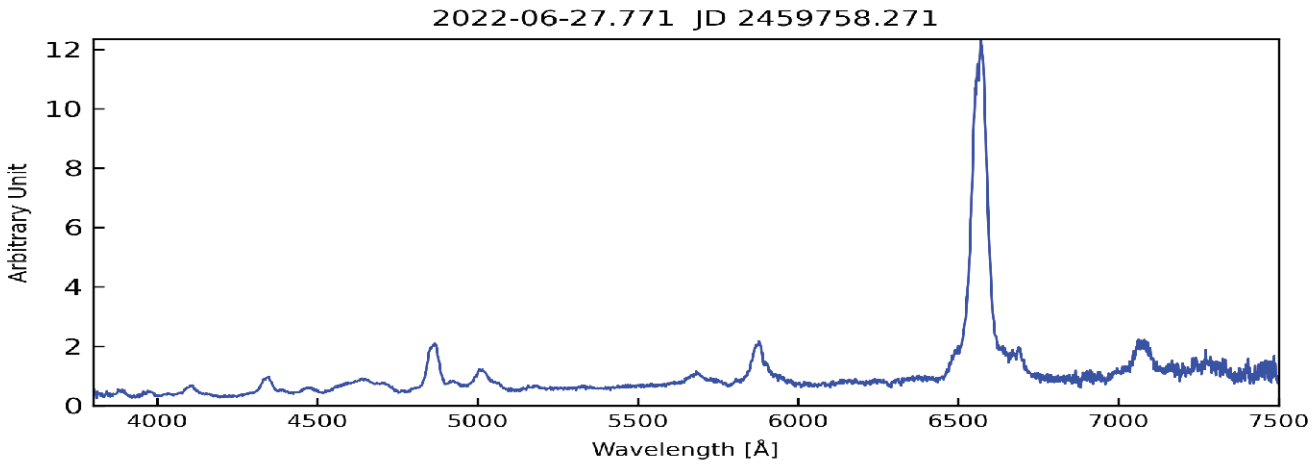

Observer: LTOC
Site: Saesteorra Instrument: RC12AF6-Alpy-ASI1600MM Resolution: 608

Nova Mus 2022

RA (2000)	13 24 31.30
DE (2000)	-72 10 30.3
Mag max V	9.2
JD max	2459742

Nova Mus 2022 (= ASASSN-22hw = AT 2022mmp)
was discovered by ASAS-SN (K. Stanek+)
on 2022 Jun 10.13 UT at 9.5 g (Sloan)
It was identified by ARAS Team as a nova
(Astronomer's Telegram #15435)

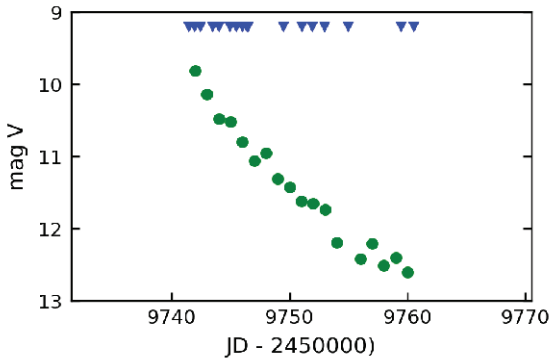

AAVSO V band lightcurve
ARAS Spectra: blue triangles

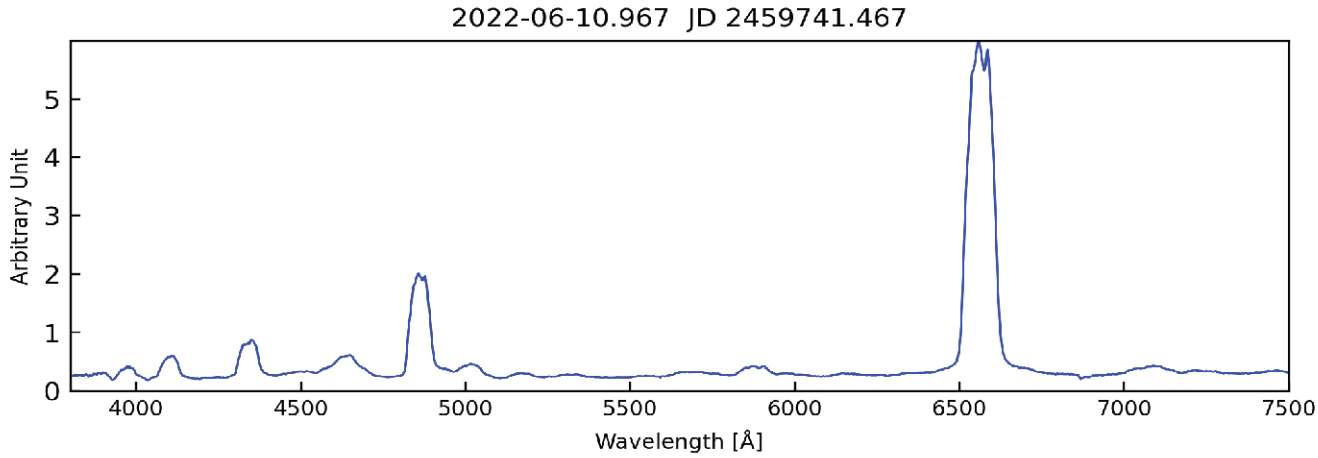

Observer: Olivier GARDE,L.Mulato,P.LeDu,Scharbonnel,TomPetit
Site: DSC Chile Instrument: RC12-Alpy-ATIK414Ex Resolution: 563

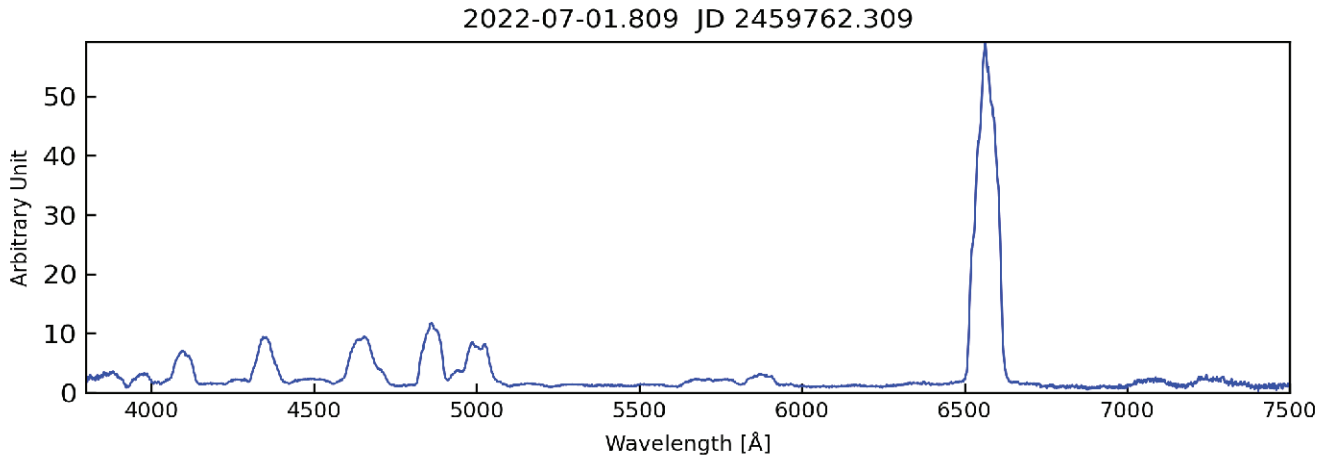

Observer: LTOC
Site: Saesteorra Instrument: RC12AF6-Alpy-ASI1600MM Resolution: 663

Nova Vel 2022

RA (2000)	16 22 30.8
DE (2000)	-17 52 43.2
Mag V max	7
JD V max	2459737

Nova Vel 2022 was discovered by Gaia (Gaiia22alz = AT2022bpq)
on 2022-02-042 UT at G = 16.87
The spectrum published by J. Brink+ (ATel#15270)
clearly identify the transcient as a classical nova event.

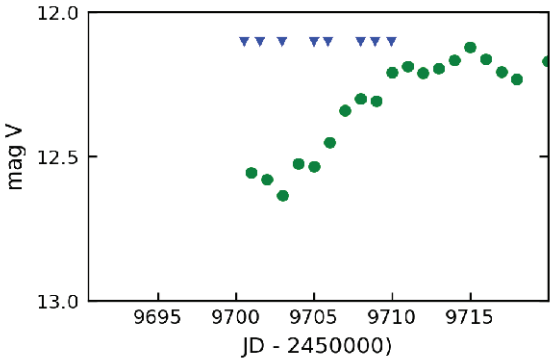

AAVSO V band lightcurve
ARAS Spectra: blue triangles

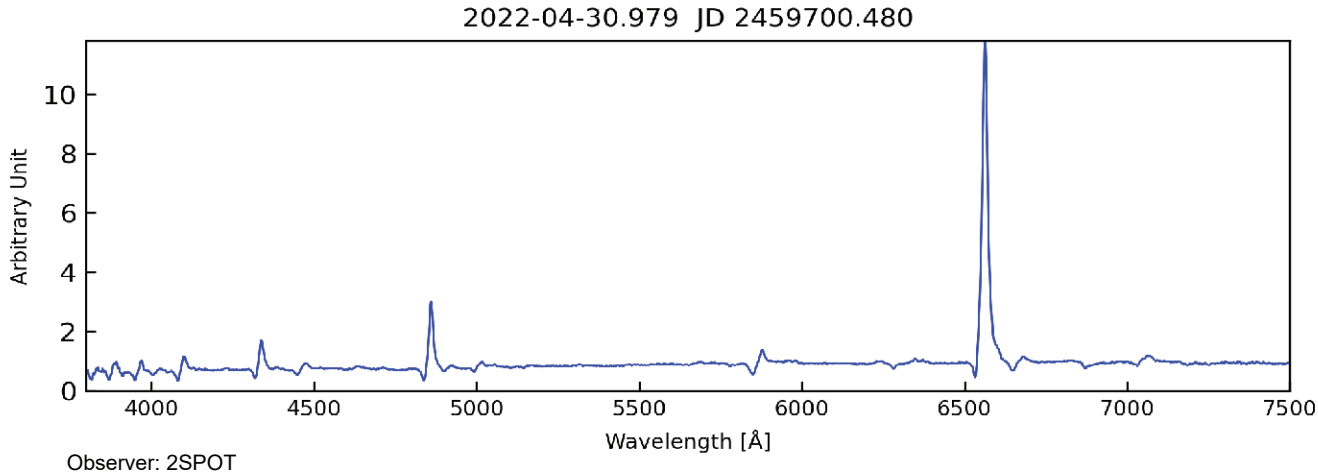

Observer: 2SPOT
Site: DSC Chile Instrument: RC12-Alpy-ATIK414Ex Resolution: 564

U Sco

RA (2000)	16 22 30.78
DE (2000)	-17 52 43.16
Mag max V	7.8
JD max	2459738

A new outburst of the recurrent nova U Sco
was detected by ASAS-SN (Stanek+) on 2022 Jun 10.13 UT
The fisrt spectra secured by ARAS team are discribed in ATel #15435

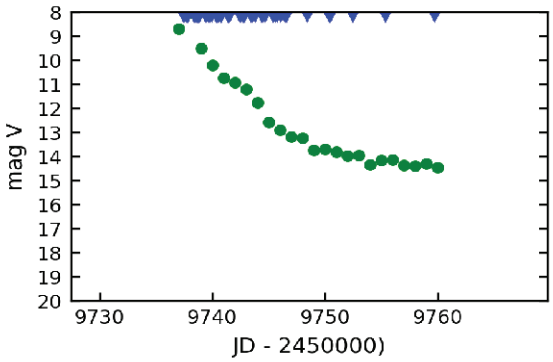

AAVSO V band lightcurve
ARAS Spectra: blue triangles

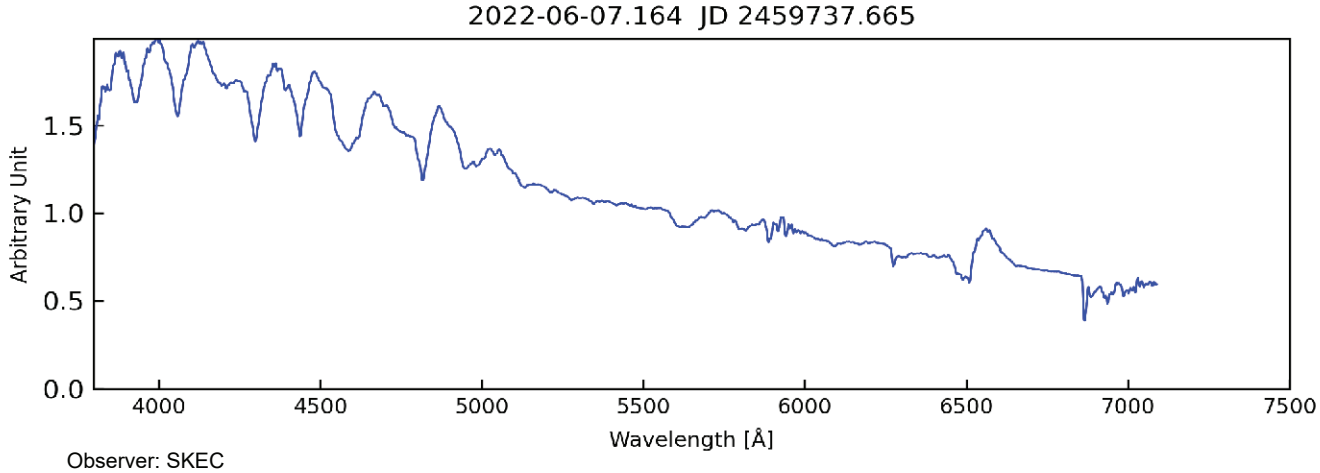

Observer: SKEC
Site: Carrollton TX Instrument: C14E@F7.6+LISA+ATIK414EX Resolution: nan

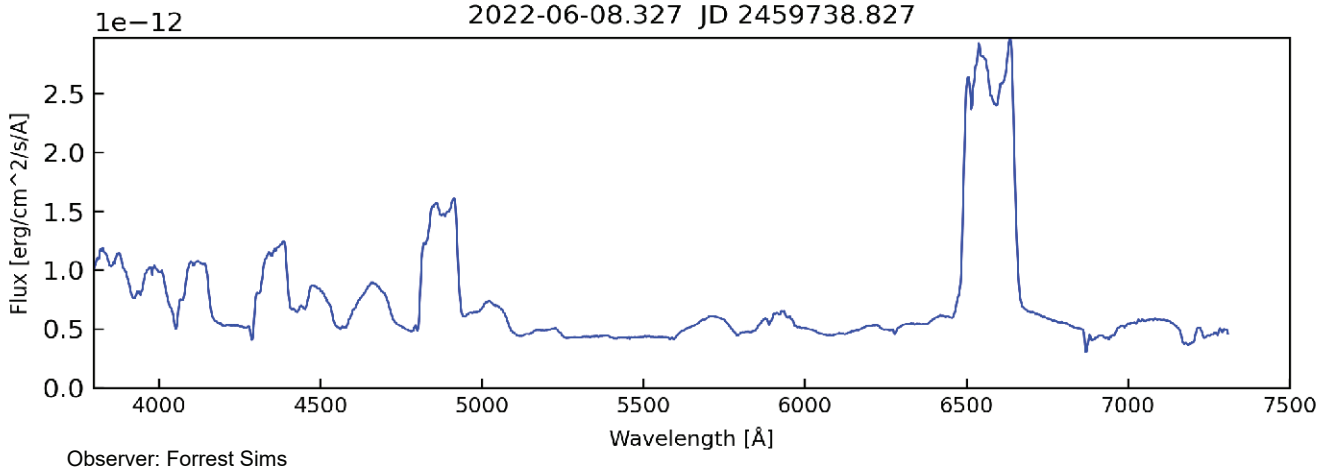

Observer: Forrest Sims
Site: Desert Celestial Observatory Instrument: CDK20 LISA Atik414ex Resolution: 1036

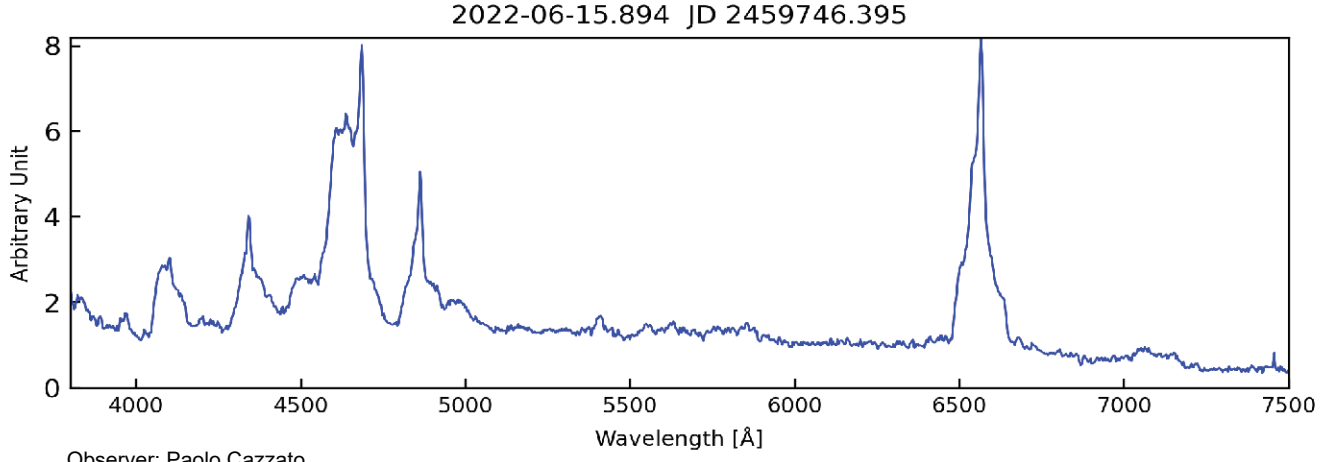

Observer: Paolo Cazzato
Site: LEC-IT Instrument: VX10_Alpy600_Atik414 Resolution: 535

Nova Per 2020

RA (2000)	04 29 18.80
DE (2000)	+43 54 23.2
Mag max V	8.2
JD max	2459187

Nova Per 2020 peaked at V = 8.2 on JD 2459187
It showed 1. oscillation at max. 2. dust event
Now in nebular phase

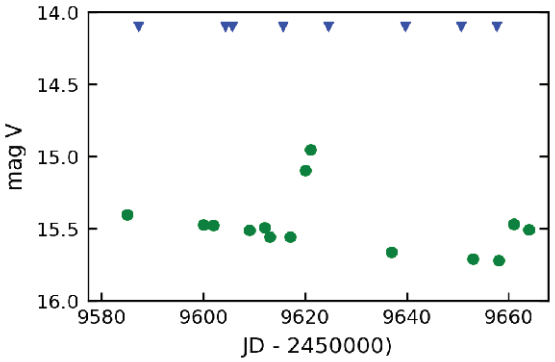

AAVSO V band lightcurve
ARAS Spectra: blue triangles

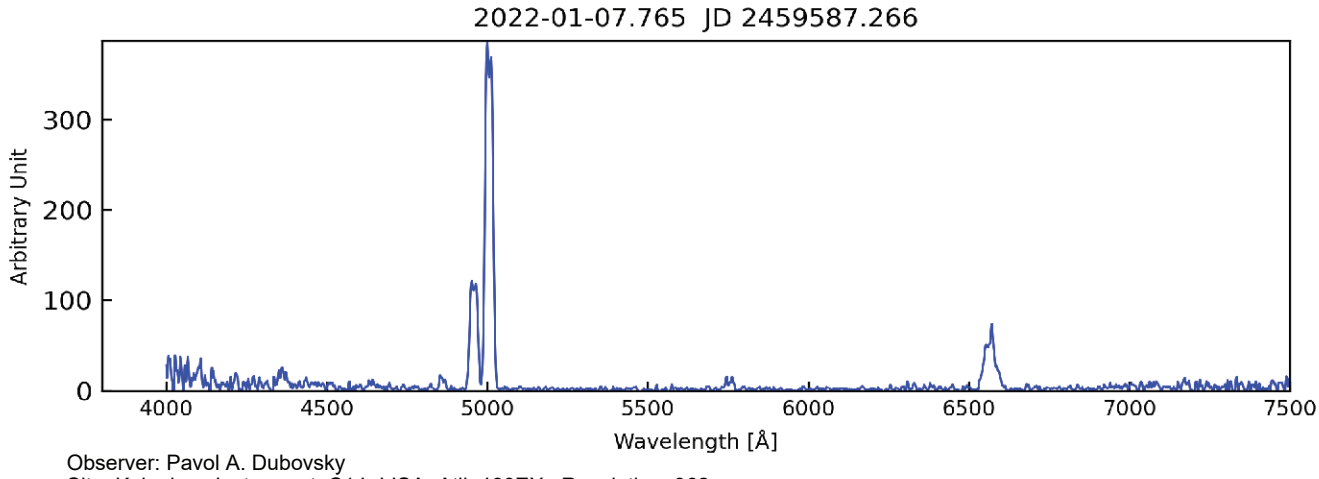

Observer: Pavol A. Dubovsky
Site: Kolonica Instrument: C14+LISA+Atik 460EX Resolution: 962

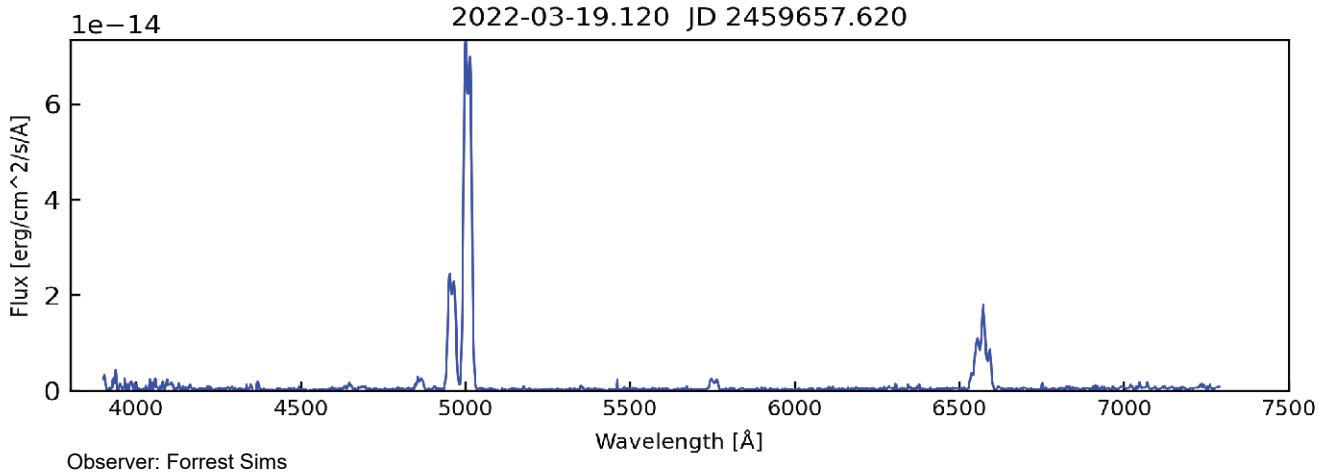

Observer: Forrest Sims
Site: Desert Celestial Observatory Instrument: CDK20 LISA Atik414ex Resolution: 957

Nova Cas 2021

RA (2000)	23 24 47.73
DE (2000)	+61 11 14.8
Mag max V	5.0
JD max	245945

Nova Cas 2021 peaked at V = 5.0 on JD 2459345
The light curve is atypical with : 1. long maximum with strong oscillations 2. jitters
Now in nebular phase
55 spectra were secured during 2022-S1

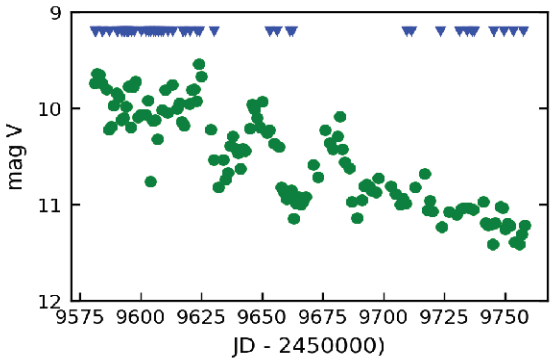

AAVSO V band lightcurve
ARAS Spectra: blue triangles

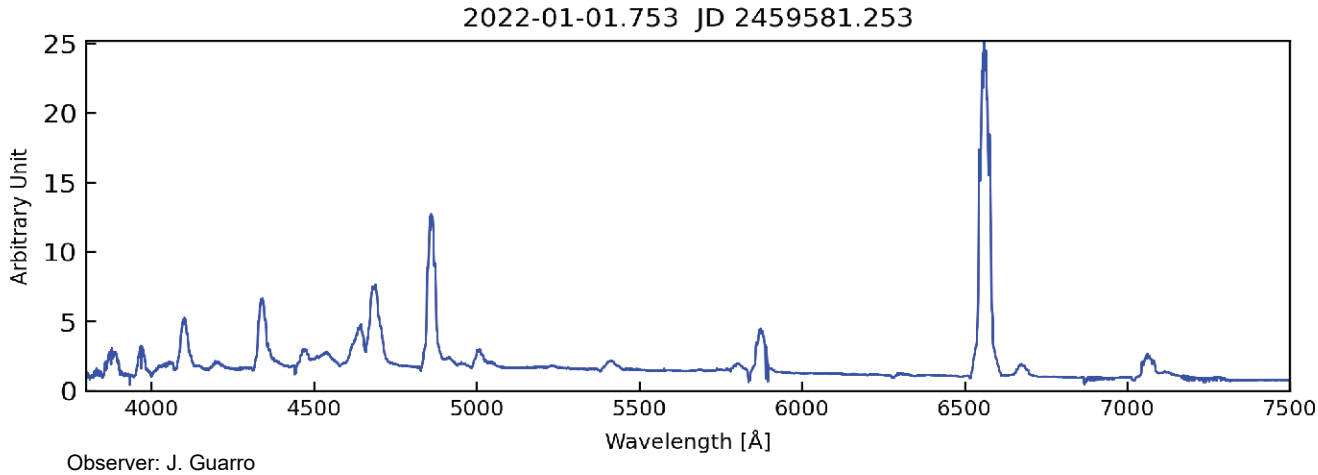

Observer: J. Guarro
Site: PIERA Instrument: PIERA Meade16 NOU_T ASI2600MM Resolution: 8500

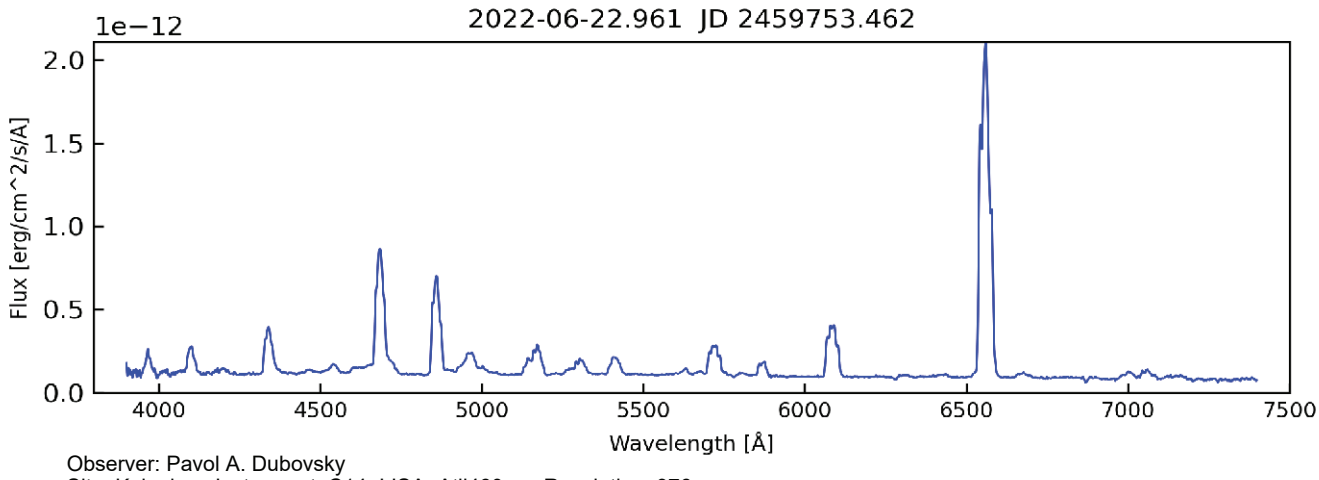

Observer: Pavol A. Dubovsky
Site: Kolonica Instrument: C14+LISA+Atil460ex Resolution: 976

Nova Vul 2021

RA (2000)	20 21 07.70
DE (2000)	+29 14 09 3
Mag max V	9.8
JD max	2459475

Nova Vul 2021 peaked at V = 5.0 on JD 2459345
The light curve is atypical with 2 maxima
Now in nebular phase at V ~ 15 after a dust event

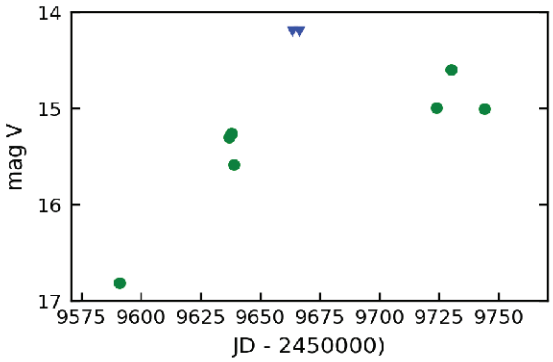

AAVSO V band lightcurve
ARAS Spectra: blue triangles

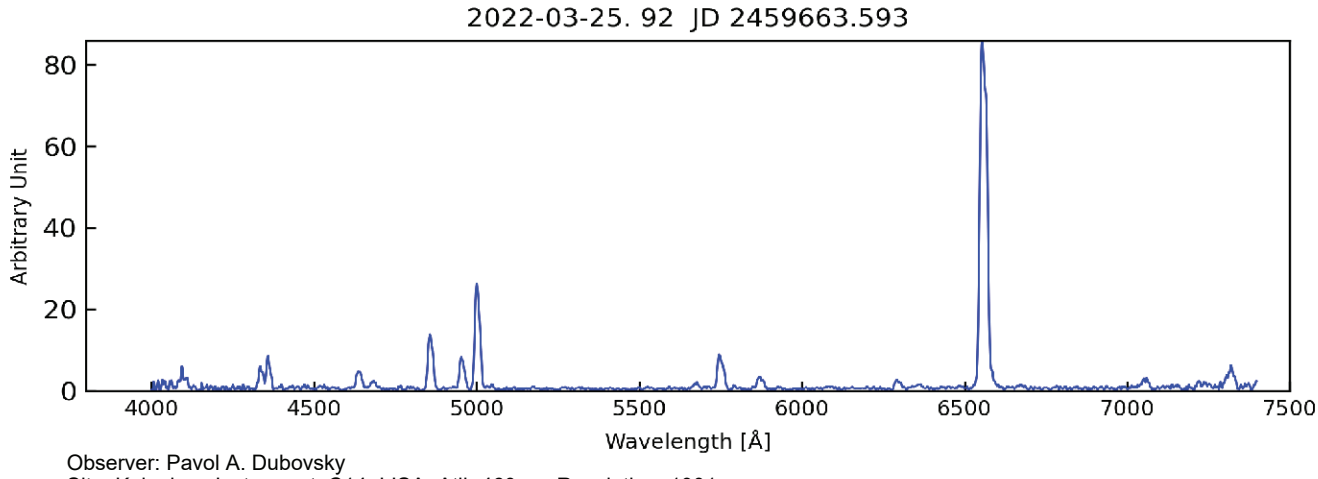

Observer: Pavol A. Dubovsky
Site: Kolonica Instrument: C14+LISA+Atik-460ex Resolution: 1001

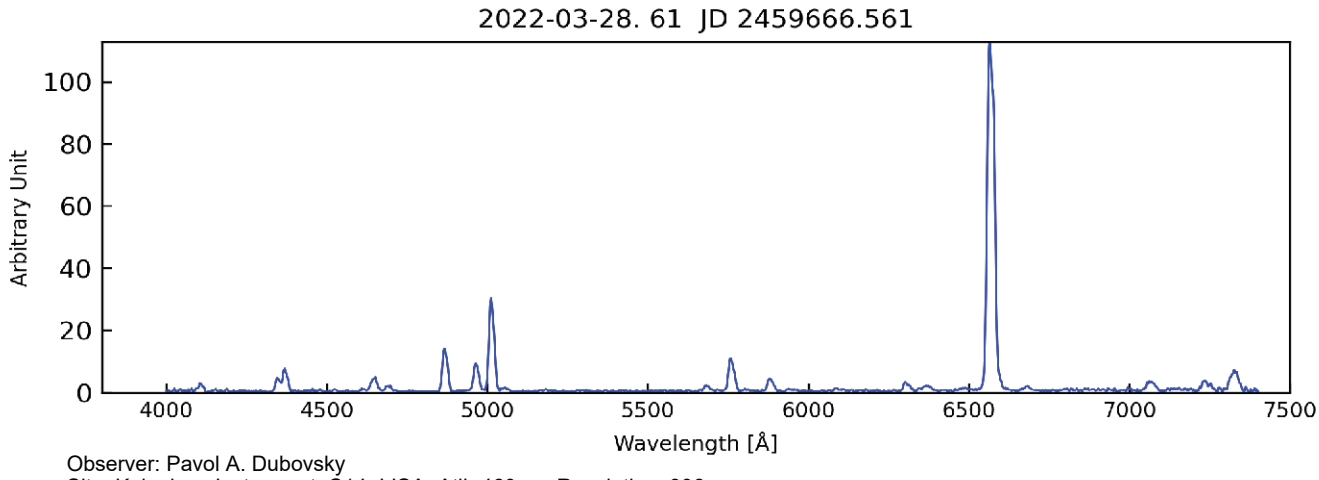

Observer: Pavol A. Dubovsky
Site: Kolonica Instrument: C14+LISA+Atik-460ex Resolution: 906

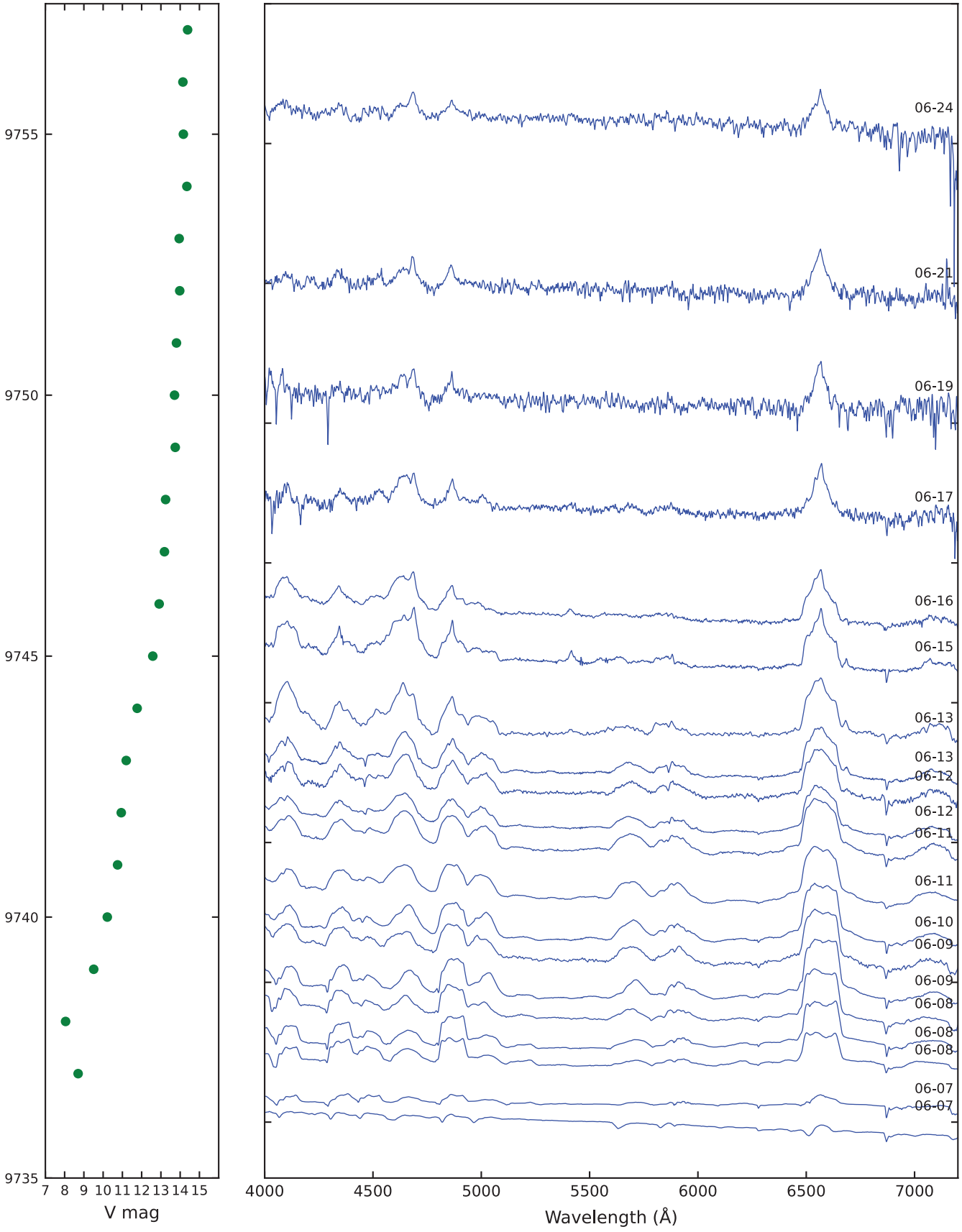
9755
9750
9745
9740
9735
7 8 9 10 11 12 13 14 15
V mag
4000 4500 5000 5500 6000 6500 7000
Wavelength (Å)
06-24
06-21
06-19
06-17
06-16
06-15
06-13
06-13
06-12
06-12
06-11
06-11
06-10
06-09
06-09
06-08
06-08
06-08
06-07
06-07

by Christophe Boussin

An overview of the outburst of U Sco in June 2022

Nova U Scorpii (U Sco) was found by Pogson on May 20, 1863 at magnitude 9,1 (Thomas 1940). This is one of about 10 known recurrent novae in our galaxy !
Recurrent novae (RNe) are cataclysmic binary systems that have several recorded nova outbursts on recurrence of Human observations timescale. U Sco has undergone seven recorded outbursts in 1863, 1906, 1936, 1979, 1987, 1999 and 2010. With the detection of three additional eruptions in 1917, 1945 and 1969 in a search of archival data (Schaefer 2010, and references therein), it appears that U Sco has had outbursts at intervals of 10 ± 2 years. The outburst in 2010 made U Sco the first star whose predicted eruption was detected (Anupama 2013). The eleven and last outburst of U Sco has been detected in June 6, 2022 (see hereafter).

During an outburst of U Sco, the increase of luminosity is very fast : in only a 6 - 12 hours, its magnitude goes from 18, in quiescent phase, to about 8 at peak luminosity (Anupama 2013). The decline is also very fast with a decrease of 3 magnitudes in 2.6 days (t_3 = 2.6) (Schaefer 2022). The classification light curve for U Sco is P which means that the light curve has relatively flat intervals superposed on the otherwise smooth declines (Strope 2010).

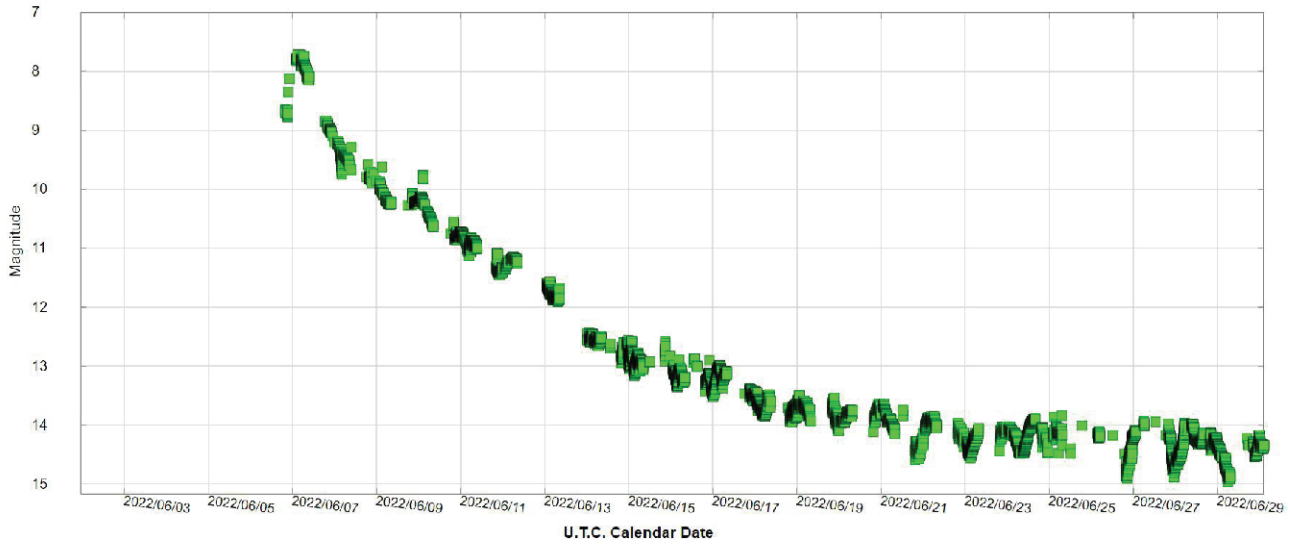

Light curve of U Sco in June 2022 (AAVSO)

(Johnson V : green squares)

Previous outbursts well-studied in 2010, 1999 and 1987 appear to be broadly similar in terms of the spectrum and its evolution. The early epoch spectra (up to roughly 10 days after outburst maximum) were dominated by broad lines due to hydrogen Balmer, He I, NI, NII, NIII and OI (Anupama 2013, Iijima 2002). Fe II (multiplet 42 at 4924, 5018 and 5169 A) and Mg II lines (4481 A blended, 7880 A) have also been identified during previous outbursts (see for example Iijima 2002).

Comparison of the intensities and profiles of the different lines in emission shows similarities from one outburst to another. For example, the profile of the Halpha line is thus composed of three main components (the reddest component being the strongest) while the Hbeta line is double peaked. Multiple absorption systems were also detected in the Balmer lines (Kafka 2011). Rapid variations are visible in the spectrum as the nova weakens. The Fe II lines are less and less visible, unlike the NII lines (Anupama 2013).

Evolution of the optical spectra at low resolution from 7 to 29 June 2022 (0 - 22 days after outburst maximum)

At the outburst maximum

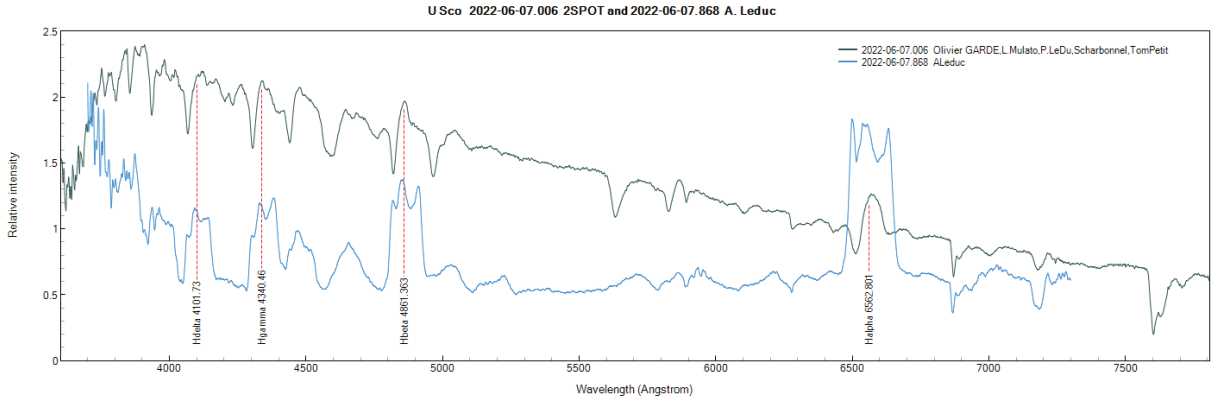

0 - 3 days after outburst maximum

The first spectrum obtained by the 2SPOT team on 7.006 June shows numerous absorption lines of which the P Cygni profile can be distinguished on some of them. The spectrum pattern remains similar until 7.321 June (Forrest Sims).

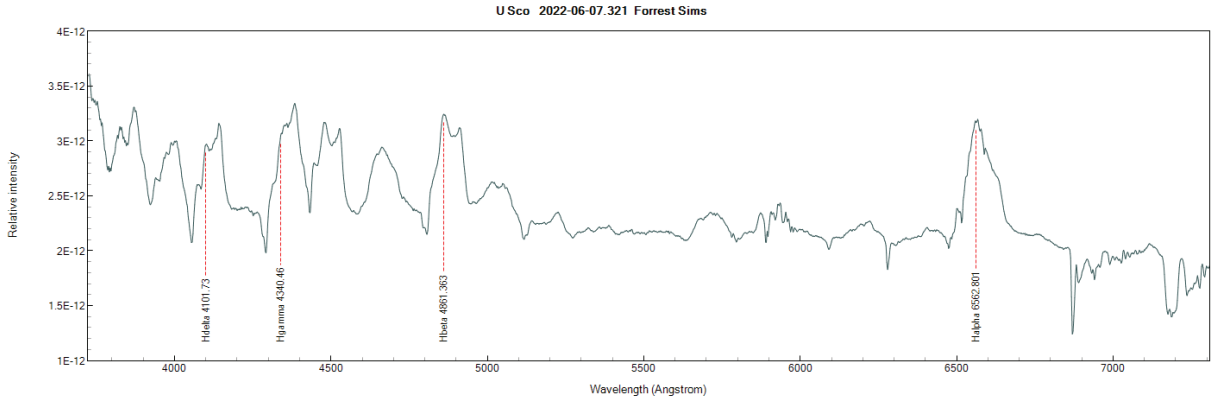

From 7.868 June, the spectrum of Arthur Leduc shows a triple peak structure around the Halpha, Hbeta, Hgamma and Hdelta lines. These structures are well visible in the ARAS database spectra (Pavol A. Dubovsky, Vincent Lecocq, 2SPOT team, Keith Shank, Forrest Sims, Arthur Leduc) up to 9.426 June (Hamish Barker). From this date, the multi-peak structure evolves much more clearly.

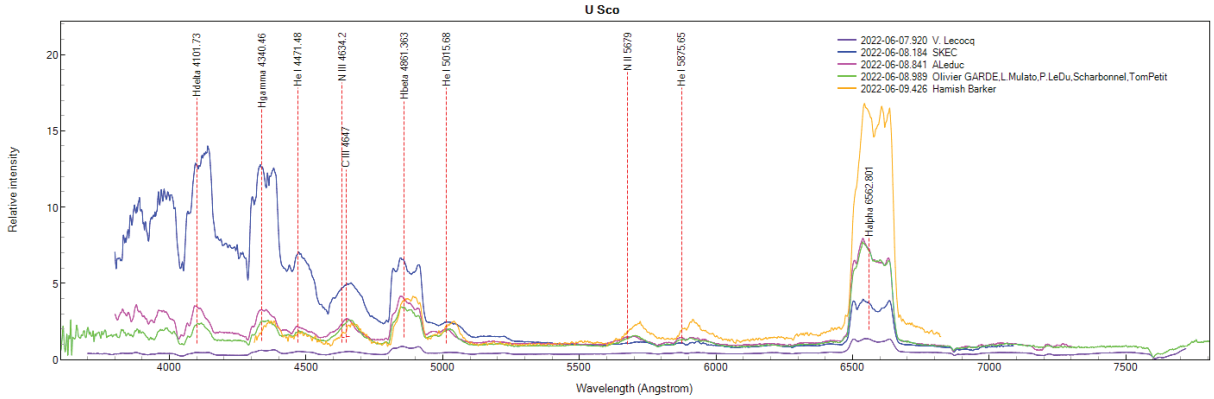

Mg II line (4481 A) is probably blended with He I line (4471 A) as well as NII and Fe II lines with He I (5015 A) (Anupama 2013).

During the previous outburst in 2010, Anupama et al. (Anupama 2013) recorded several spectra of U Sco. The following figure shows the evolution during the first 4 days after the maximum outburst. There are strong similarities between the spectra of the 2010 and 2022 outbursts, in particular the similar complex structures in the Balmer lines.

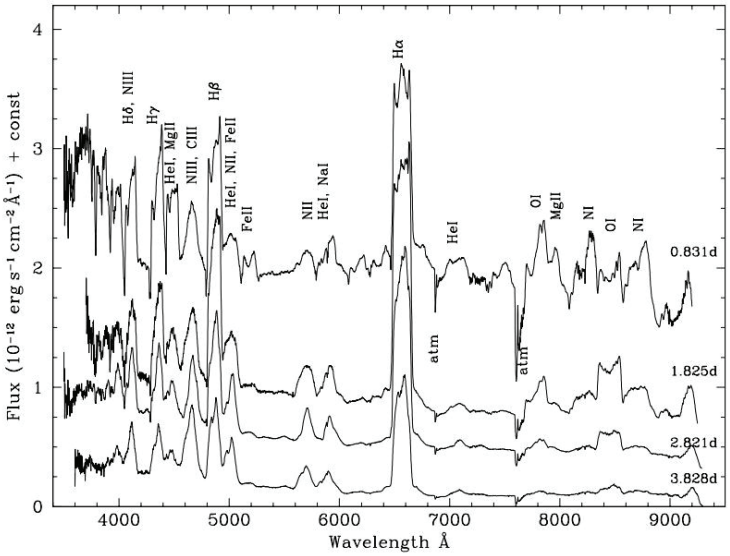

Fig. 2. Optical spectra of U Sco during days 0.83–3.83 after outburst maximum. The emission line identifications and day since the estimated maximum are marked. Note the changes in the line profile. For clarity, the zero level of the spectra of days 0.831, 1.825 and 2.821 are offset, respectively, by a constant value of 0.8, 0.5 and 0.3 in flux units.

4 - 7 days after outburst maximum

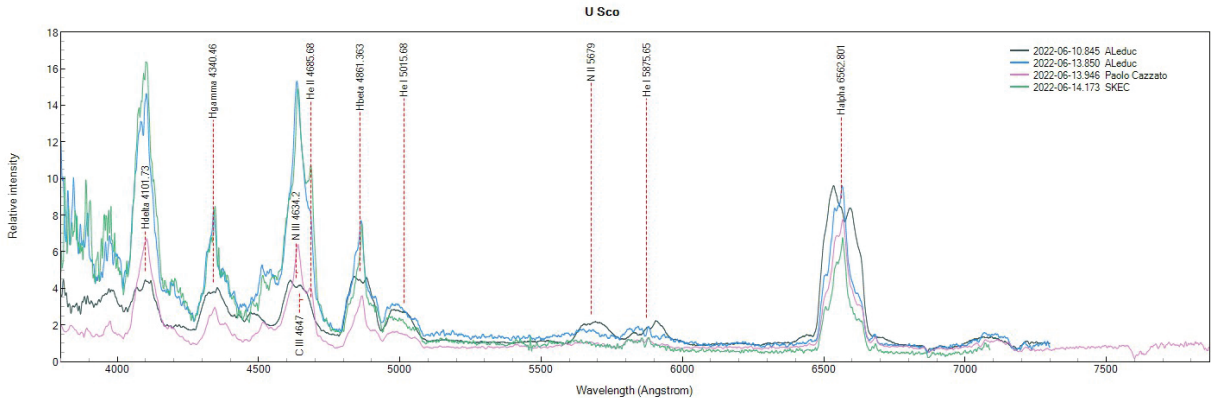

About 4 days after the maximum outburst, the boxy profile of the Balmer lines starts to evolve into a peak profile.

During the previous outburst in 2010, the Balmer lines also evolved into a shape closer and closer to a simple peak.

The spectral region of the NIII (4634 - 4642 A) and CIII (4647 - 4665 A) lines develops progressively from the beginning and then a more complex structure appears from 10.845 June (Arthur Leduc). From 13.850 June (Arthur Leduc), this spectral region looks more like a peak.

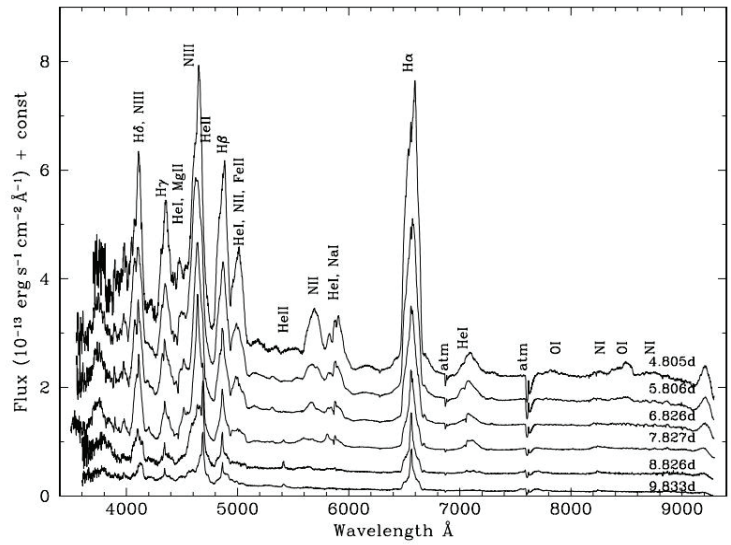

Fig. 3. Optical spectra of U Sco during days 4.81–9.83 after outburst maximum. The time since estimated maximum and emission line identifications are marked. Note the changes in the line profile, and the decrease in the strength of the oxygen and nitrogen lines by day ~7. For clarity, the zero level of the spectra of days 4.805, 5.806, 6.826, 7.827 and 8.826 are offset, respectively, by a constant value of 1.6, 1.3, 1.0, 0.7 and 0.3 in flux units.

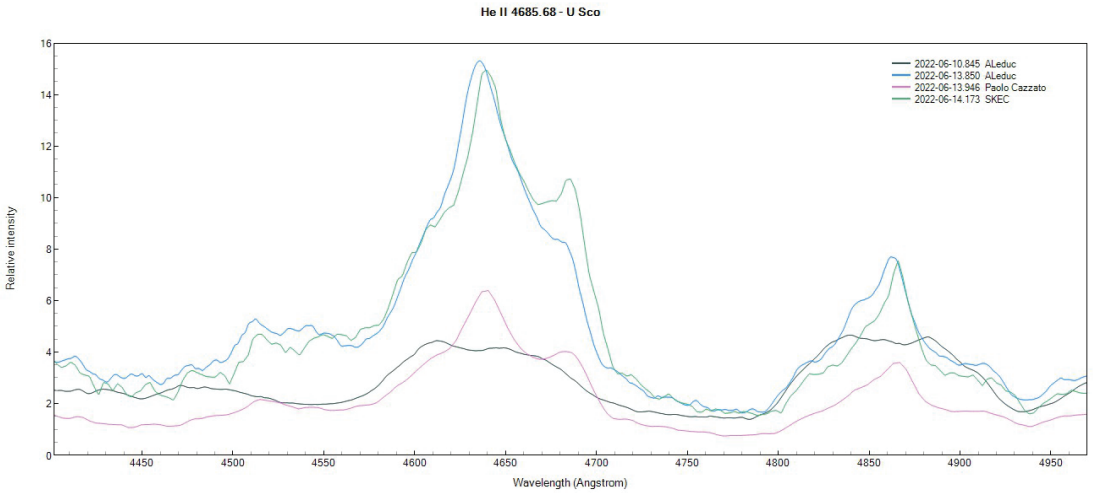

The HeII line at 4686 A starts to emerge from the NIII-CIII spectral region clearly between 13.946 (Paolo Cazzato) and 14.173 June (Keith Shank) i.e. about 7 days after the outburst maximum. This line becomes dominant in this spectral region from 14.839 June and remains well visible until 29.200 June (Forrest Sims).

The evolution of the HeII line at 4686 A is very similar to that noted during the 2010 outburst (Anupama 2013). The emergence of this line is noted 6.826 days after the outburst, i.e. about the same time as for this outburst.

Around the Balmer lines, a single-peak form clearly emerges from 14.173 June (Keith Shank) and remains until 29.200 June (Forrest Sims). The evolution of the Halpha line at low resolution is detailed in the next paragraph.

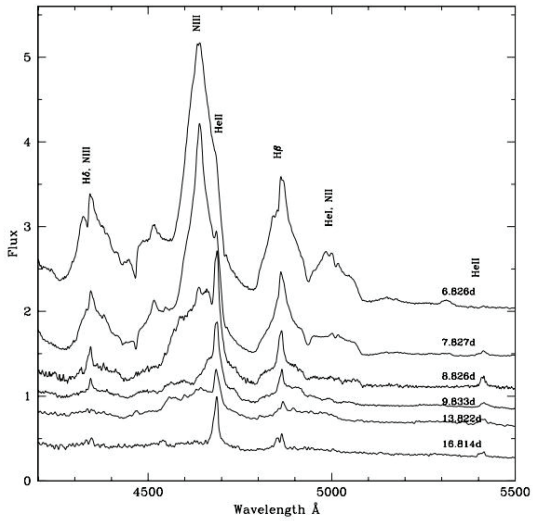

Fig. 4. Spectrum of U Sco during days 6.8–16.8 after outburst maximum, showing the emergence and increase in the strength of the He II lines. Note also the relative increase in the strength of the N III 4660 feature on days 8.83 and 13.82.

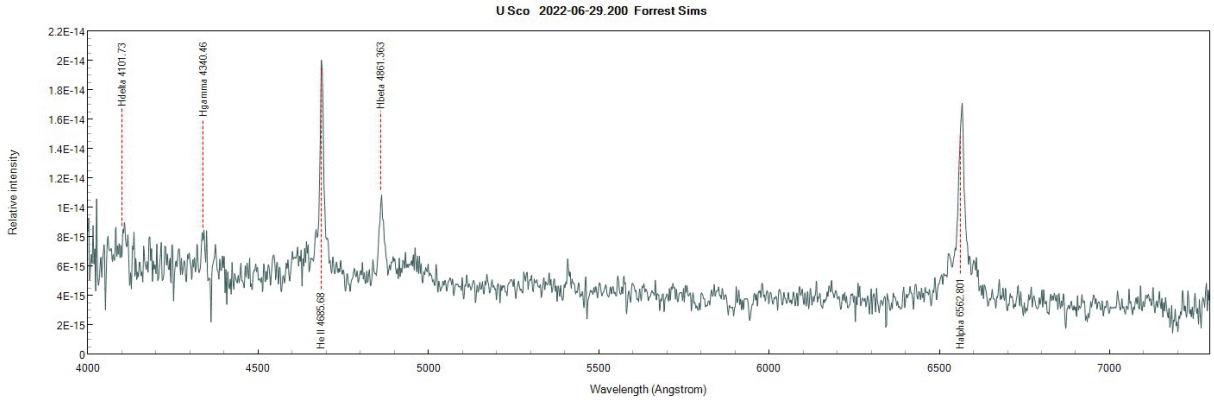

Evolution of the Halpha line at low resolution from 7.165 to 29.200 June 2022

The three-peak structure appears on 7.901 June in the spectrum of Pavol A. Dubovsky spectrum (consistent with Umberto Sollecchia's high-resolution observation on 7.836 June) but is not visible in the previous spectrum obtained by Forrest Sims on 7.321 June.

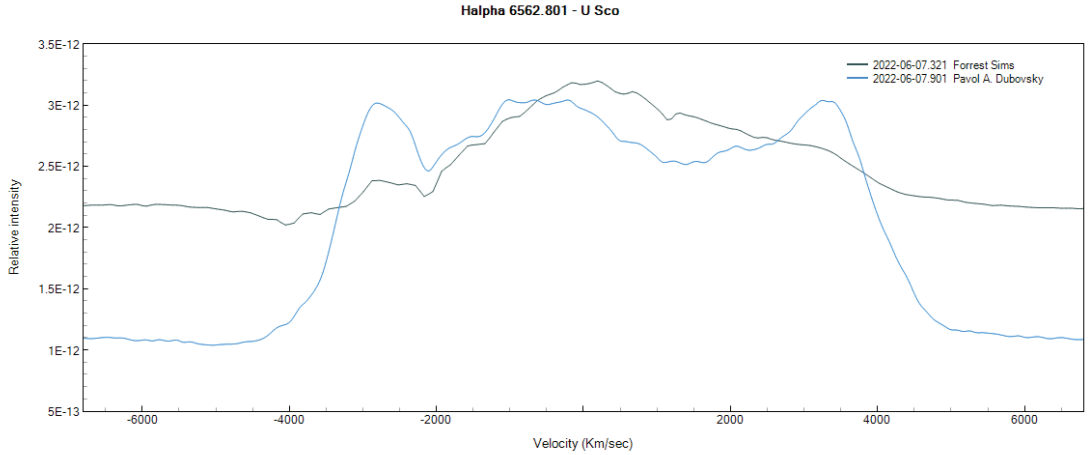

Visible until 9.426 June in the Hamish Barker spectrum, this structure changes significantly from 10.236 June (Forrest Sims) and the reddest component gradually decreases from 11.887 June (Pavol A. Dubovsky).

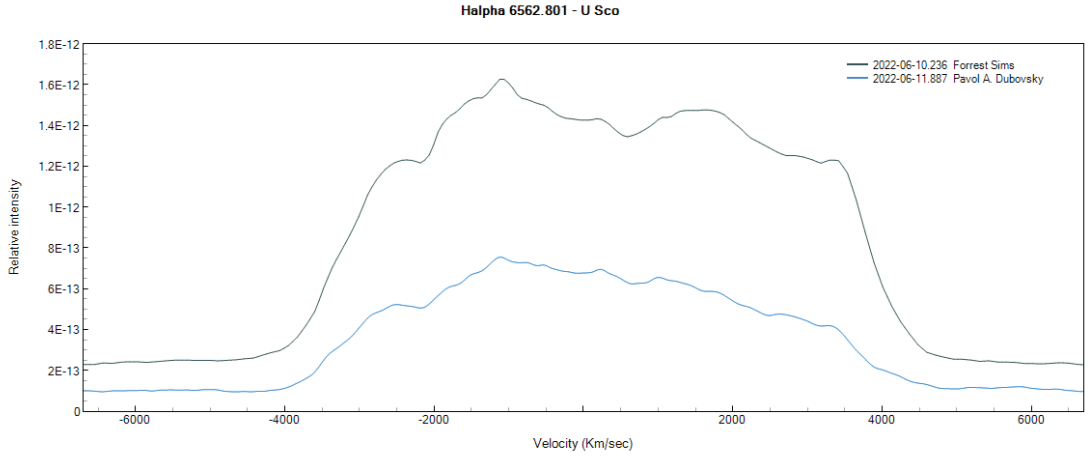

From 14.173 June (Keith Shank) the structure of the Halpha line remains complex but a central peak now clearly dominates in the reddest part and remains well visible on the spectra of 14.889 (Pavol A. Dubovsky) and 15.216 (Forrest Sims) then progressively decreases until 29.200 June (Forrest Sims).

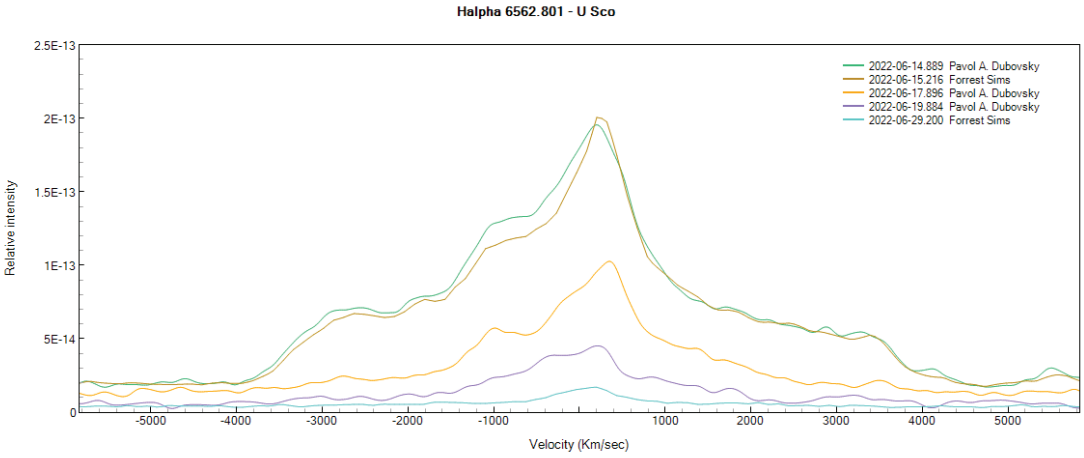

Evolution of the Halpha line at high resolution from 6.866 to 10.892 June 2022

The first high resolution spectra (R = 15000) obtained by Umberto Sollecchia on 6.866 and 7.836 June show a very fast evolution of the profile in less than 24 hours.

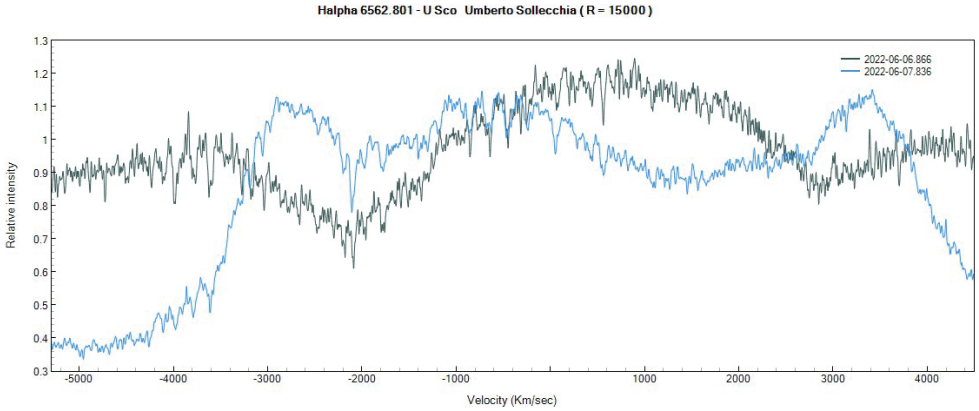

The echelle spectra obtained by Joan Guarro Flo (R = 9000) show a complex multi-peak structure that evolves clearly between 9.09 and 10.854 June.

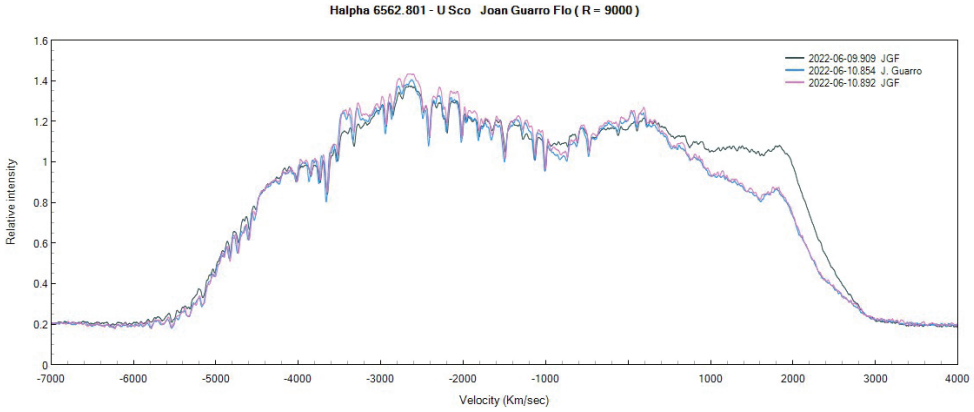

This evolution is also visible on the low resolution spectra (R = 1000) with a better temporal resolution (see above).

Christophe Boussin

ARAS observers involved in the monitoring of the U Sco outburst

2 SPOT Team (2SPOT), Arthur Leduc (ALE), Terry Bohlsen (BHQ), Forrest Sims (FAS), Hamish Barker (HBA), Joan Guarro Flo (JGF), Keith Shank (KSH, SKEC), Pavol A. Dubovsky (PAD), Paolo Cazzato (PCA), Umberto Sollecchia (SOL), Vincent Lecoq (VLE).

References

Anupama G.C. et al. 2013, A&A, 559, A121
Iijima, T. 2002, A&A, 387, 1013
Kafka S. et al. 2011, A&A 526, A83
Schaefer B.E. et al. 2010, AJ, 140, 925
Schaefer B.E. 2022, MNRAS, 516, 4497
Siviero et al. 2022, ATEL 15417
Strope R.J. et al. 2010 AJ, 140, 34
Thomas H.L. 1940, Harvard College Observatory, Bulletin No. 912, 10

Monitoring of the U Sco outburst in 2022 by ARAS observers

The last outburst of U Sco was announced on 2022 June 6.720 UT by Masayuki Moriyama via VSNET alert N°26798 reporting the nova at a magnitude of 11.4 unfiltered about 10 hours before the maximum luminosity (see Siviero A. 2022). The first spectra secured in the Aras database were obtained by Umberto Sollecchia (6447-6661 A, R = 14552) on 2022 June 6.866 and by the 2SPOT team (3603-7809 A, R = 570) on 2022 June 7.006 respectively 5 and 3 hours before the maximum of luminosity ! Between June 6 and 29, 2022, 67 spectra were recorded in the ARAS database.

Some features of U Sco outburst monitoring by Aras observers :

- Resolution of the recorded spectra is between 500 and 15000.
- Time interval between 2 spectra in the first 10 days of observation is less than 24h !
- Average time interval between 2 spectra is about 8 hours during the monitoring.

Date	Time (UT)	JD+24.....	Days from max luminosity	Interval (days)	Interval (hours)	Observer	Site	R	λ_{min}	λ_{max}
2022-06-06	22:26:00	59737.435	-0.209	0.000	0.000	SOL	AQL-IT	14552	6447	6661
2022-06-07	00:17:00	59737.512	-0.132	0.077	1.848	2SPOT	DSC-CL	570	3603	7809
2022-06-07	04:12:00	59737.675	0.031	0.163	3.912	KSH	CAR-US	1000	3800	7089
2022-06-07	06:10:00	59737.757	0.113	0.082	1.968	FAS	DCO-US	1024	3723	7311
2022-06-07	07:00:00	59737.792	0.148	0.035	0.840	FAS	DCO-US	1036	3723	7311
2022-06-07	08:08:00	59737.839	0.195	0.047	1.128	FAS	DCO-US	1035	3723	7311
2022-06-07	20:58:00	59738.374	0.730	0.535	12.840	ALE	NSH-FR	608	3700	7300
2022-06-07	21:50:00	59738.410	0.766	0.036	0.864	PAD	KOL-SK	1107	3850	7400
2022-06-07	21:57:00	59738.415	0.771	0.005	0.120	SOL	AQL-IT	14694	6445	6662
2022-06-07	22:23:00	59738.433	0.789	0.018	0.432	VLE	ORL-FR	508	3700	7720
2022-06-08	00:23:00	59738.516	0.872	0.083	1.992	2SPOT	DSC-CL	566	3603	7809
2022-06-08	03:07:00	59738.630	0.986	0.114	2.736	2SPOT	DSC-CL	571	3602	7809
2022-06-08	03:43:00	59738.655	1.011	0.025	0.600	KSH	CAR-US	1000	3800	7089
2022-06-08	04:35:00	59738.691	1.047	0.036	0.864	KSH	CAR-US	1000	3800	7089
2022-06-08	04:43:00	59738.697	1.053	0.006	0.144	2SPOT	DSC-CL	548	3602	7809
2022-06-08	05:28:00	59738.728	1.084	0.031	0.744	FAS	DCO-US	1020	3724	7312
2022-06-08	06:08:00	59738.756	1.112	0.028	0.672	FAS	DCO-US	1039	3724	7311
2022-06-08	06:50:00	59738.785	1.141	0.029	0.696	FAS	DCO-US	1044	3724	7311
2022-06-08	07:30:00	59738.813	1.169	0.028	0.672	FAS	DCO-US	1037	3724	7311
2022-06-08	08:16:00	59738.845	1.201	0.032	0.768	FAS	DCO-US	1036	3724	7311
2022-06-08	20:31:00	59739.355	1.711	0.510	12.240	ALE	NSH-FR	606	3800	7300
2022-06-08	23:49:00	59739.493	1.849	0.138	3.312	2SPOT	DSC-CL	567	3603	7808
2022-06-09	03:02:00	59739.627	1.983	0.134	3.216	2SPOT	DSC-CL	567	3603	7808
2022-06-09	05:44:00	59739.739	2.095	0.112	2.688	FAS	DCO-US	1007	3725	7310
2022-06-09	06:47:00	59739.783	2.139	0.044	1.056	FAS	DCO-US	1004	3725	7311
2022-06-09	10:23:00	59739.933	2.289	0.150	3.600	HBA	RSO-NZ	950	4310	6826
2022-06-09	20:18:00	59740.346	2.702	0.413	9.912	ALE	NSH-FR	642	3800	7300
2022-06-09	20:58:00	59740.374	2.730	0.028	0.672	ALE	NSH-FR	669	3800	7300
2022-06-09	21:36:00	59740.400	2.756	0.026	0.624	VLE	ORL-FR	509	3700	7721
2022-06-09	21:38:00	59740.402	2.758	0.002	0.048	ALE	NSH-FR	675	3800	7300
2022-06-09	23:03:00	59740.461	2.817	0.059	1.416	JGF	SMM-SP	9000	3839	9356
2022-06-10	01:53:00	59740.579	2.935	0.118	2.832	2SPOT	DSC-CL	567	3603	7808
2022-06-10	06:01:00	59740.751	3.107	0.172	4.128	FAS	DCO-US	1014	3724	7312
2022-06-10	06:47:00	59740.783	3.139	0.032	0.768	FAS	DCO-US	1019	3724	7312
2022-06-10	07:32:00	59740.814	3.170	0.031	0.744	FAS	DCO-US	1033	3725	7311
2022-06-10	21:01:00	59741.376	3.732	0.562	13.488	ALE	NSH-FR	503	3800	7300
2022-06-10	22:09:00	59741.423	3.779	0.047	1.128	JGF	PIE-SP	9000	3833	9355
2022-06-10	22:33:00	59741.440	3.796	0.017	0.408	VLE	ORL-FR	515	3701	7721
2022-06-10	22:39:00	59741.444	3.800	0.004	0.096	JGF	SMM-SP	9000	3834	9483
2022-06-11	01:07:00	59741.547	3.903	0.103	2.472	2SPOT	DSC-CL	567	3603	7808
2022-06-11	21:41:00	59742.404	4.760	0.857	20.568	PAD	KOL-SK	1154	4000	7400
2022-06-11	21:41:00	59742.404	4.760	0.000	0.000	VLE	ORL-FR	506	3700	7720
2022-06-12	01:13:00	59742.551	4.907	0.147	3.528	2SPOT	DSC-CL	567	3751	7807
2022-06-12	05:29:00	59742.729	5.085	0.178	4.272	FAS	DCO-US	978	3724	7311
2022-06-12	06:14:00	59742.760	5.116	0.031	0.744	FAS	DCO-US	980	3724	7311
2022-06-12	07:00:00	59742.792	5.148	0.032	0.768	FAS	DCO-US	980	3724	7311
2022-06-12	07:58:00	59742.832	5.188	0.040	0.960	FAS	DCO-US	1022	3724	7311
2022-06-12	22:10:00	59743.424	5.780	0.592	14.208	PAD	KOL-SK	1104	4000	7400
2022-06-13	01:36:00	59743.567	5.923	0.143	3.432	2SPOT	DSC-CL	566	3751	7807
2022-06-13	06:28:00	59743.770	6.126	0.203	4.872	FAS	DCO-US	950	3725	7312
2022-06-13	20:44:00	59744.364	6.720	0.594	14.256	ALE	NSH-FR	538	3800	7300
2022-06-13	23:11:00	59744.466	6.822	0.102	2.448	PCA	LEC-IT	507	3802	7868
2022-06-14	04:23:00	59744.683	7.039	0.217	5.208	KSH	CAR-US	1000	3801	7089
2022-06-14	20:38:00	59745.360	7.716	0.677	16.248	ALE	NSH-FR	568	3800	7300
2022-06-14	21:46:00	59745.407	7.763	0.047	1.128	PAD	KOL-SK	1022	4000	7400
2022-06-15	01:26:00	59745.560	7.916	0.153	3.672	2SPOT	DSC-CL	564	3751	7807
2022-06-15	05:51:00	59745.744	8.100	0.184	4.416	FAS	DCO-US	1031	3723	7311
2022-06-15	12:34:00	59746.024	8.380	0.280	6.720	BHQ	ARM-AU	1542	3900	6999
2022-06-15	22:13:00	59746.426	8.782	0.402	9.648	PCA	LEC-IT	535	3802	7867
2022-06-16	01:26:00	59746.560	8.916	0.134	3.216	2SPOT	DSC-CL	567	3751	7807
2022-06-17	21:50:00	59748.410	10.766	1.850	44.400	PAD	KOL-SK	1158	4000	7400
2022-06-19	21:10:00	59750.382	12.738	1.972	47.328	ALE	NSH-FR	562	3800	7300
2022-06-19	21:37:00	59750.401	12.757	0.019	0.456	PAD	KOL-SK	1146	4000	7400
2022-06-19	22:45:00	59750.448	12.804	0.047	1.128	PCA	LEC-IT	524	3802	7401
2022-06-21	22:37:00	59752.443	14.799	1.995	47.880	PCA	LEC-IT	532	3802	7399
2022-06-24	20:48:00	59755.367	17.723	2.924	70.176	ALE	NSH-FR	580	3800	7300
2022-06-29	05:26:00	59759.727	22.083	4.360	104.640	FAS	DCO-US	982	4001	7296

Nova Per 2020

by David Boyd

Nova Per 2020 (= V1112 Per) now in the nebular phase

Throughout 2022 Nova Per 2020 has been in the nebular phase producing forbidden emission lines.

At the start of 2022 Nova Per 2020 was at V magnitude 15.41 and for the rest of the year steadily faded at a mean rate of 4 mmag/day. 8 spectra of Nova Per 2020 were submitted to the ARAS database during 2022 by Pavol Dubovsky, Tomas Medulka and Woody Sims. These were all recorded using LISA spectroscopes with spectral resolution ~1000. Some of these had been calibrated in absolute flux by the observer. The others were calibrated using V magnitudes linearly interpolated to the time of each spectrum using daily averaged V magnitudes in the AAVSO photometry database. The plot below shows these 8 spectra along with their concurrent V magnitudes.

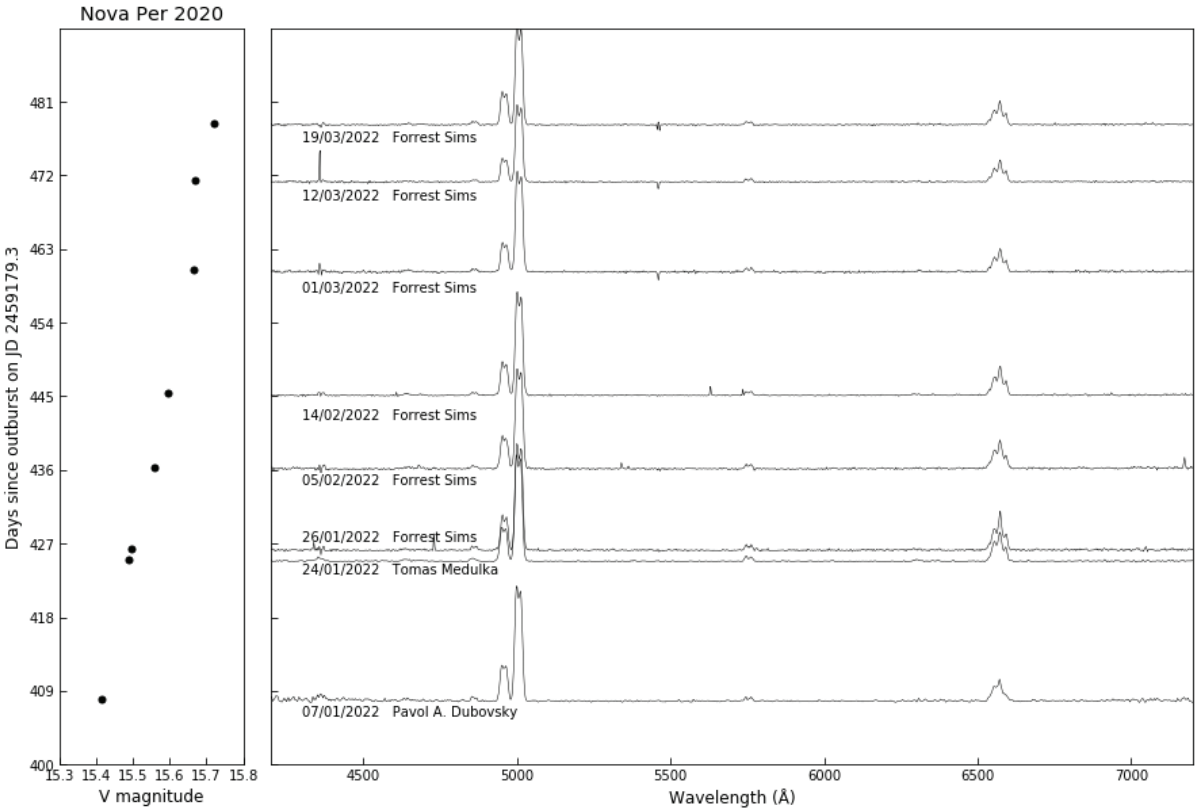

The most prominent features in these spectra are forbidden emission lines of [O III] 4959, 5007, [N II] 5755, 6583 and a weak line of [N II] 6548. These lines all have double peaks as shown below. There is also double peaked but relatively weak Hα and Hβ emission. In all cases the emission peaks are displaced by around ±400 km/s with respect to the rest wavelength of the line.

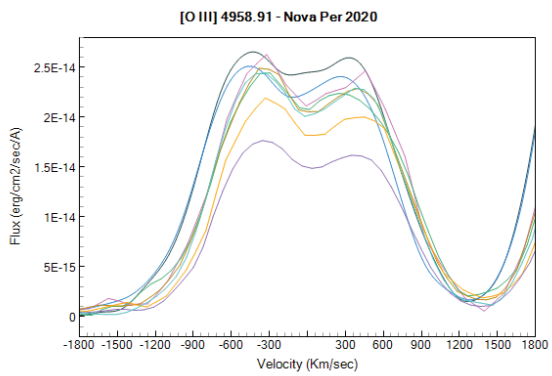

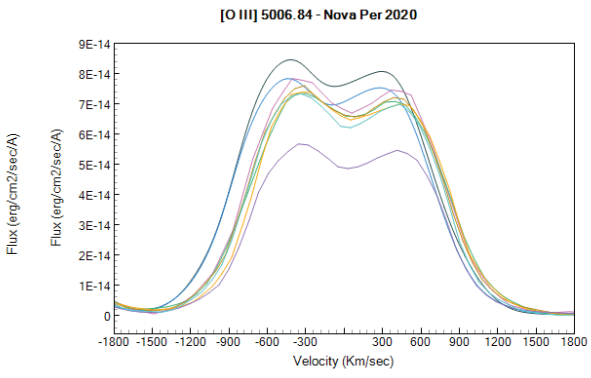

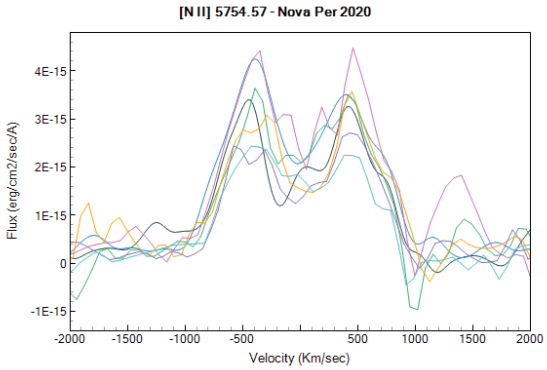

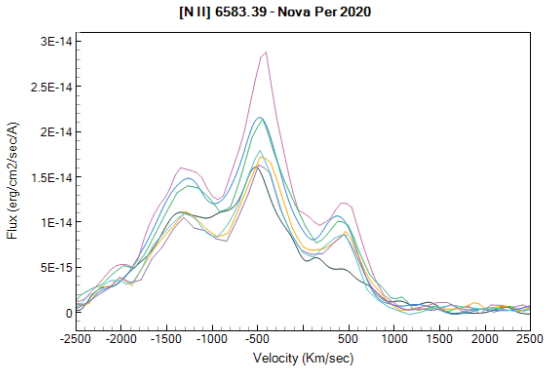

The line feature around 6560 Å is complex. It is a blend of [N II] 6583 and Hα 6563 double-peaked emission lines with a small contribution from double-peaked [N II] 6548.

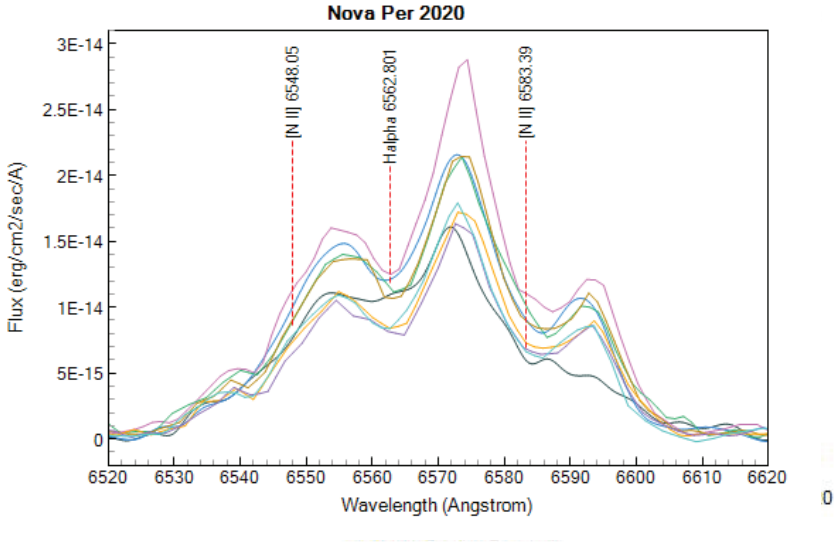

Fitting overlapping Gaussian profiles to the [O III] lines in these 8 spectra gives the following mean parameters.

Line	Wavelength (Å)	Blue peak (Å)	Blue shift (km/s)	Red peak (Å)	Red shift (km/s)
[O III] 4959	4958.91	4951.9 ± 1.0	-426 ± 61	4965.9 ± 1.0	420 ± 60
[O III] 5007	5006.84	4999.9 ± 1.1	-418 ± 68	5014.0 ± 1.1	426 ± 66

These emission lines are produced in optically thin shell-like ejecta which currently surround the nova. The blue shifted emission is from the section of ejecta moving toward us while the red-shifted component is from the ejecta behind the nova which is moving away from us.

Nova Cas 2021 = V1405 Cas

Coordinates (2000.0)	
RA(2000)	23 24 47.73
DE (2000)	+61 11 14.79
Mag V max	5.0

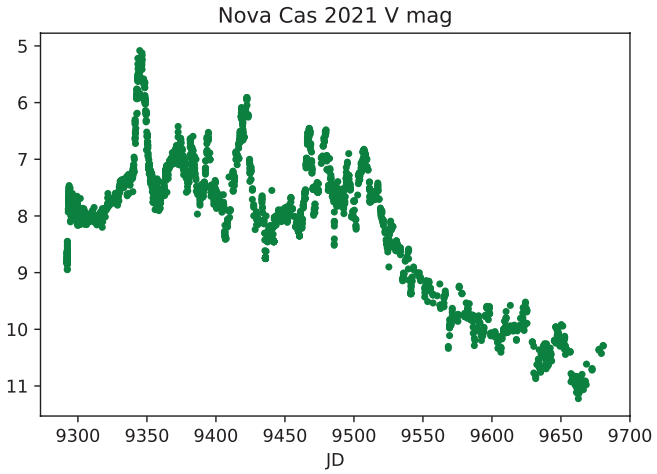

Nova Cas 2021 (V1405 Cas; PNV J23244760+6111140, was discovered on 2 by S. Korotkiy (ATel #13903).
It reached its maximum luminosity on JD 24590752 at mag V =10.6 .
After a classical first decline (ΔV ~2.4) to mag V 13.0 on JD 245078 (t2 ~ 4 days), it showed a series of flares during 113 days until JD 2459206 (Mag V = 13.9) before dimming steeply to mag V = 20.5 on JD 2459206 (ΔV = 0.44 mag/day).

481 spectra were secured by ARAS observers from 2021-03-19 to 2022-02-13

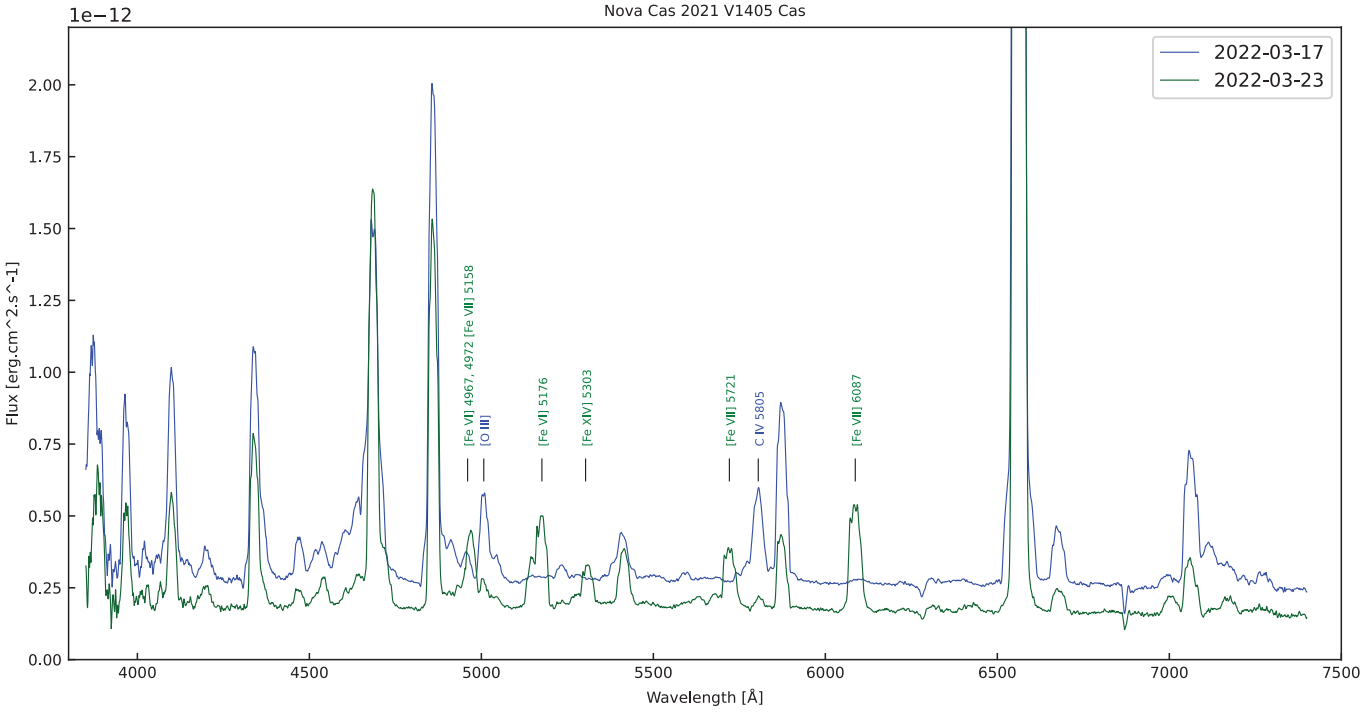

Flux calibrated spectra obtained by P. A. Dubovski, witha LISA R = 1000

The monitoring by Pavol Dubovsky allows to detect a sudden change of the ionization state of the spectrum at a time scale of 5 days. We note the fading of high ionization lines such as [O III] or CIV and the emergence of bright very high ionized iron lines from [Fe VI] to [Fe XIV] along with the decrease of the intensity of Balmer, He I and He II lines.

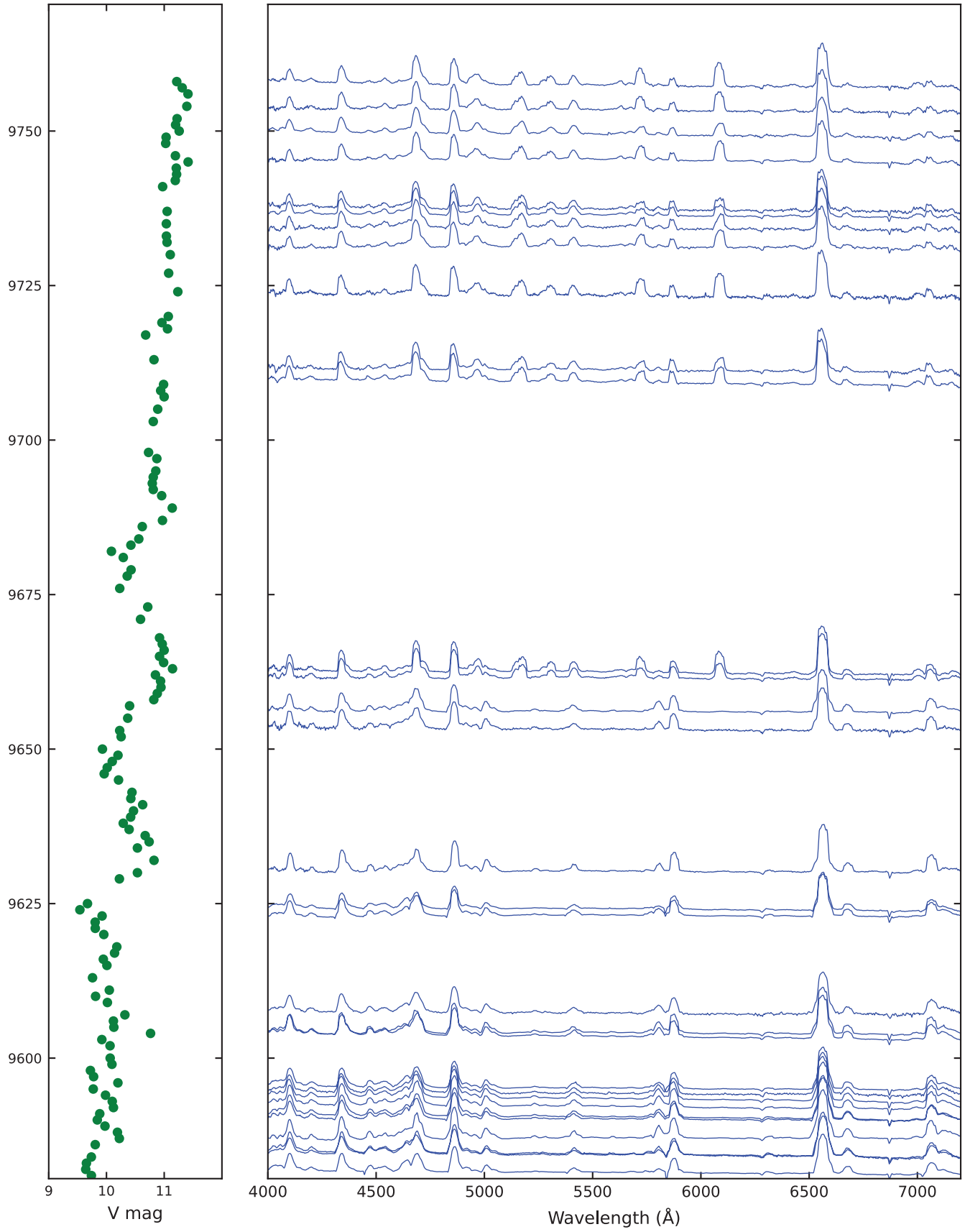

Time series - Y scale = JD -245000 - Green dots: AAVSO V Band
with low res spectra gathered by P.A. Dubovsky (23), H. Allen (3), K. Shank (3),. F. Sims (2), C. Boussin (1), T. Medulka (1). Left: AAVSO V lightcurve.

Nova Vul 2021 in nebular phase

by David Boyd

Report on the outburst of Nova Vul 2021 = V606 Vul

2021

The discovery of Nova Vul 2021 was reported as TCP J20210770+2914093 on the CBAT Transient Object Followup Reports webpage on 2021 07 16.4919 UT at unfiltered magnitude 12.0. Over the next 6 months, the nova brightened twice to V mag 10.0 before eventually fading to V mag 18.7. A V magnitude light curve for 2021 is shown below with daily averaged measurements from the AAVSO photometry database in blue. The dates of 67 spectra reported to the ARAS database in 2021 are marked along the top of the plot. Also shown in red are V magnitudes interpolated to the dates of these ARAS spectra and used to calibrate in absolute flux any spectra not already so calibrated by their observer.

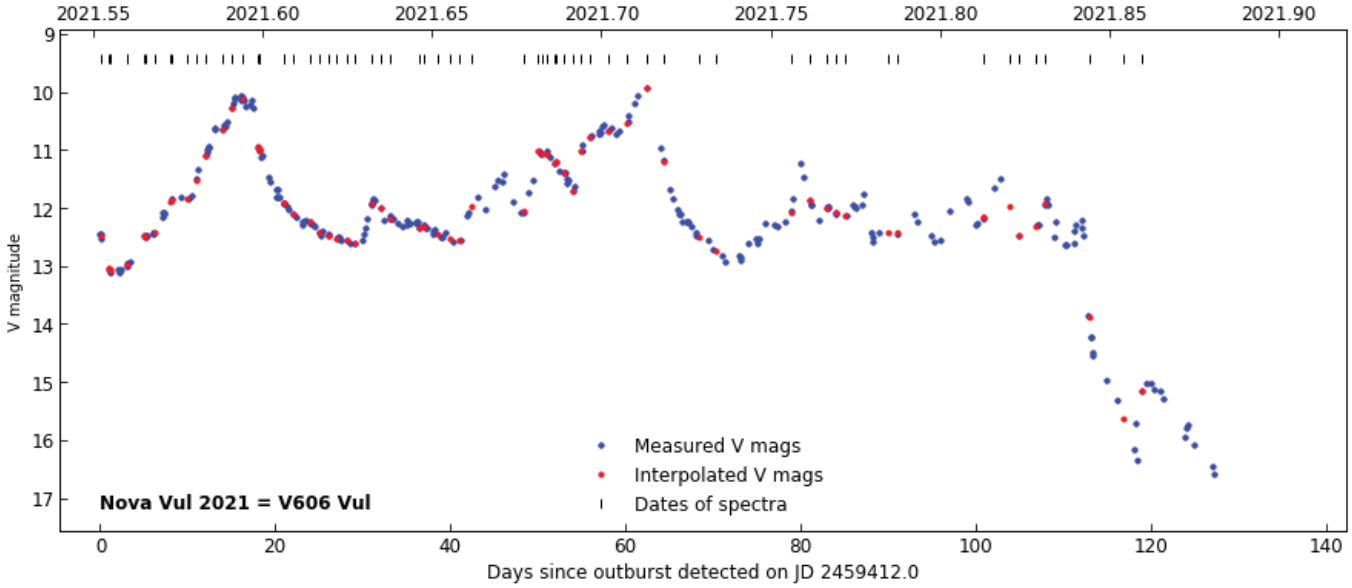

Spectra of Nova Vul were recorded in the ARAS database by Robert Barsa, David Boyd, Pavol Dubovsky, James Foster, Robin Leadbeater, Vincent Lecocq, Yana Markus and Tomas Medulka. Three-quarters of the spectra were taken with LISA spectrographs (R ~1000), the others with Alpys (R ~500). The following plot shows 16 LISA spectra of Nova Vul which illustrate the progressive changes in the spectral profile which occurred during 2021.

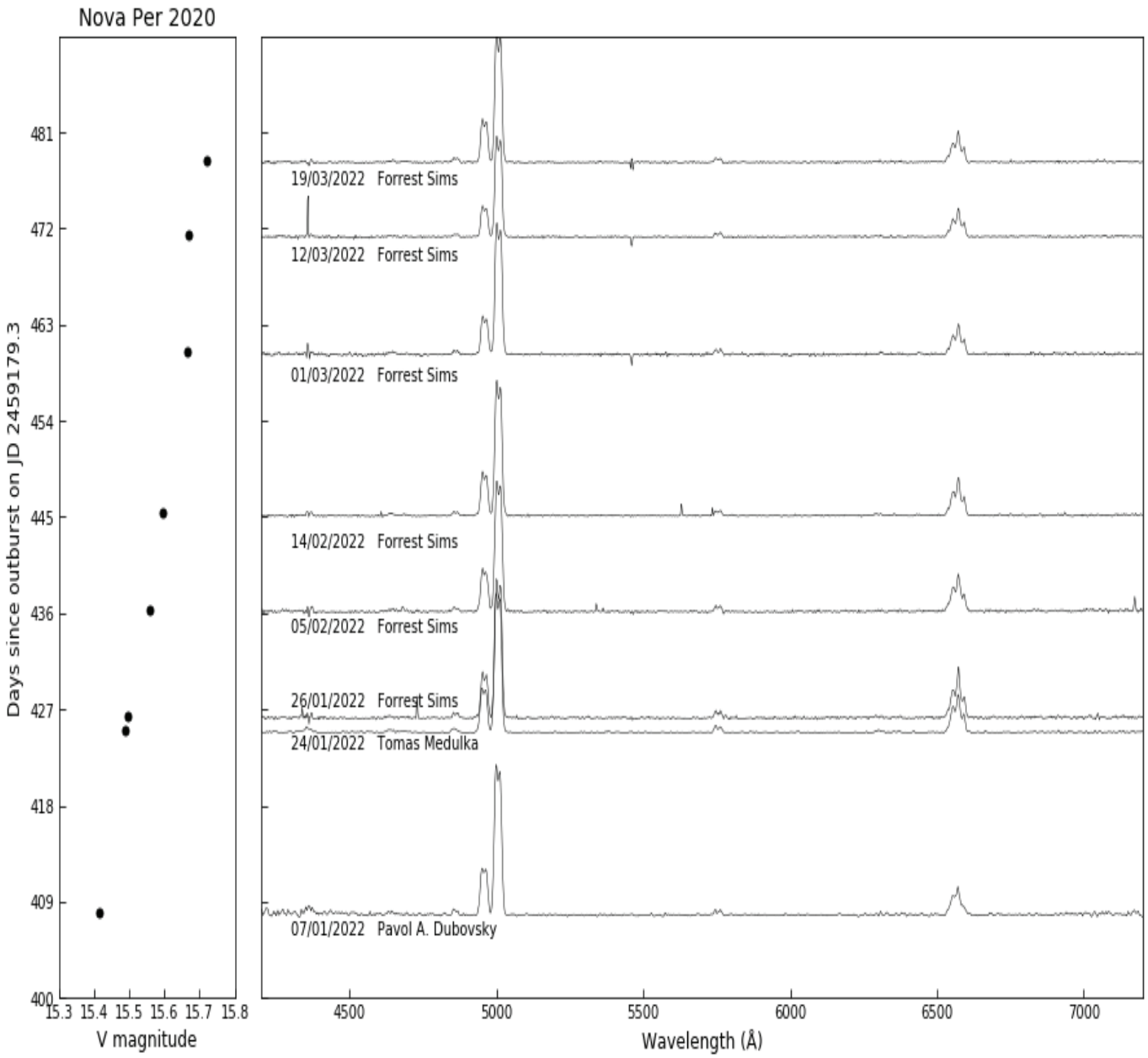

During the first 4 days, the spectrum showed emission lines of H I, He I, C II and N II. The Balmer lines all had P Cyg profiles with absorption troughs at -800 km/s and extending to -1500 km/s relative to their rest wavelengths.

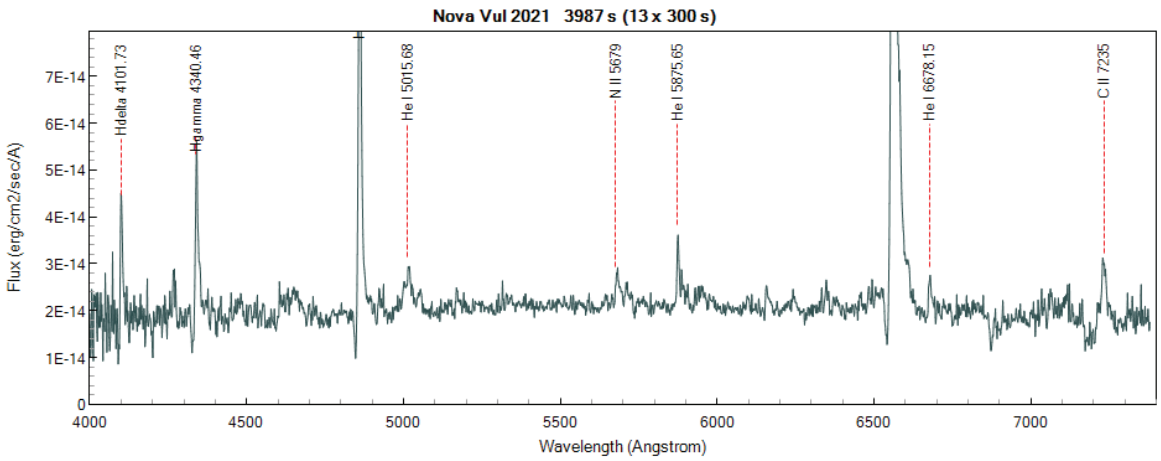

By 28th July (day 12), only the Balmer lines of those listed above were still present and there were growing Fe II emission lines including the multiplets Fe II (42), Fe II (49), Fe II (48) and Fe II (74).

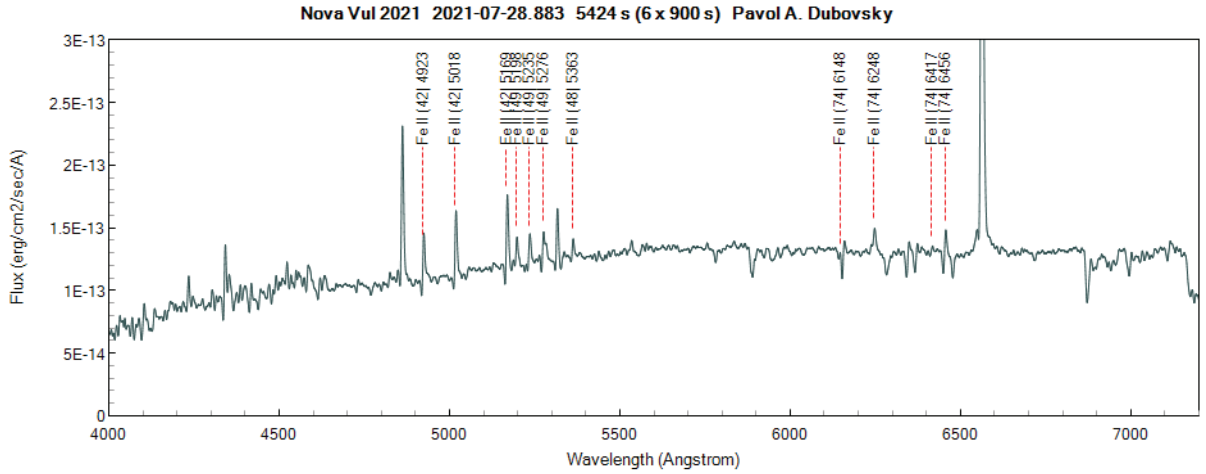

All Fe II lines had P Cyg profiles with absorption troughs at -350 km/s and extending to -700 km/s relative to their rest wavelengths. The appearance of Fe lines led to the nova being classified as a Fe-type nova in ATel 14816.

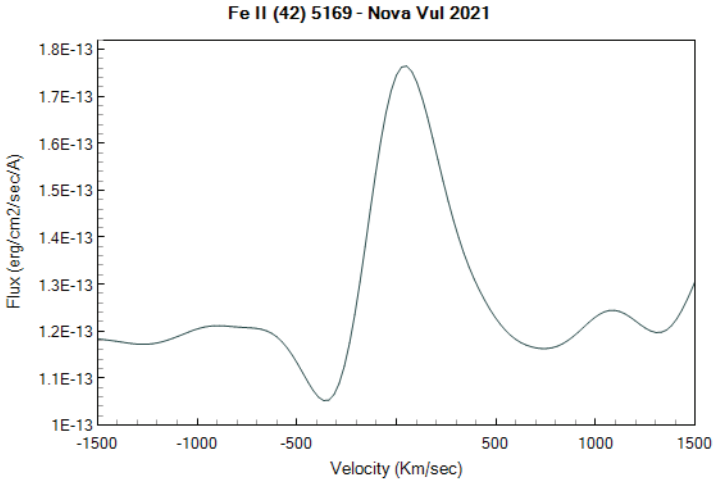

Between 28th July and 25th August (days 12 to 40) there were large changes in emission lines as shown in this plot of the Hα line. As the nova peaked at V=10.0 on 2nd August (day 17), the line first broadened and developed an absorption trough centred on -300 km/s relative to the Hα rest wavelength. This absorption then disappeared as the Hα line widened and increased in flux. P Cyg troughs were much reduced during this period.

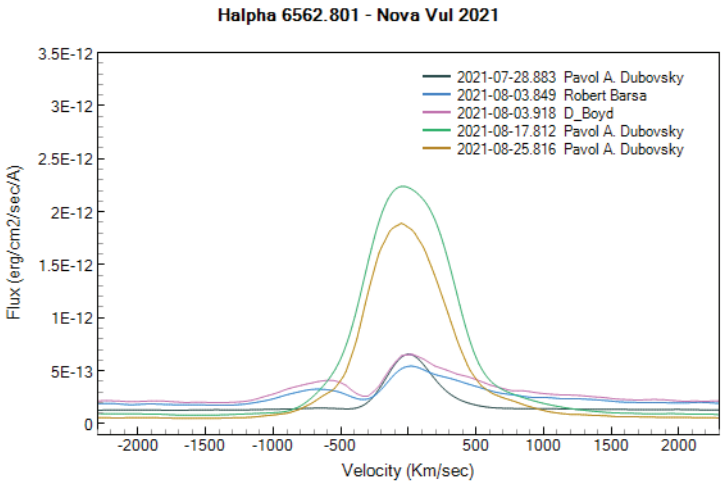

Meanwhile the nova faded rapidly by 2.5 magnitudes before recovering slowly and irregularly.

By 17th August (day 32) double-peaked [O I] emission lines had appeared at 5577, 6300 and 6364 Å with components at approximately -200 km/s and +200 km/s relative to their rest wavelengths. The 6300 Å line in particular persisted in the spectra until the nova faded in November. Fe II lines had by now also become double-peaked with similar component separation.

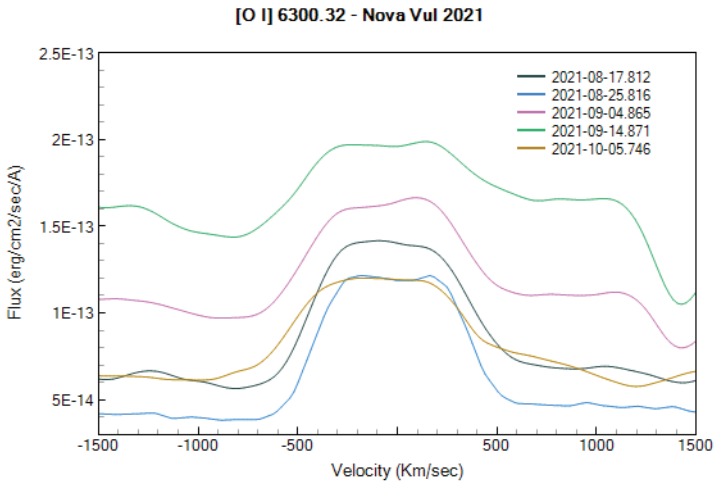

By 4th September (day 50), P Cyg profiles had returned on the Balmer and Fe II emission lines. Initially these had absorption troughs at -800 km/s which extended to -1150 km/s. During October the P Cyg troughs moved to -1000 km/s and extended to -1500 km/s. This plot shows these changes in the Hβ line.

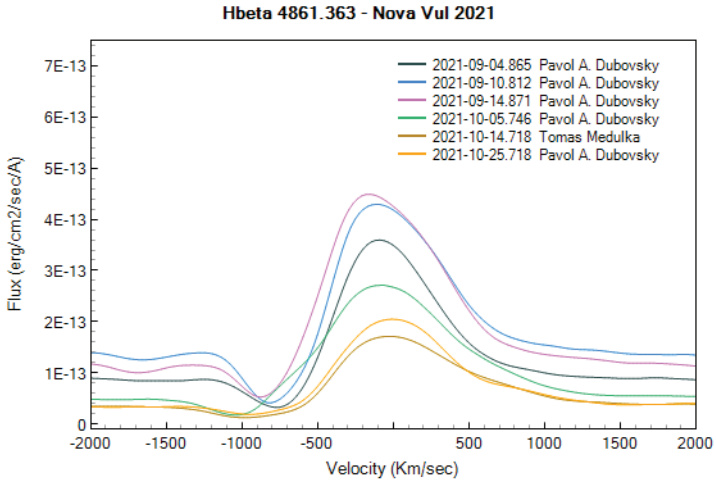

Flux in the Fe lines reached maximum amplitude during September (days 50-60).

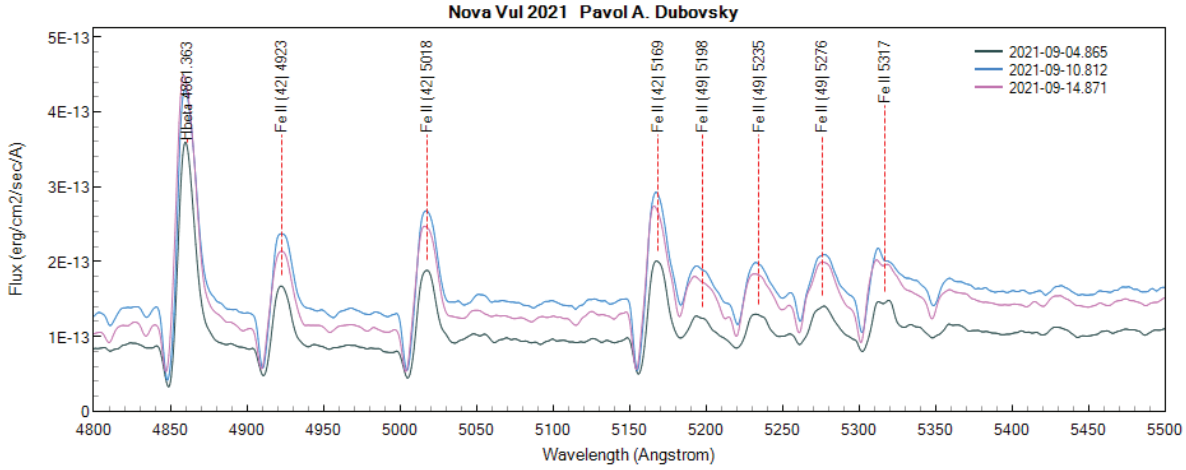

The nova brightened again to mag 10.0 on 17th September (day 63) then faded rapidly by 3 magnitudes. It maintained that level for a further 35 days with little change in the spectrum. On 5th November (day 112) the nova began to fade rapidly, possibly due to the creation of dust, and emission features in the spectrum became much weaker.

2022

During 2022, V magnitude measurements on 11 days in the AAVSO database showed the nova gradually brightening to V=15.0 before undergoing a slow, steady decline. Only the 4 spectra shown below were submitted to the database during 2022.

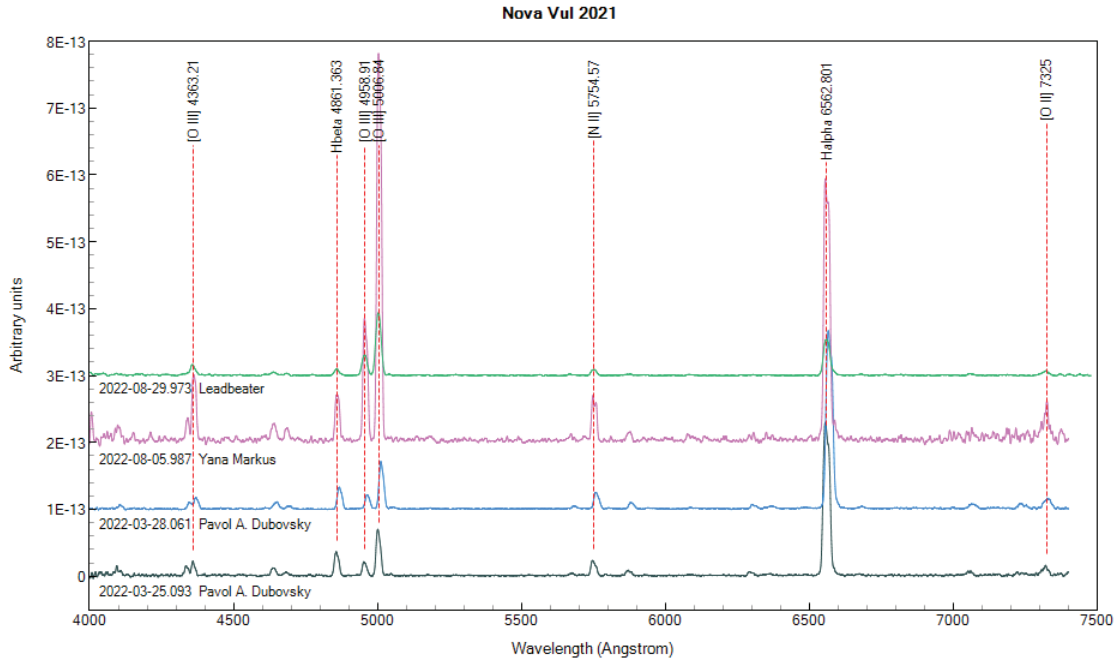

The spectrum by Markus on day 386 clearly shows the nova to be in the nebular phase with double peaked emission lines of [O III] 4363, 4959, 5007 and [N II] 5755.

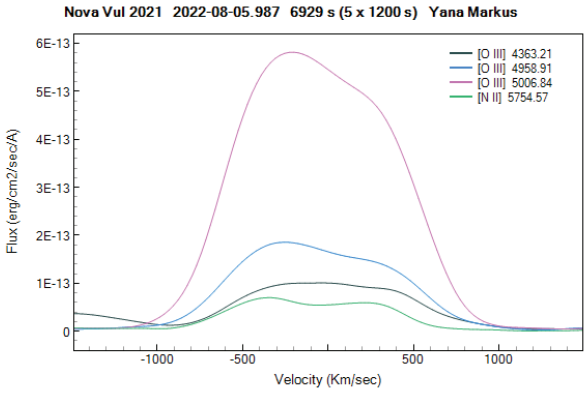

Fitting two Gaussian profiles to the [O III] 4959 and 5007 lines, gives the following wavelength shifts and velocities for the blue- and red-shifted components of the lines relative to their rest wavelengths.

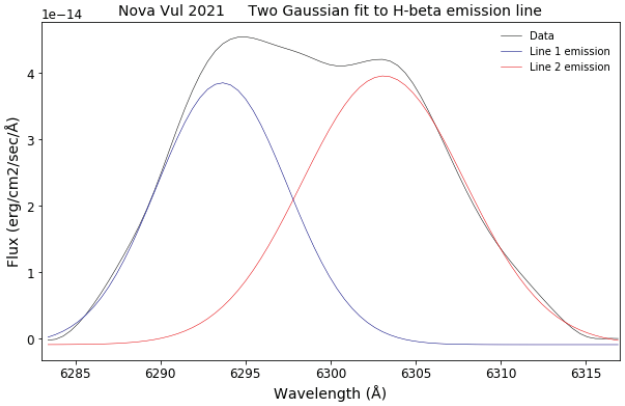

Line	Wavelength (Å)	Blue peak (Å)	Blue shift (km/s)	Red peak (Å)	Red shift (km/s)
[O III] 4959	4958.91	4953.6	-323	4963.5	+280
[O III] 5007	5006.84	5001.6	-313	5011.4	+273

Eruptive stars spectroscopy
Cataclysmics, Symbiotics, Novae

Eruptive Stars
Information Letter n° 50 #2022-01 12-05-2023

Spectroscopic observations of symbiotic stars in 2022-S1

Authors:
Authors: F. Teyssier, C. Boussin, D. Boyd, F. Sims, J.P. Nougayrede, K. Shank, P. A. Dubovsky, J. Guarro, Y. Markus, S. Curry, I. Diabassoura, V. Bouttard, J. F. Coliac,C. Laulhère, C. Eldridge, P. Velez, R. Ehlert, F. Boubault, H. Barker, P. Luckas, T. Bohlsen, B. Buccheim, P. Somogyi, U. Sollecchia, M. Le Lain, V. Lecocq, G. Bertrand,J. Hinnefeld, J. Michelet, D. Cujedo, J.Coffin, T. Love, L. Franco, 2SPOT (O. Garde;L.Mulato;P. LeDu;S. Charbonnel; T. Petit)

Stars: AG Dra, AG Peg, AR Pav, AX Per, BF Cyg, CH Cyg, CI Cyg, CN Cha, EG And, FG Ser, Hen 4-204, HM Sge, IV Vir, LT Del, omi Cet, PU Vul, R Aqr, RR Tel, RS Oph, SS Lep, StHA 190, SU Lyn, T CrB, V1016 Cyg, V1261 Ori, V1329 Cyg, V1413 Aql, V335 Vul, V399 Pav, V407 Cyg, V426 Sge, V443 Her, V471 Per, V627 Cas, V648 Car, V694 Mon, WY Vel, Z And,

Abstract:
Continuous monitoring of 38 symbiotic stars.
Egress of eclipse of BX Mon.

AG Dra

RA (2000)	16 01 41.01
DE (2000)	+66 48 10.13
Mag V	9.77
Orb. Phase	0.05 - 0.38

Yellow Symbiotic

Continuous monitoring in quiescence
upon the request of R. Gàlis & J. Merc
Quiescent State
Orbital Variations

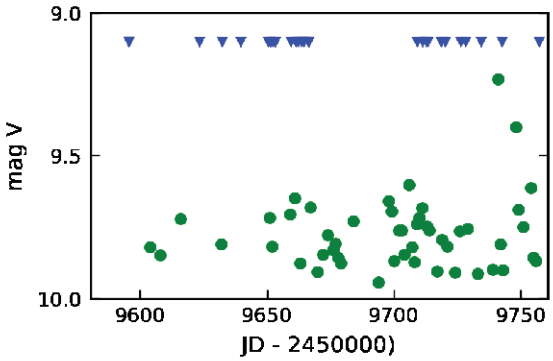

AAVSO V band lightcurve
ARAS Spectra: blue triangles

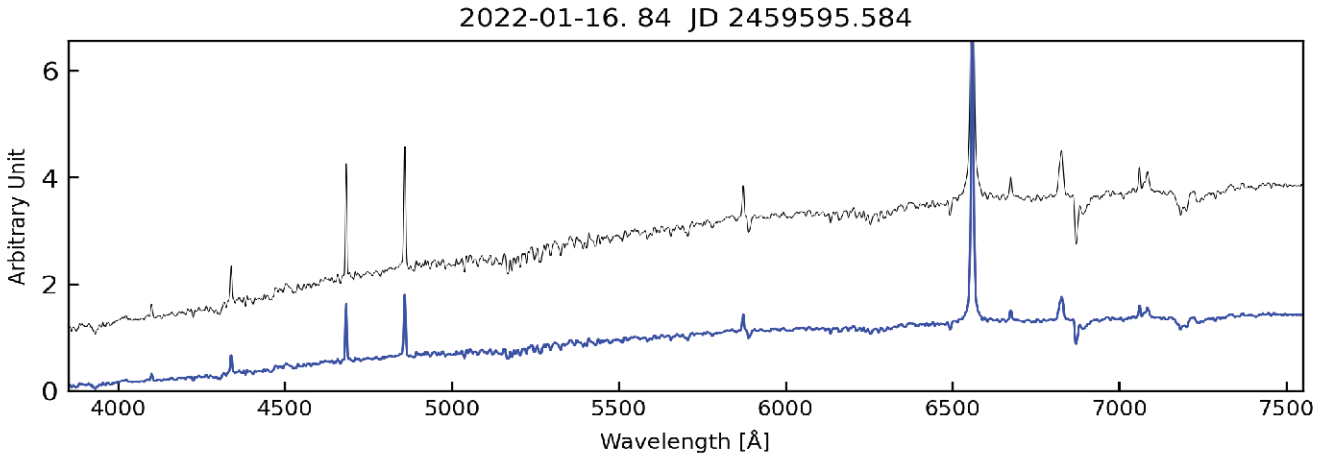

Observer: Pavol A. Dubovsky
Site: Kolonica Instrument: C14+LISA+Atik 460EX Resolution: 855

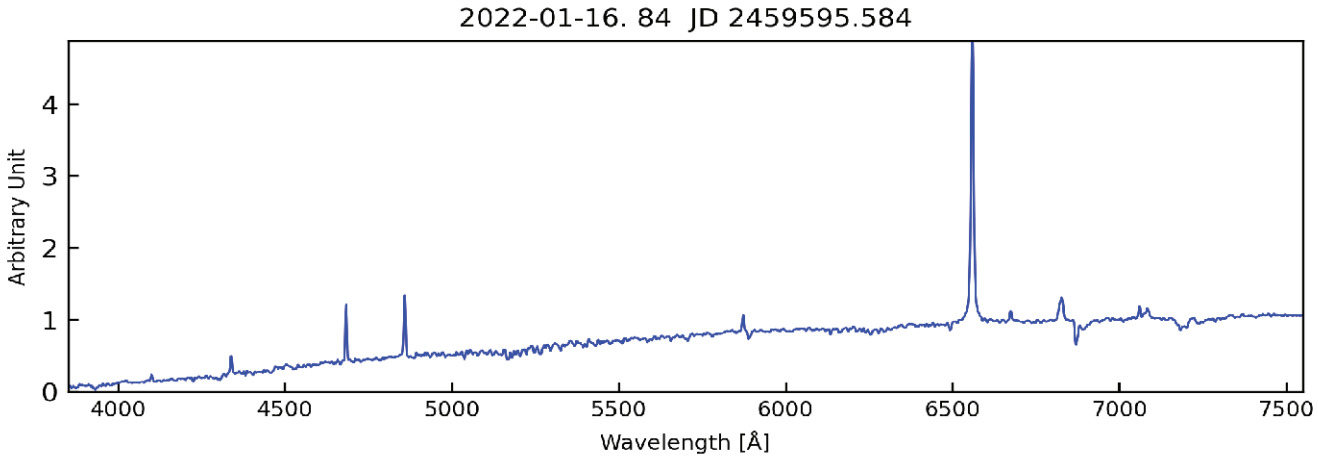

Observer: Pavol A. Dubovsky
Site: Kolonica Instrument: C14+LISA+Atik 460EX Resolution: 855

AG Peg

RA (2000)	21 51 01.97
DE (2000)	+12 37 32.12
Mag V	8.62
Orb. Phase	0.61 - 0.83

Symbiotic Nova (1850:)
Classical Symbiotic (2010 ~>)

Quiescent State
Orbital Variations

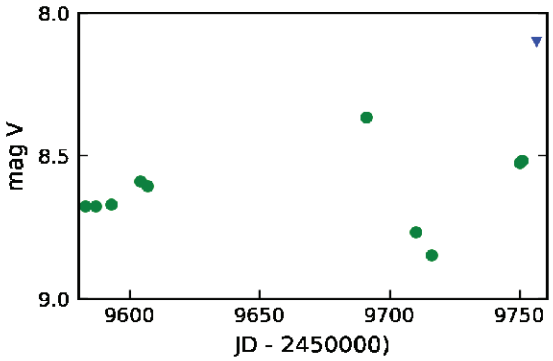

AAVSO V band lightcurve
ARAS Spectra: blue triangles

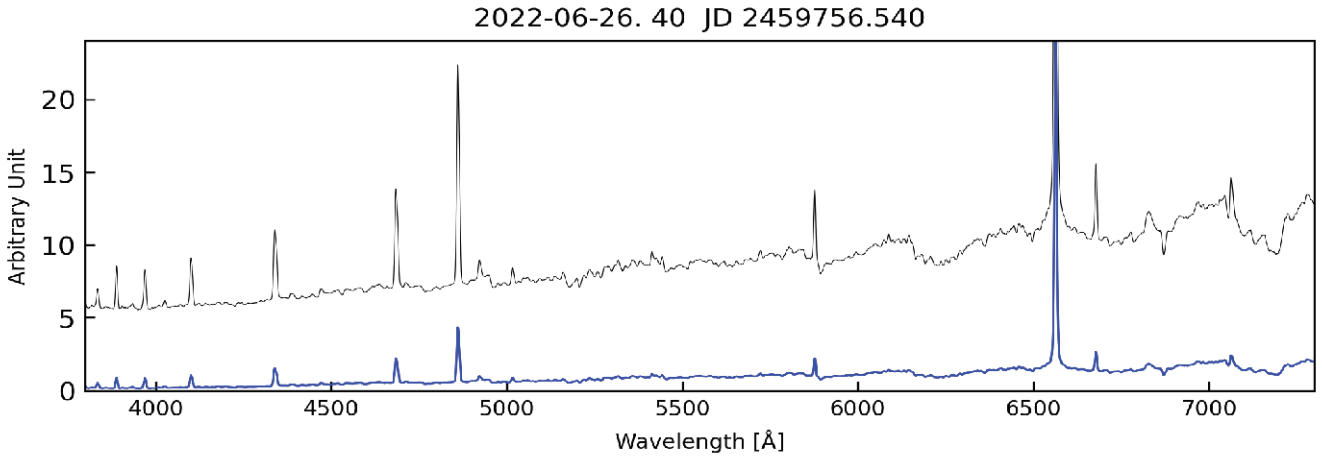

Observer: ALeduc
Site: Nice Shakespeare Instrument: N200F5 Starex 300t 23mic asi183mmpro Resolution: 786

AX Per

RA (2000)	01 36 22.70
DE (2000)	+54 15 02.41
Mag V	11.61
Orb. Phase	0.67 - 0.93

Classical Symbiotic

Quiescent State
Orbital Variations

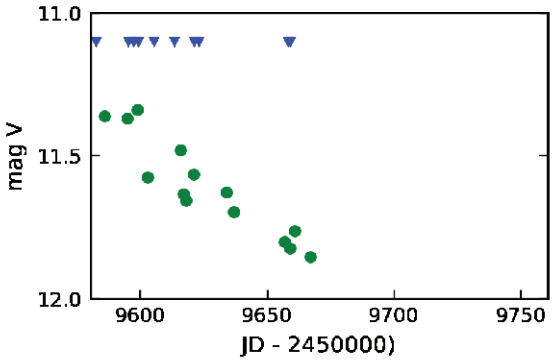

AAVSO V band lightcurve
ARAS Spectra: blue triangles

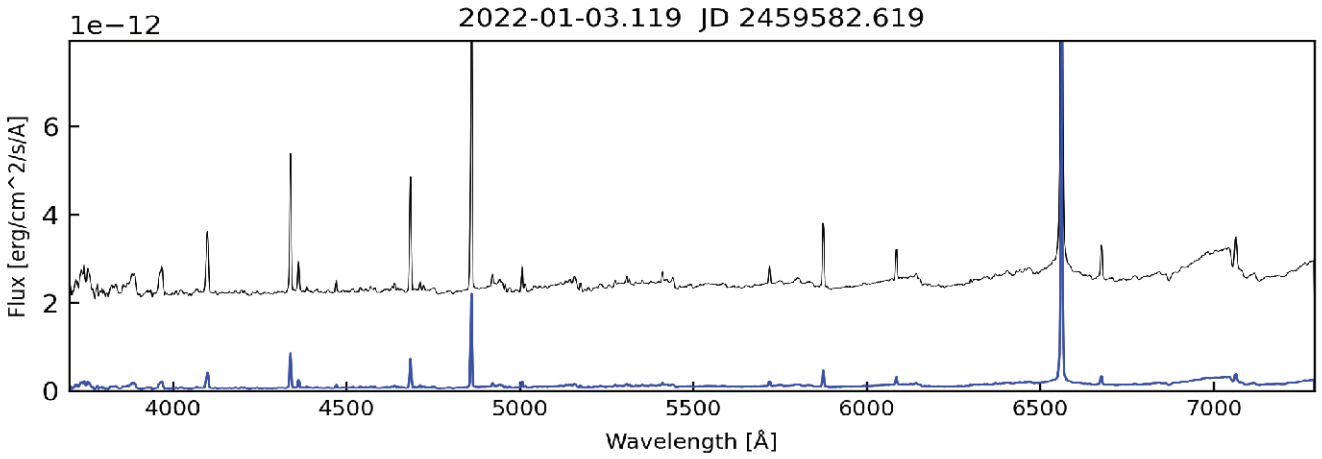

Observer: Forrest Sims
Site: Desert Celestial Observatory Instrument: CDK14 LISA Atik414ex Resolution: 994

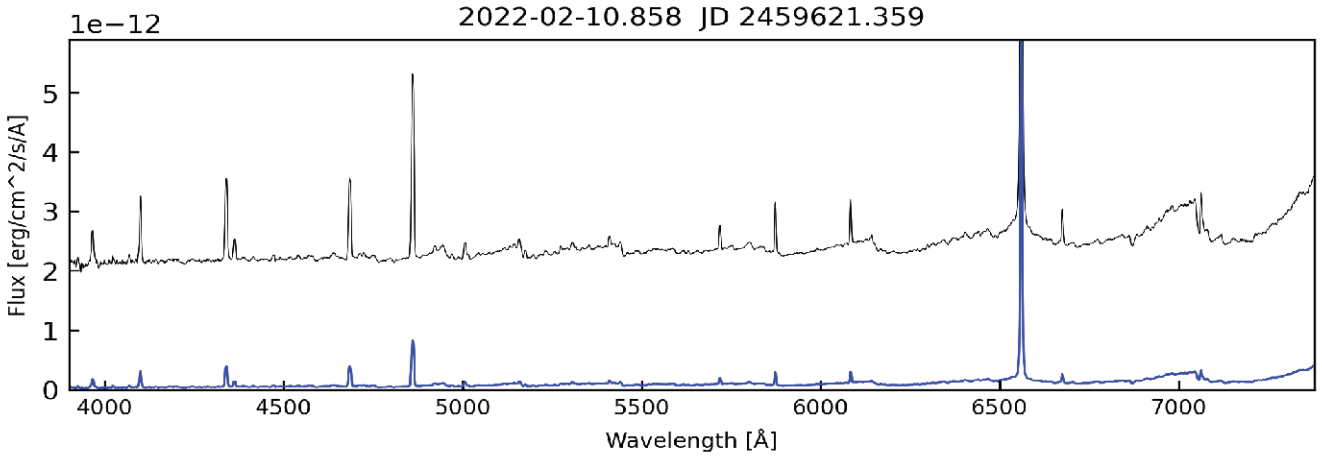

Observer: D_Boyd
Site: West Challow Observatory Instrument: C11 + LISA + SXVR-H694 Resolution: 1064

BD Cam

RA (2000)	03 42 09.33
DE (2000)	+63 13 00.46
Mag V	no data
	-

Symbiotic in UV

No emission lines detected
Quiescent State

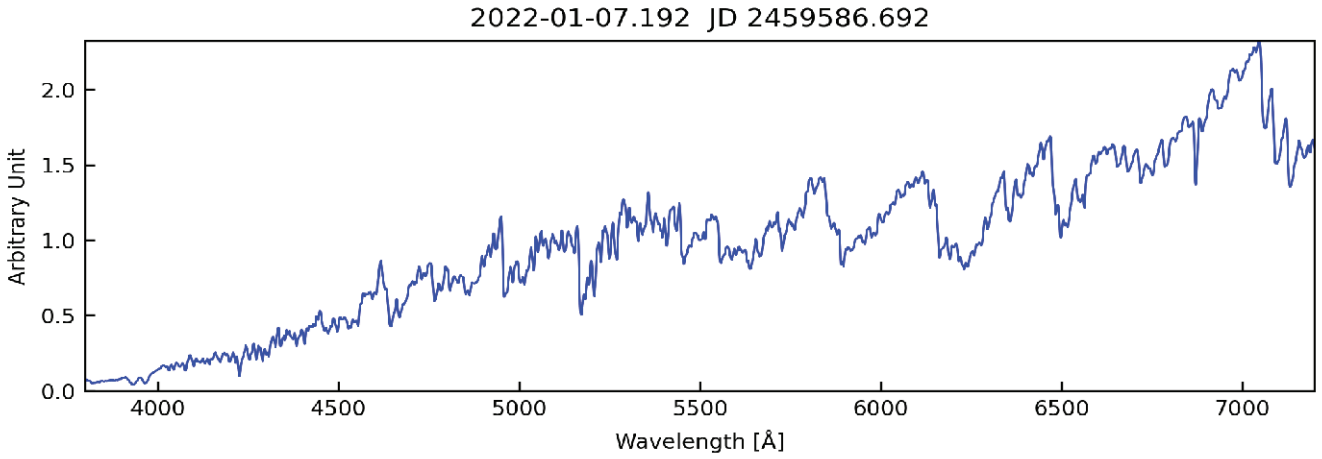

Observer: K. Shank
Site: Carrollton TX Instrument: C14E@F7.6+LISA+SX Tirus825M Pro Resolution: nan

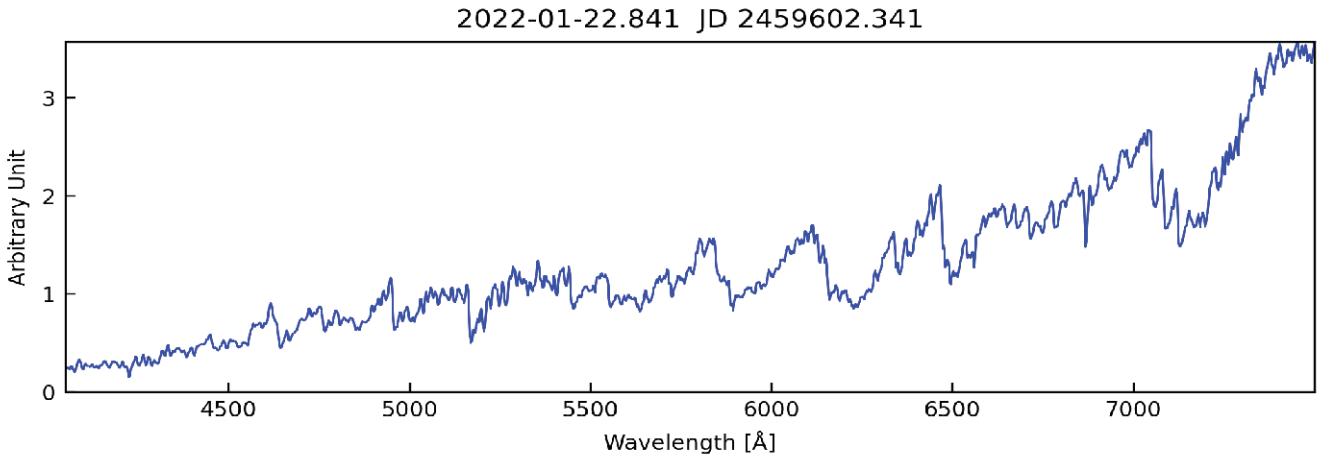

Observer: F. Boubault
Site: Saint-Jean-d'Illac Instrument: C8_LISA_ATIK414 Resolution: nan

BF Cyg

RA (2000)	19 23 53.50
DE (2000)	+29 40 29.17
Mag V	10.5
	-

Low ionisation symbiotic

Quiescent State

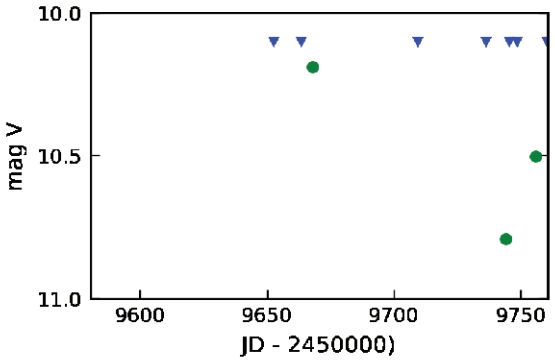

AAVSO V band lightcurve
ARAS Spectra: blue triangles

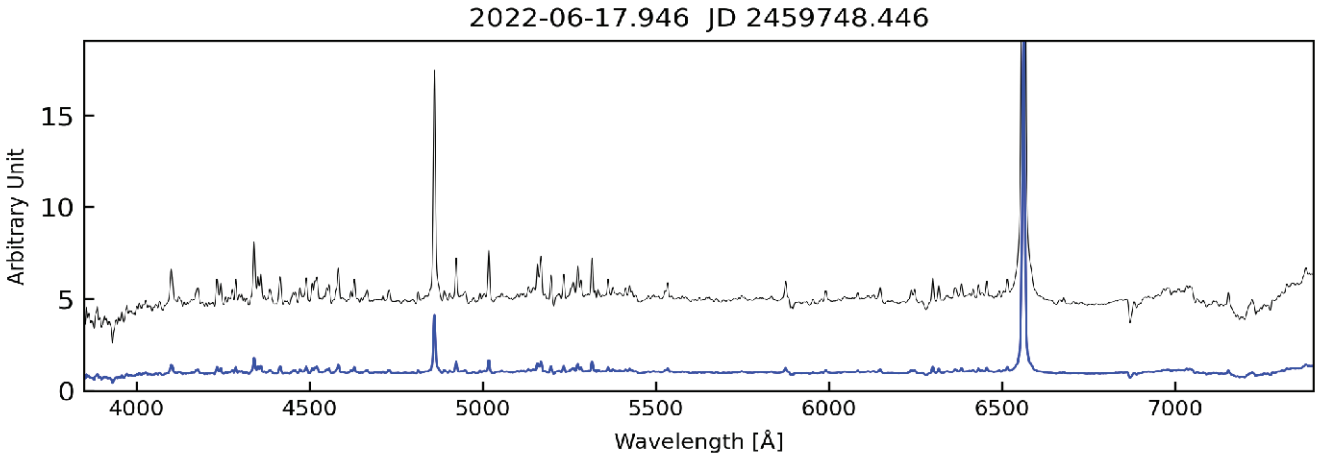

Observer: Pavol A. Dubovsky
Site: Kolonica Instrument: C14+LISA+Atil460ex Resolution: 1011

BX Mon

RA (2000)	07 25 22.76
DE (2000)	-03 35 50.64
Mag V	10.01
Phase	0.77 - 0.91

Low ionisation Symbiotic Star

Eclipsing

Quiescent State
Egress of Eclipse

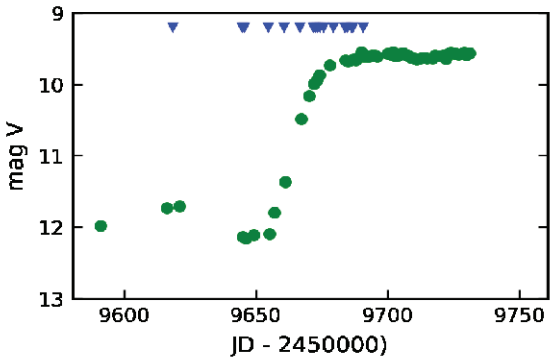

AAVSO V band lightcurve
ARAS Spectra: blue triangles

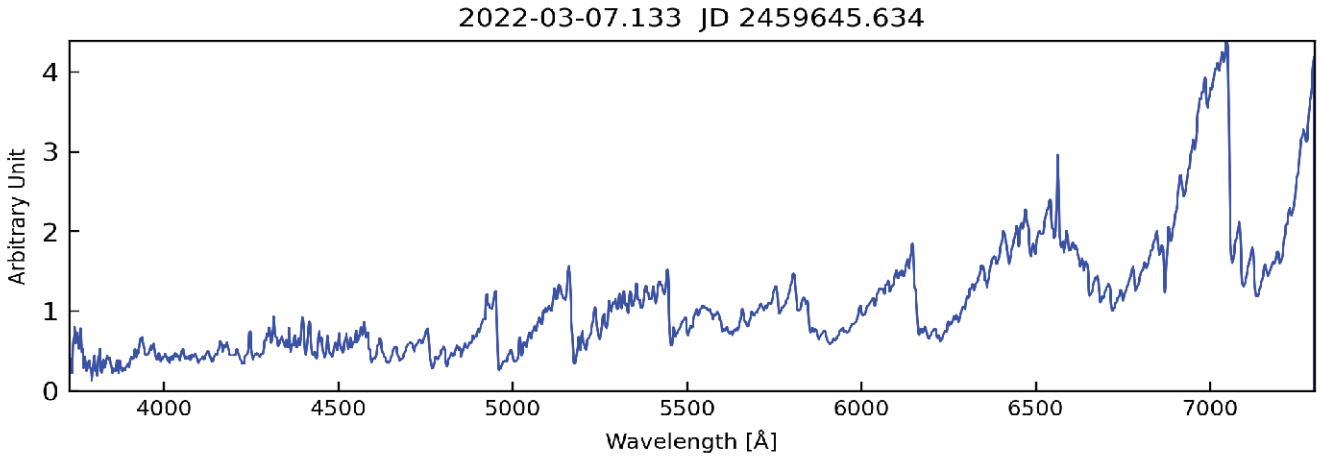

Observer: Forrest Sims
Site: Desert Celestial Observatory Instrument: CDK20 LISA Atik414ex Resolution: 1036

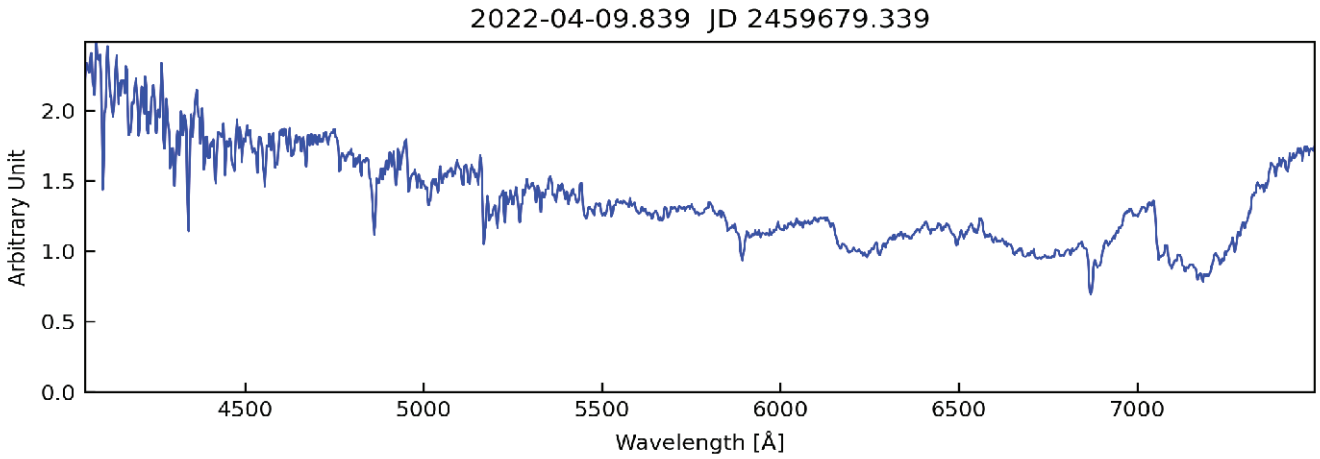

Observer: F. Boubault
Site: Saint-Jean-d'Illac Instrument: C8_LISA_ATIK414 Resolution: nan

CH Cyg

RA (2000)	19 24 33.07
DE (2000)	+50 14 29.06
Mag V	6.93
	-

Accretion powered symbiotic

Weak [OIII] 5007
Quiescent State
Balmer lines in emission

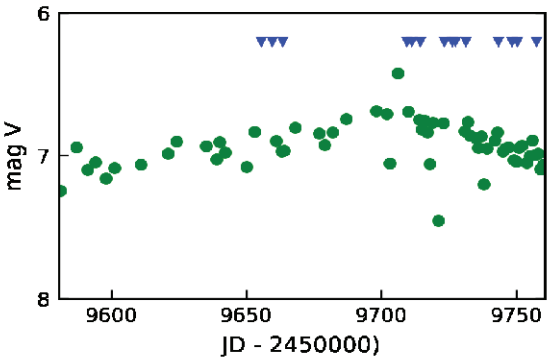

AAVSO V band lightcurve
ARAS Spectra: blue triangles

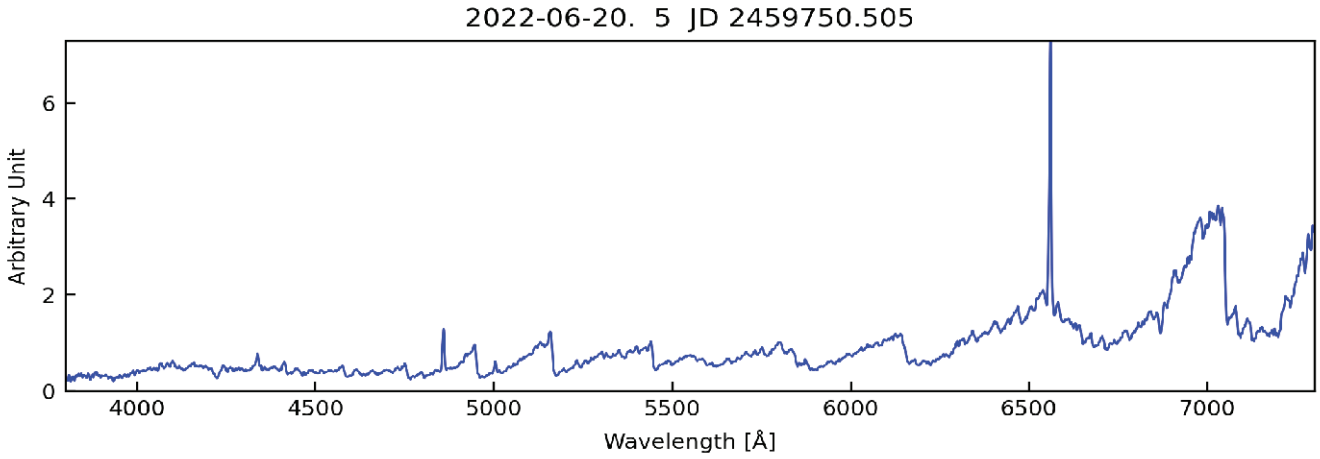

Observer: A. Leduc
Site: Nice Shakespeare Instrument: N200F5 Starex 300t 23mic asi183mmpro Resolution: 988

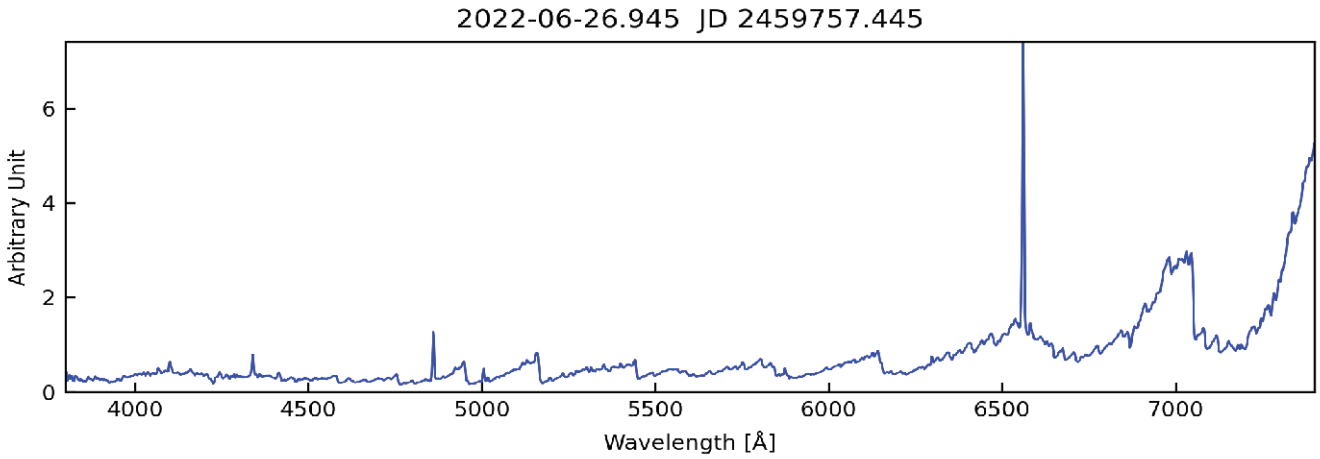

Observer: P. A. Dubovsky
Site: Kolonica Instrument: C14+LISA+Atil460ex Resolution: 1043

CI Cyg

RA (2000)	19 50 11.83
DE (2000)	+35 41 03.00
Mag V	11.04
	-

Classical Symbiotic Star

Quiescent State
Orbital Variations

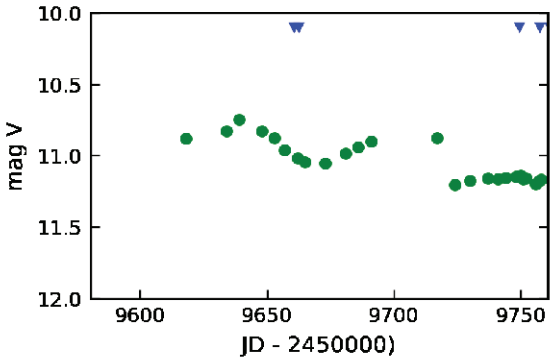

AAVSO V band lightcurve
ARAS Spectra: blue triangles

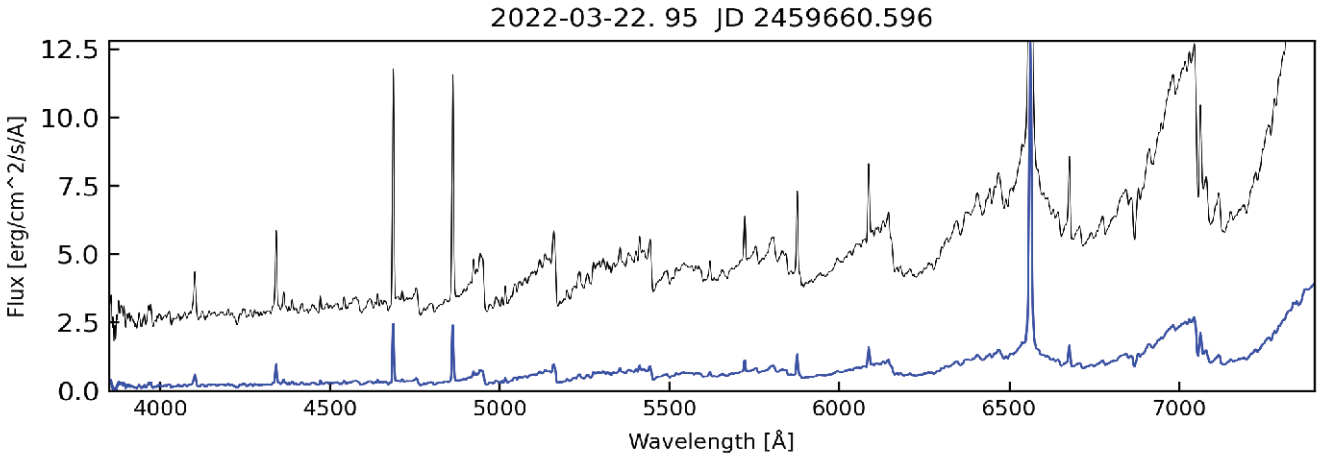

Observer: Pavol A. Dubovsky
Site: Kolonica Instrument: C14+LISA+Atik-460ex Resolution: 975

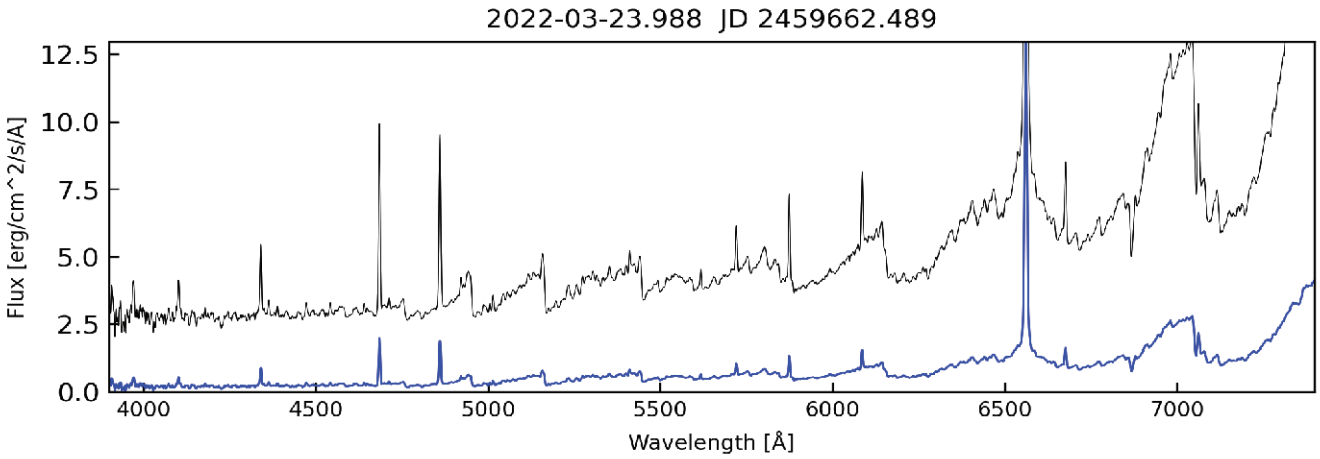

Observer: Pavol A. Dubovsky
Site: Kolonica Instrument: C14+LISA+Atik-460ex Resolution: 1017

CN Cha

RA (2000)	10 59 57.62
DE (2000)	-79 57 01.06
Mag V	no data
	-

Symbiotic Nova (~ 2012)

Nebular spectrum
Strong [OIII]
Nova Outburst

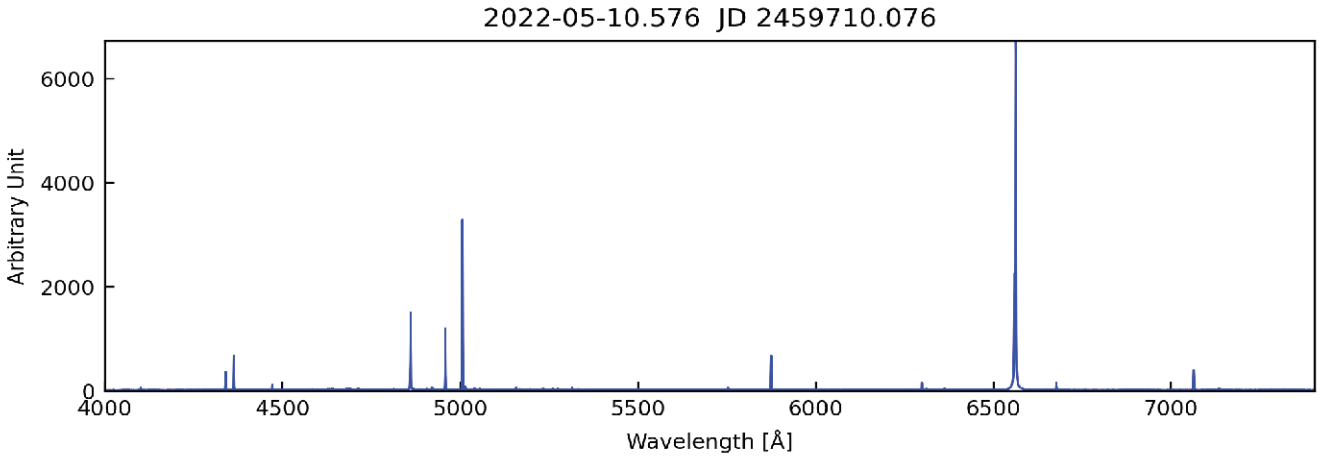

Observer: C. Eldridge
Site: Mardella Instrument: CDK1000-eShel-Atik-460ex Resolution: nan

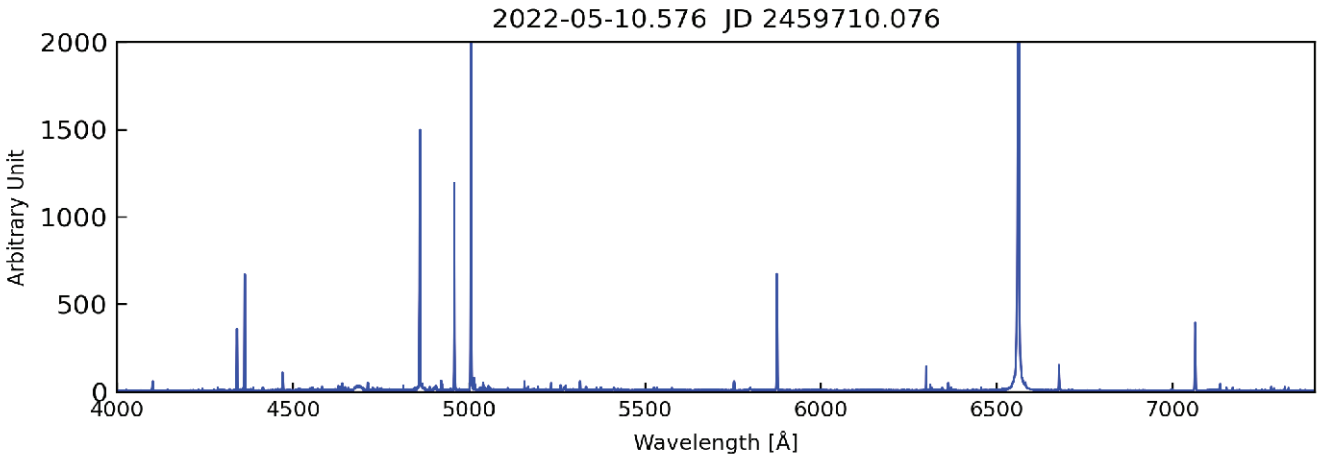

Observer: Colin Eldridge
Site: Mardella Instrument: CDK1000-eShel-Atik-460ex Resolution: nan

CQ Dra

RA (2000)	12 30 06.67
DE (2000)	+69 12 03.99
Mag V	no data
	-

Symbiotic Star in UV

Quiescent State
No emission lines detected

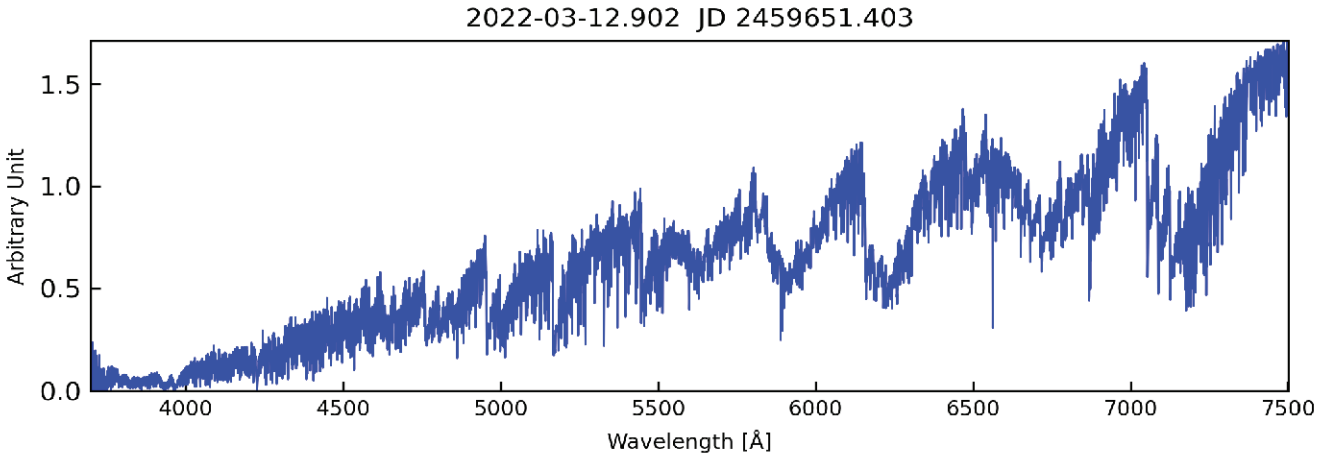

Observer: J. Guarro
Site: PIERA Instrument: PIERA Meade16 NOU_T ASI2600MM Resolution: 8500

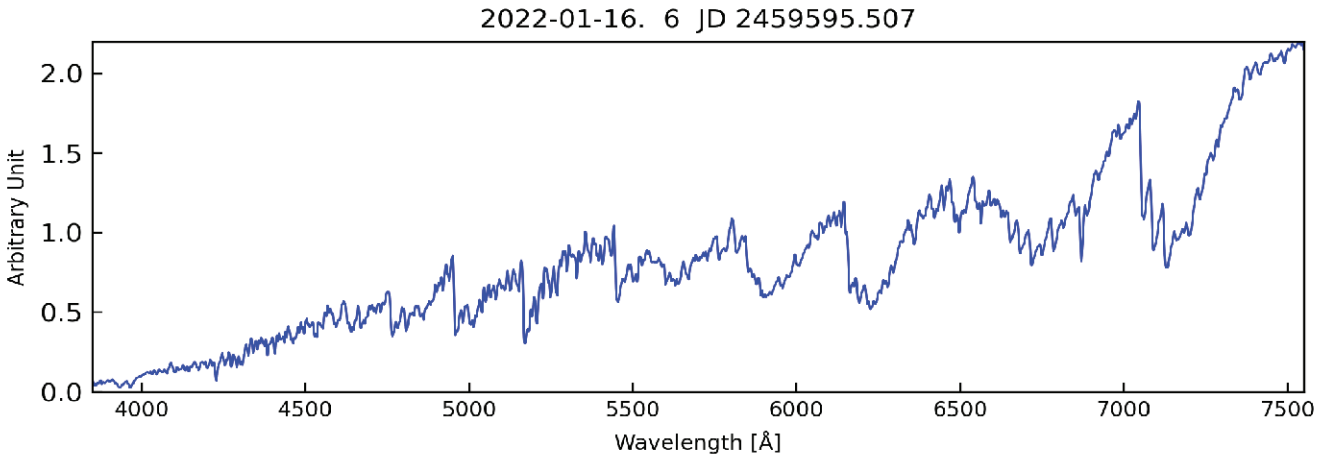

Observer: Pavol A. Dubovsky
Site: Kolonica Instrument: C14+LISA+Atik 460EX Resolution: 865

EG And

RA (2000)	00 44 37.19
DE (2000)	+40 40 45.70
Mag V	7.23
Orb. Phase	0.14 - 0.52

Accretion Powered Symbiotic

He I 5876 very weak if present
Quiescent State
Balmer lines in emission

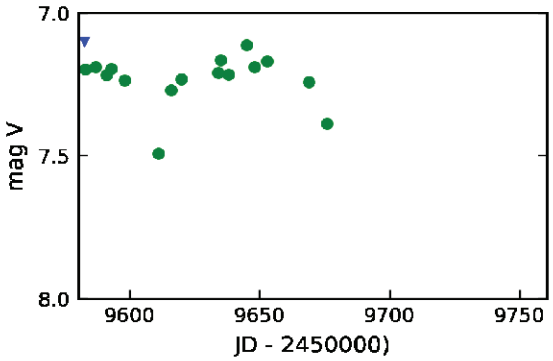

AAVSO V band lightcurve
ARAS Spectra: blue triangles

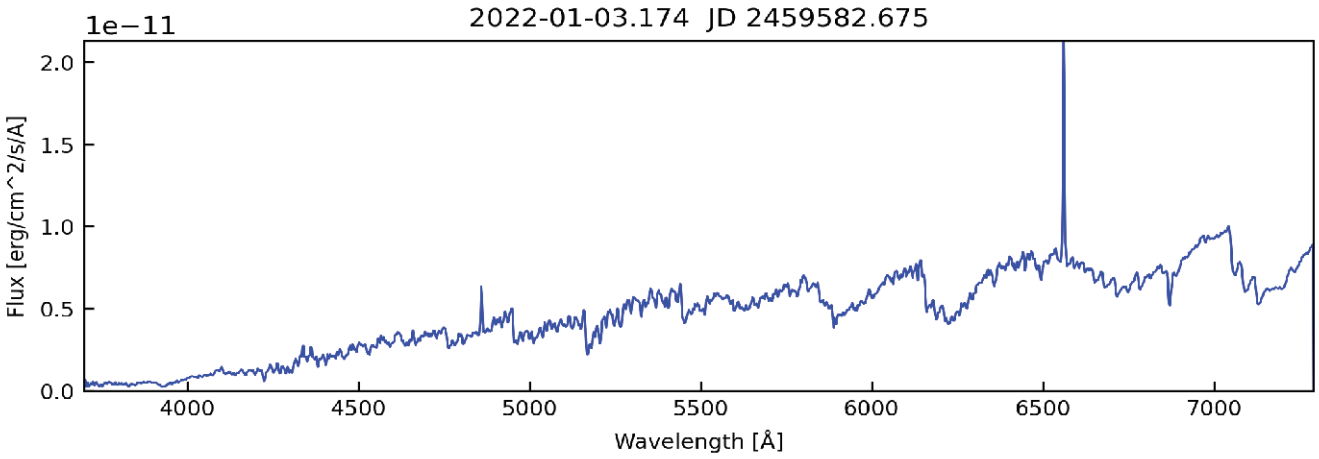

Observer: F. Sims
Site: Desert Celestial Observatory Instrument: CDK14 LISA Atik414ex Resolution: 1003

GH Gem

RA (2000)	07 04 12.77
DE (2000)	+12 03 34.24
Mag V	12.64
	-

Yellow Symbiotic Star

Quiescent State
H alpha in emission

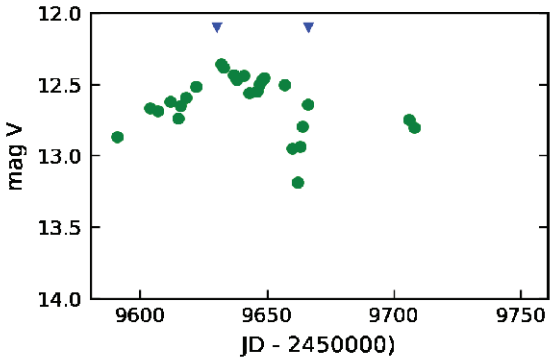

AAVSO V band lightcurve
ARAS Spectra: blue triangles

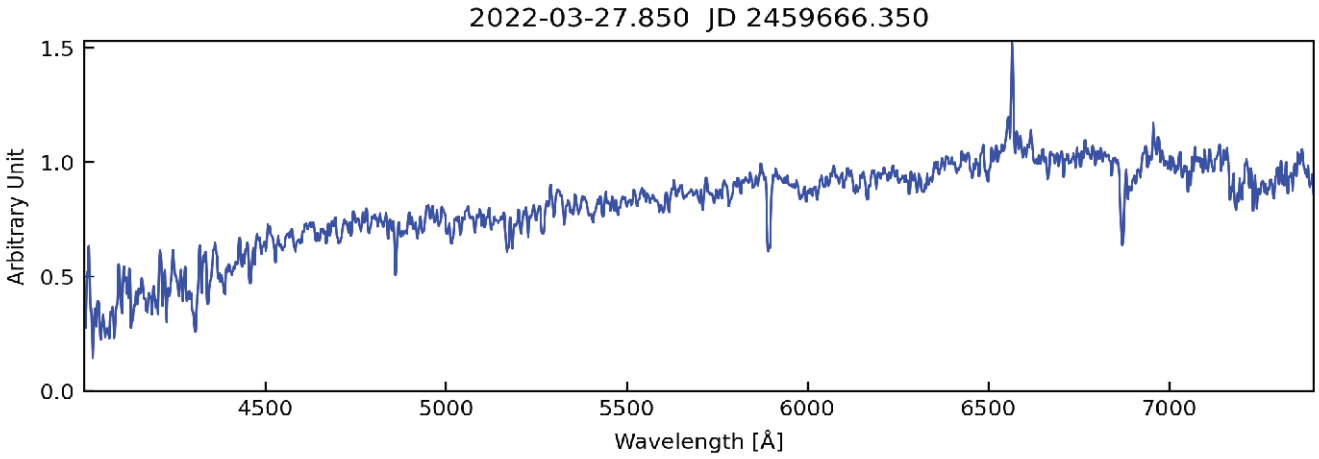

Observer: P. A. Dubovsky
Site: Kolonica Instrument: C14+LISA+Atik-460ex Resolution: 991

IV Vir

RA (2000)	14 16 34.29
DE (2000)	-21 45 50.04
Mag V	no data
	-

Yellow symbiotic star

Quiescent State

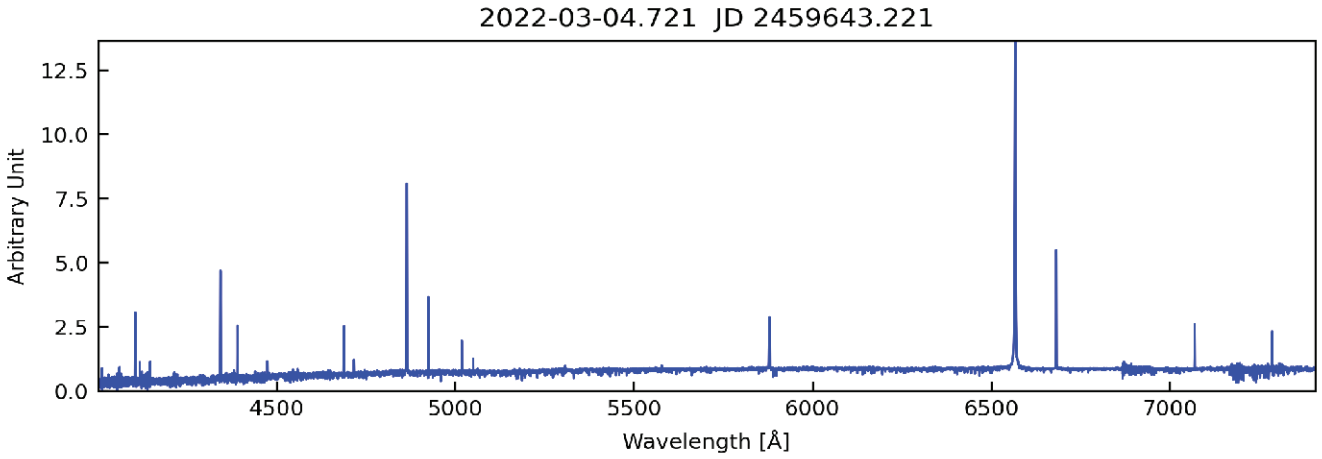

Observer: C. Eldridge
Site: Mardella Instrument: eShel on CDK-1000 Resolution: nan

NQ Gem

RA (2000)	07 31 54.52
DE (2000)	+24 30 12.54
Mag V	no data
	-

Low ionisation Symbiotic

Carbon M giant

H alpha in emission

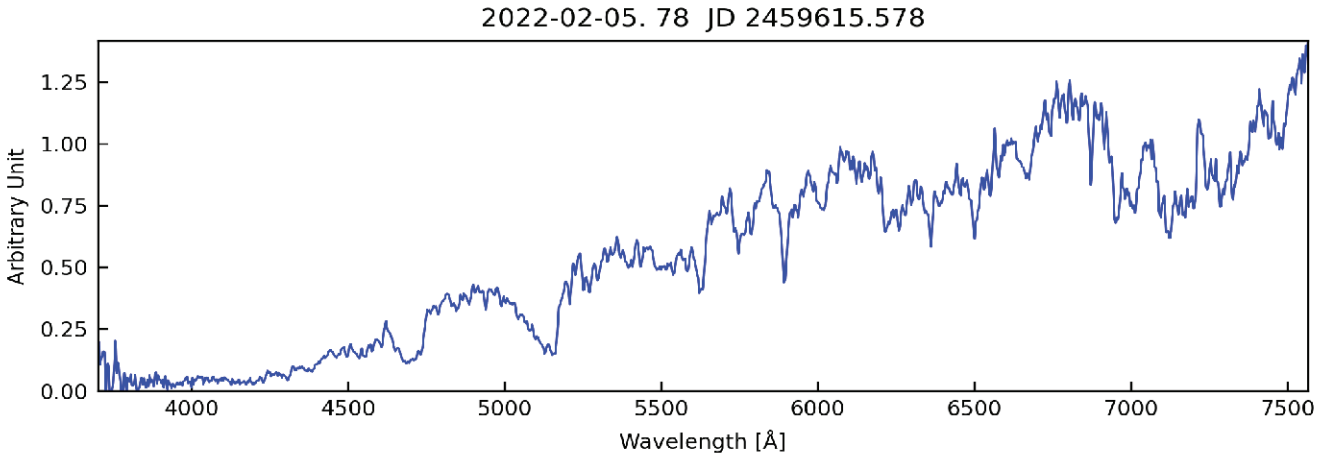

Observer: C. Boussin
Site: OCT-FR Instrument: N200mmF/5+Alpy600 Resolution: 528

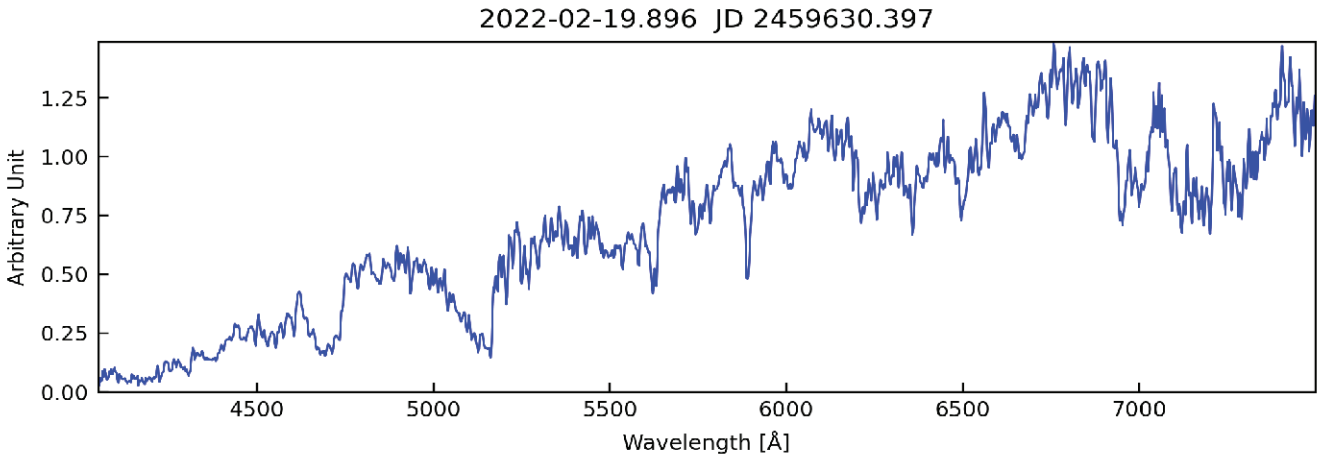

Observer: F. Boubault
Site: Saint-Jean-d'Illac Instrument: C8_LISA_ATIK414 Resolution: nan

omi Cet

RA (2000)	02 19 20.79
DE (2000)	-02 58 39.50
Mag V	8.31
Phot. Phase	0.41 - 0.95

Mira Symbiotic Star (in UV)

Mira declining
Mira near max Luminosity

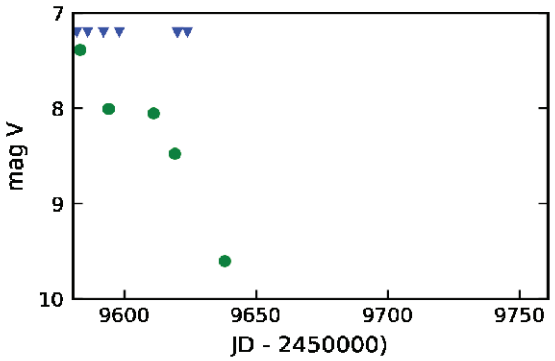

AAVSO V band lightcurve
ARAS Spectra: blue triangles

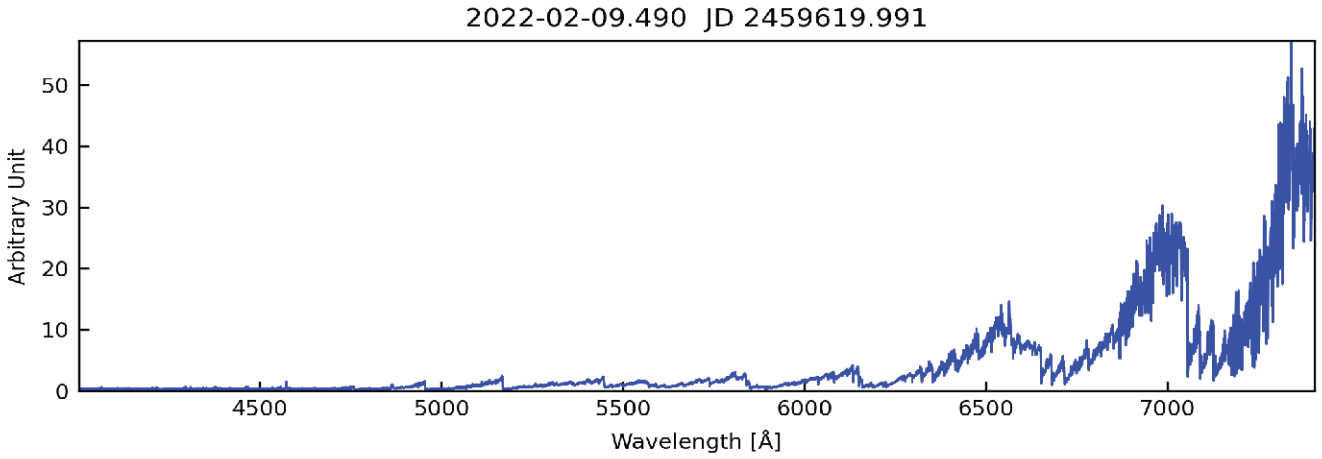

Observer: C. Eldridge
Site: Mardella Instrument: eShel on CDK-1000 Resolution: nan

RS Oph

RA (2000)	17 50 13.16
DE (2000)	-06 42 28.48
Mag V	11.5
	-

Recurrent Symbiotic Nova

Relaxing after the RN event in 2021
Orbital Variations

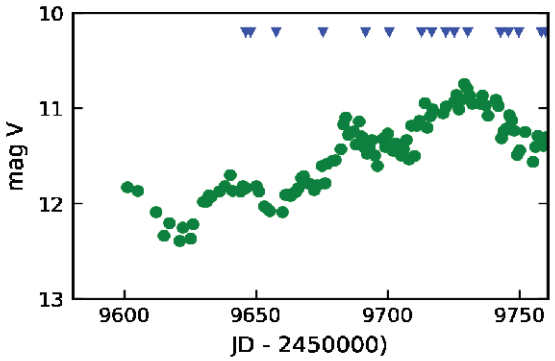

AAVSO V band lightcurve
ARAS Spectra: blue triangles

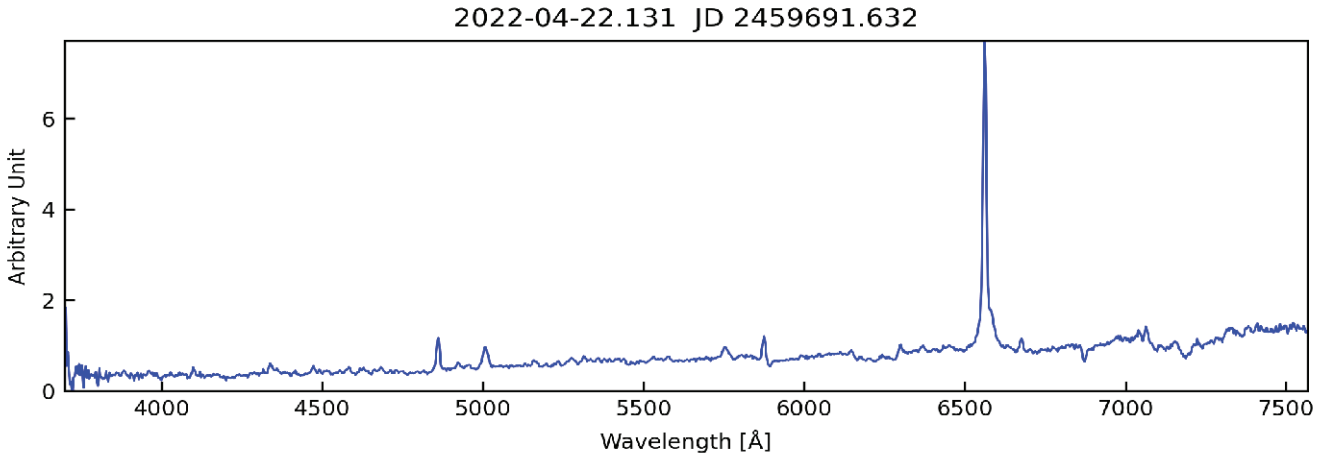

Observer: C. Boussin
Site: OCT-FR Instrument: N200mmF/5+Alpy600 Resolution: 523

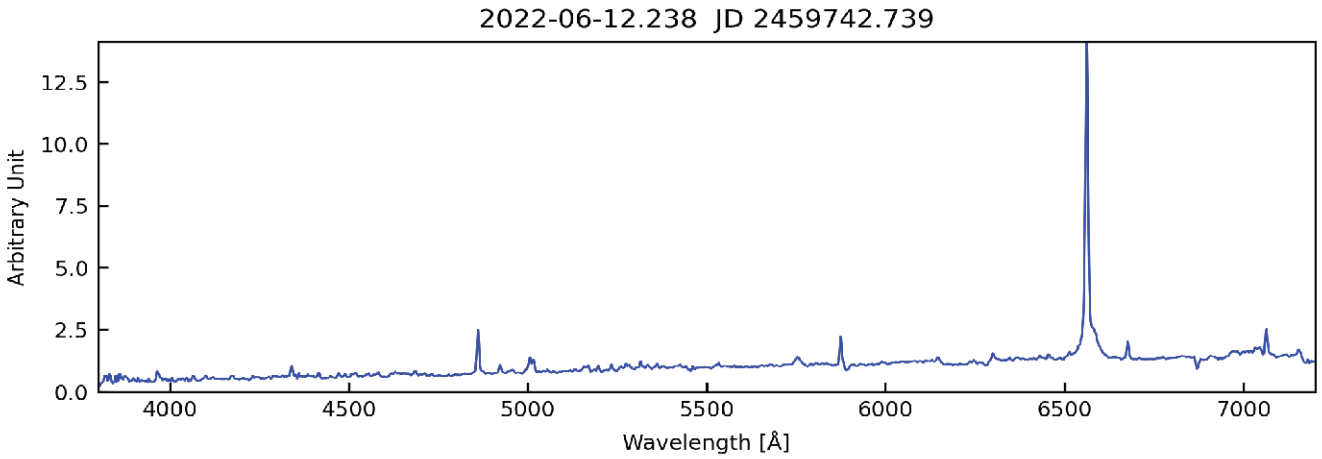

Observer: K. Shank
Site: Carrollton TX Instrument: C14E@F7.6+LISA+ATIK414EX Resolution: nan

RW Hya

RA (2000)	13 34 18.13
DE (2000)	-25 22 48.89
Mag V	no data
	-

Classical Symbiotic Star

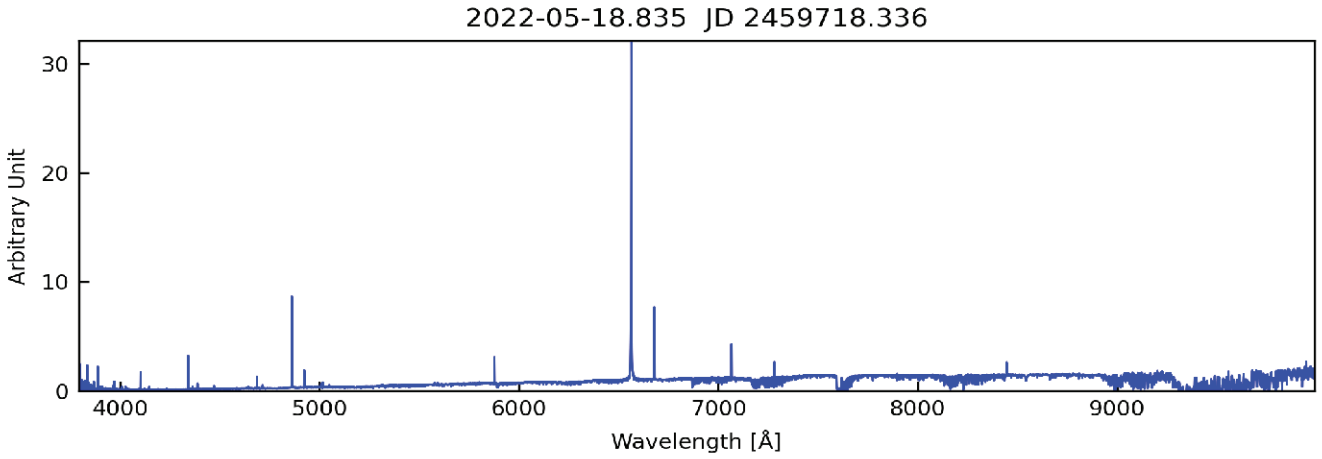

Observer: J. Guarro
Site: PIERA Instrument: PIERA Meade16 NOU_T ASI2600MM Resolution: 9000

SS Lep

RA (2000)	06 04 59.13
DE (2000)	-16 29 03.97
Mag V	4.99
	-

Peculiar Symbiotic

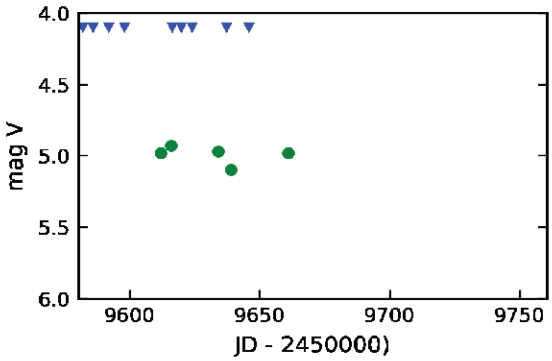

AAVSO V band lightcurve
ARAS Spectra: blue triangles

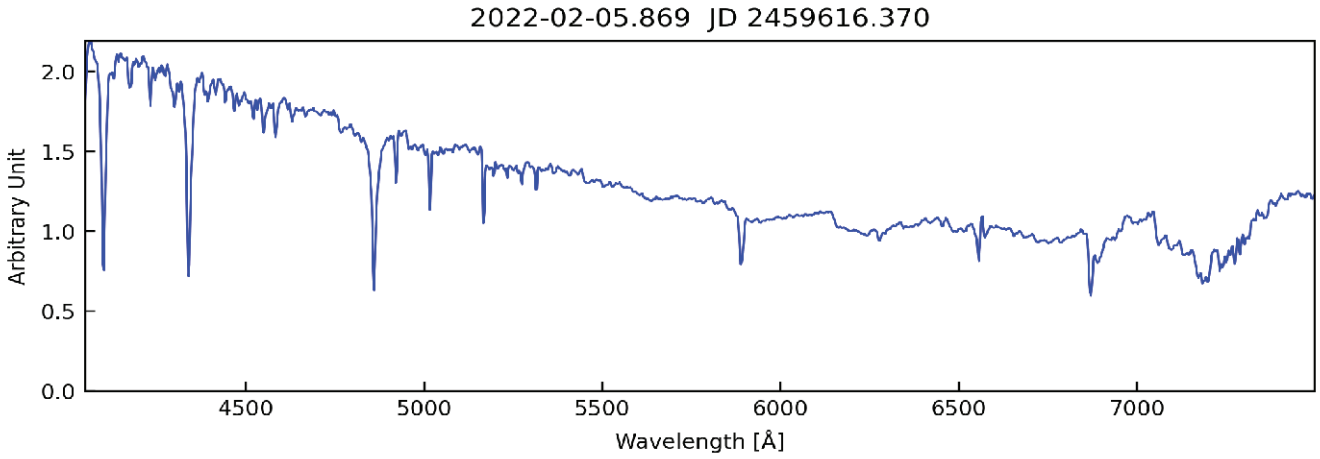

Observer: F. Boubault
Site: Saint-Jean-d'Illac Instrument: C8_LISA_ATIK414 Resolution: nan

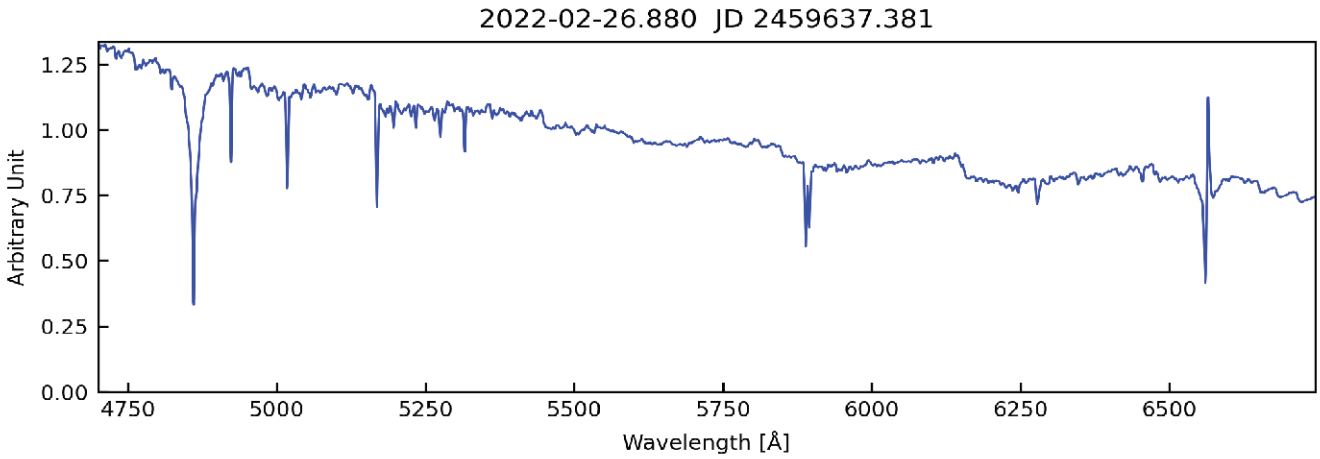

Observer: J. Michelet
Site: Claix Instrument: RC12-Uvex600-Atik460EX Resolution: nan

StHA 149

RA (2000)	18 18 55.87
DE (2000)	+27 26 27.73
Mag V	no data
	-

Classical Symbiotic Star

Quiescent State
Orbital Variations

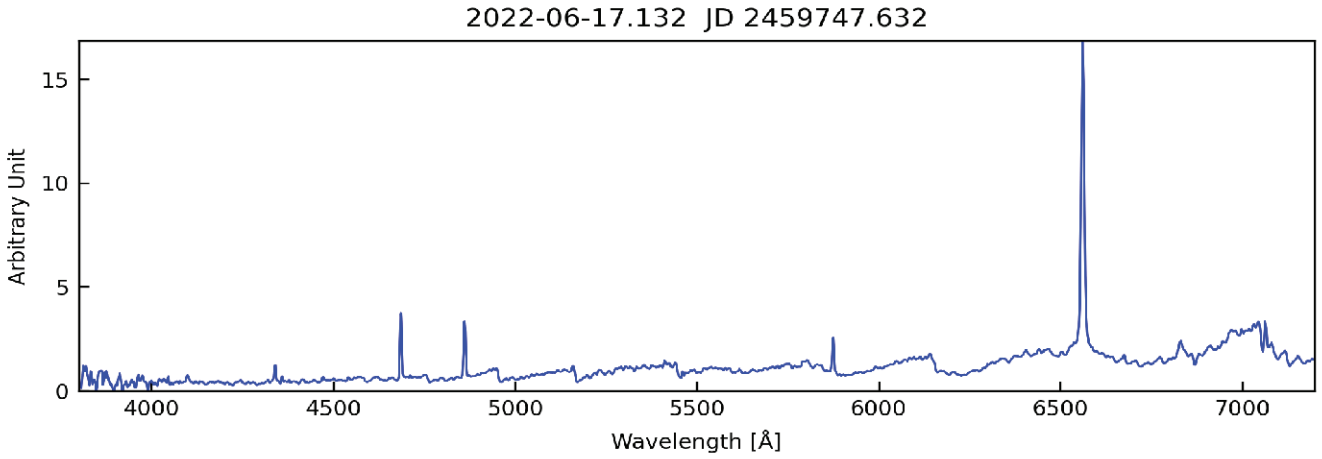

Observer: K. Shank
Site: Carrollton TX Instrument: C14E@F7.6+LISA+ATIK414EX Resolution: nan

StHA 32

RA (2000)	04 37 45.63
DE (2000)	-01 19 11.90
Mag V	no data
	-

Classical Symbiotic Star

Quiescent State
Orbital Variations

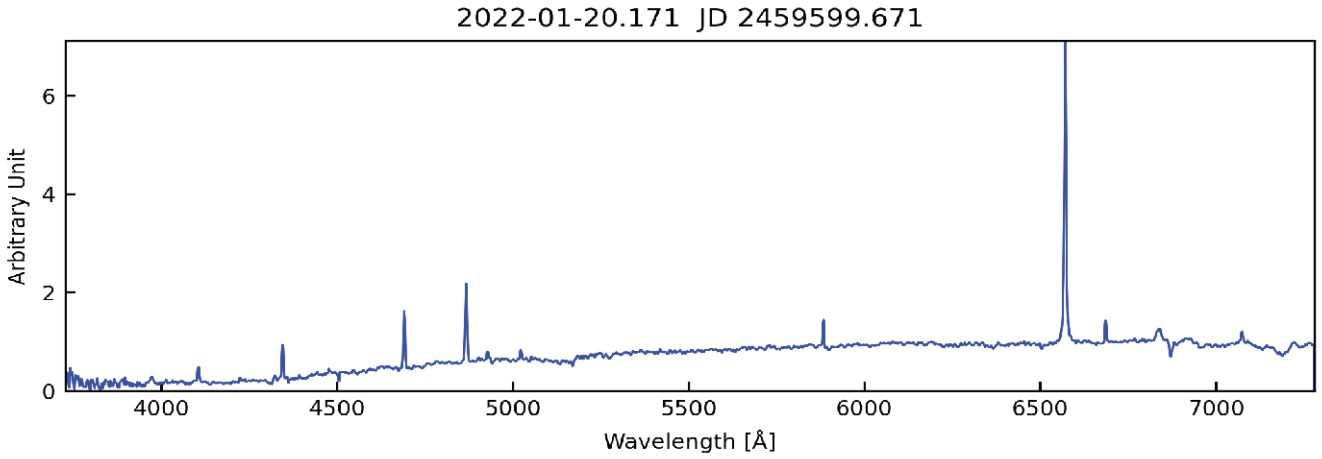

Observer: F. Sims
Site: Desert Celestial Observatory Instrument: CDK14 LISA Atik414ex Resolution: 962

StHA 55

RA (2000)	05 46 42.08
DE (2000)	+06 43 47.08
Mag V	no data
	-

Mira Symbiotic Star

H alpha in emission

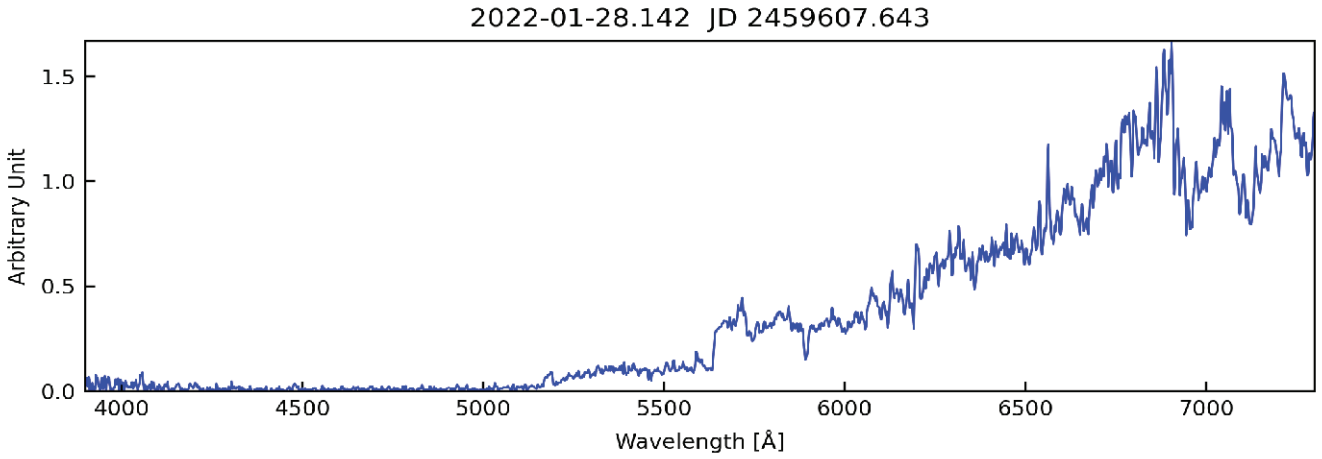

Observer: F. Sims
Site: Desert Celestial Observatory Instrument: CDK14 LISA Atik414ex Resolution: 1047

SU Lyn

RA (2000)	06 42 55.14
DE (2000)	+55 28 27.23
Mag V	8.56
	-

low ionization symbiotic

Quiescent State
No emission lines detected

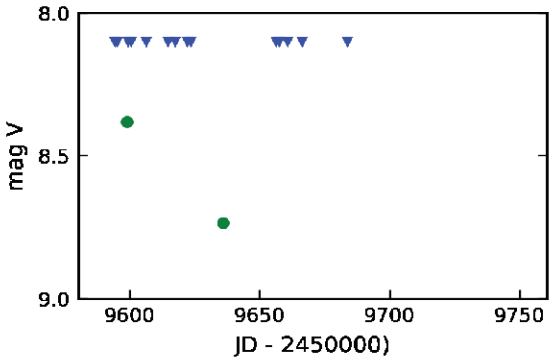

AAVSO V band lightcurve
ARAS Spectra: blue triangles

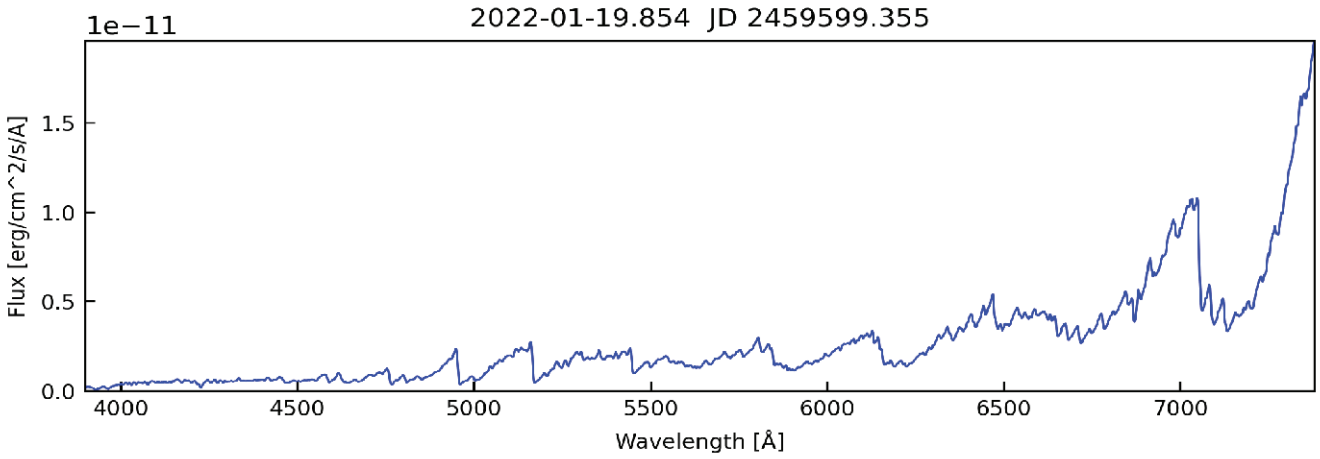

Observer: D. Boyd
Site: West Challow Observatory Instrument: C11 + LISA + SXVR-H694 Resolution: 1067

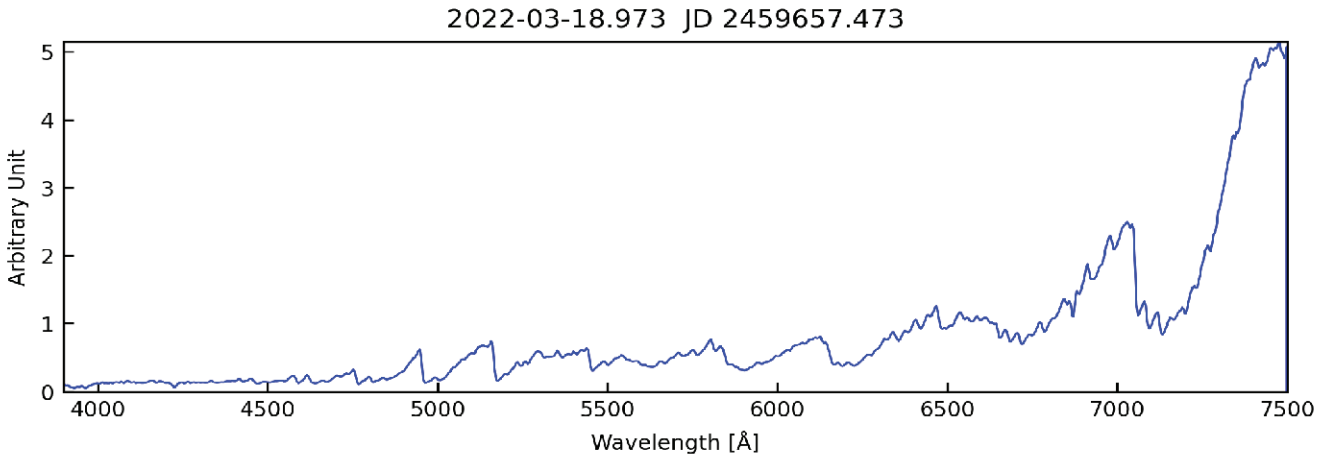

Observer: J.Coffin
Site: East Essex,UK Instrument: C8 0.7xFR + ALPY 600 + Atik 460EX Resolution: 556

SY Mus

RA (2000)	11 32 10.00
DE (2000)	-65 25 11.46
Mag V	11.22
	-

Classical Symbiotic Star

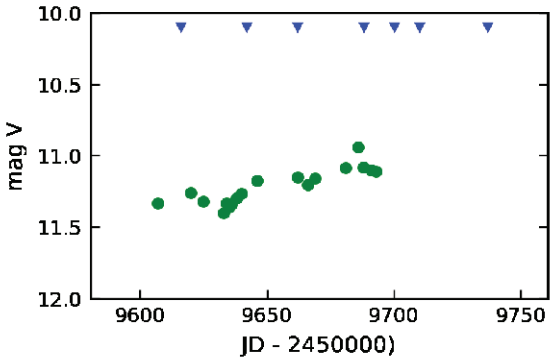

AAVSO V band lightcurve
ARAS Spectra: blue triangles

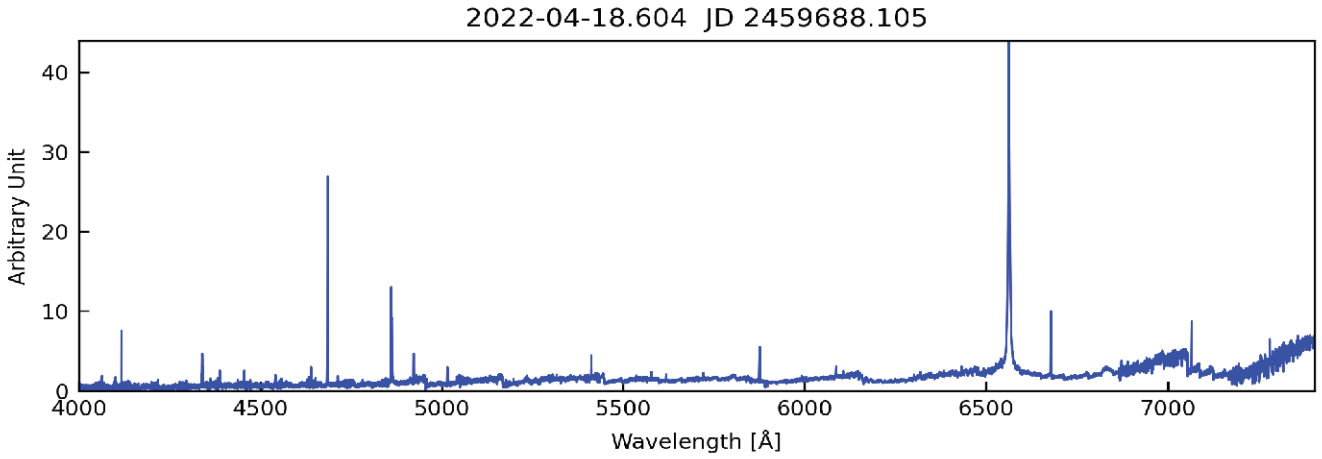

Observer: C. Eldridge
Site: Mardella Instrument: CDK1000-eShel-Atik-460ex Resolution: nan

T CrB

RA (2000)	15 59 30.16
DE (2000)	+25 55 12.61
Mag V	9.87
	-

Accretion powered Symbiotic

Recurrent Symbiotic Nova

Pre-outburst state
Balmer + He I + He II
Continuous monitoring before the next RN event

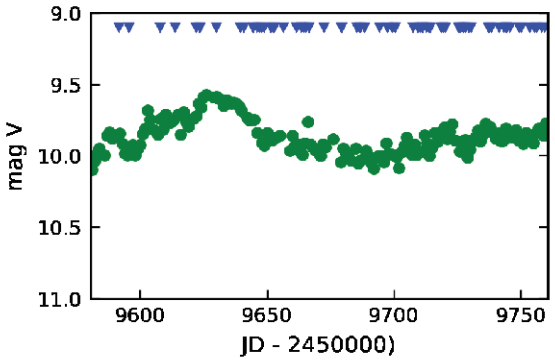

AAVSO V band lightcurve
ARAS Spectra: blue triangles

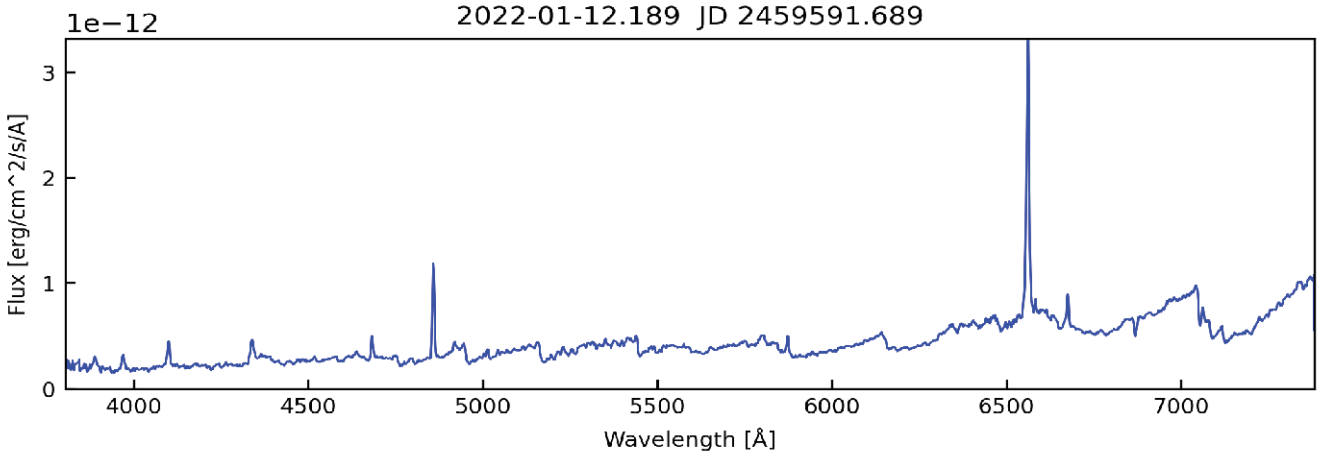

Observer: H. Boussier
Site: K21-FR_St_Saturnin Instrument: FLT110_LISA_ATIK414EX Resolution: 790

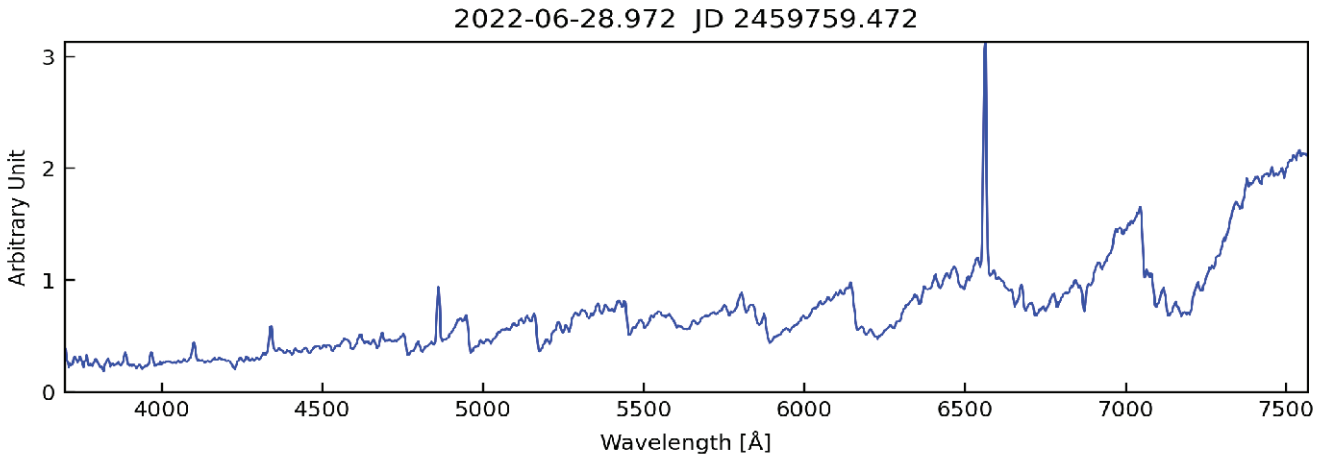

Observer: C. Boussin
Site: OCT-FR Instrument: N200mmF/5+Alpy600 Resolution: 542

TX CVn

RA (2000)	12 44 42.06
DE (2000)	+36 45 50.62
Mag V	9.97
	-

Low ionisation Symbiotic

H alpha in emission

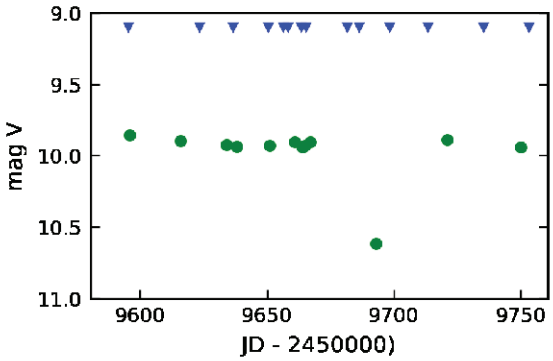

AAVSO V band lightcurve
ARAS Spectra: blue triangles

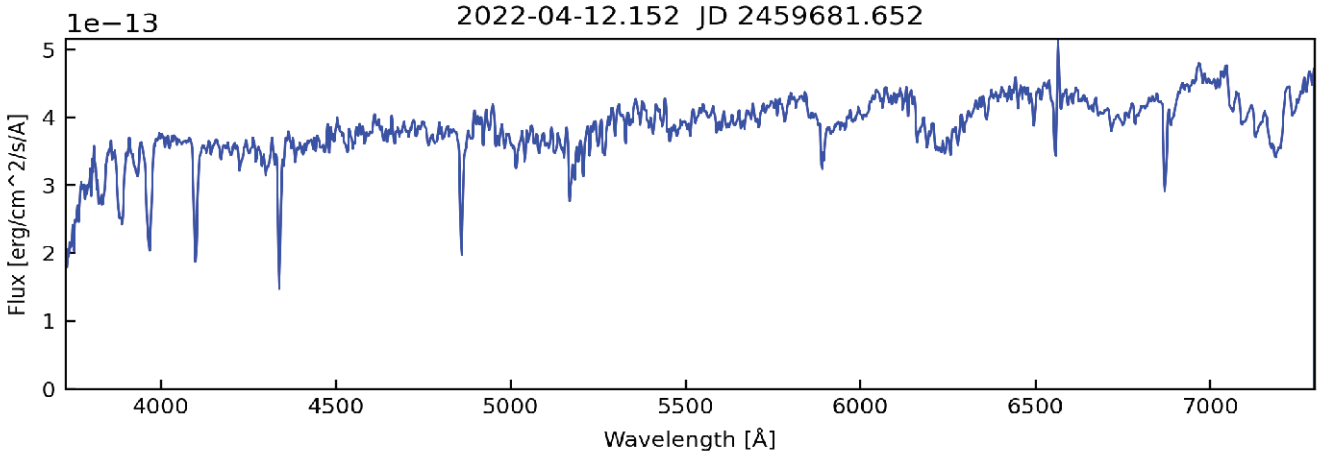

Observer: F. Sims
Site: Desert Celestial Observatory Instrument: CDK20 LISA Atik414ex Resolution: 1064

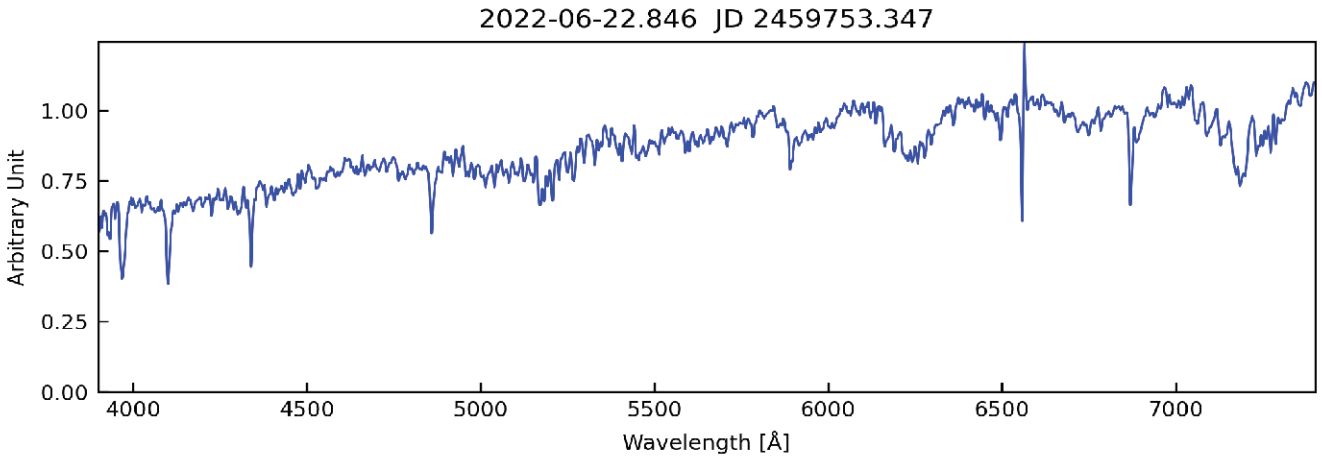

Observer: P. A. Dubovsky
Site: Kolonica Instrument: C14+LISA+Atik-460ex Resolution: 1134

UV Aur

RA (2000)	05 21 48.91
DE (2000)	+32 30 40.18
Mag V	8.21
Phot. Phase	0.04 - 0.49

Carbon Mira Symbiotic Star

Balmer lines in emission
Mira declining

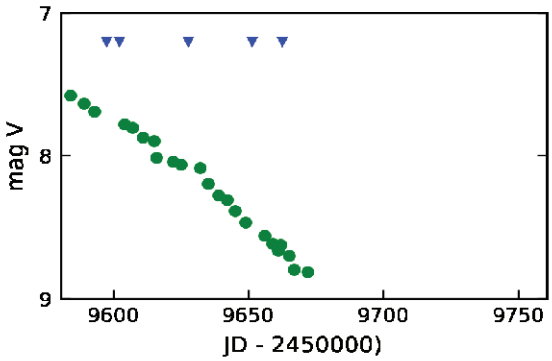

AAVSO V band lightcurve
ARAS Spectra: blue triangles

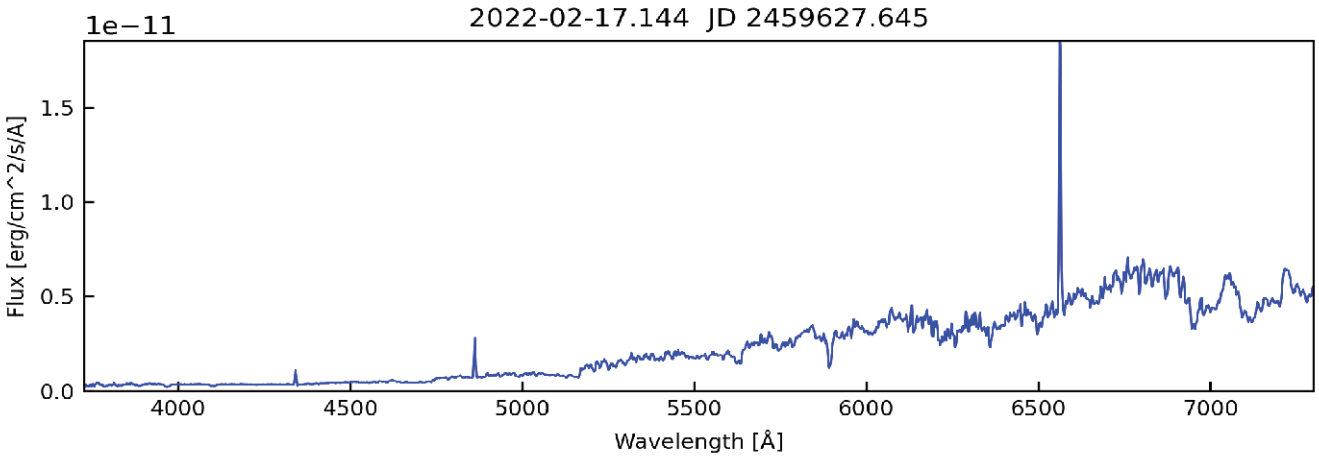

Observer: F. Sims
Site: Desert Celestial Observatory Instrument: CDK14 LISA Atik414ex Resolution: 1051

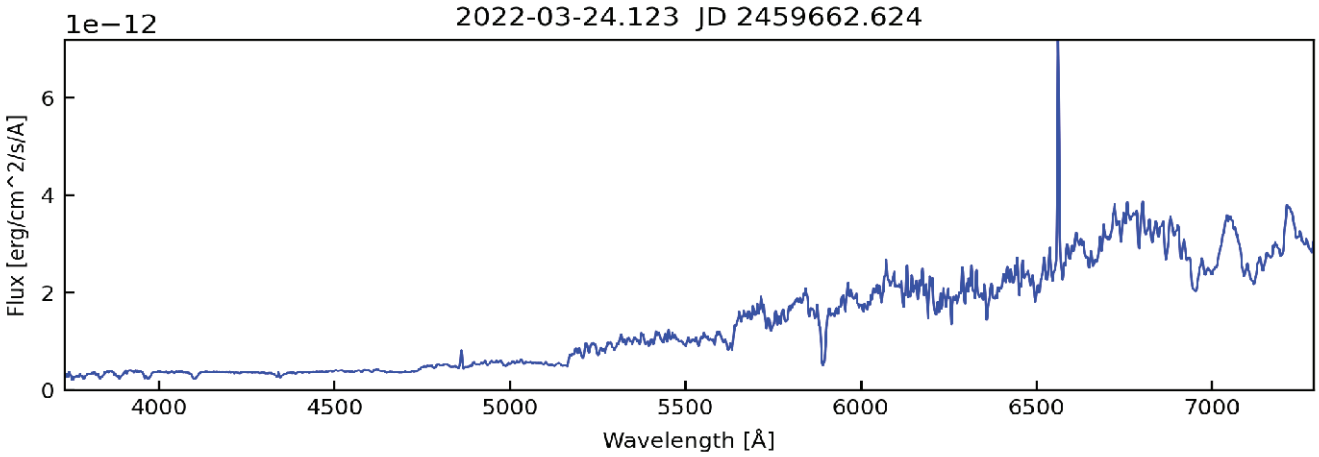

Observer: F. Sims
Site: Desert Celestial Observatory Instrument: CDK20 LISA Atik414ex Resolution: 946

V1016 Cyg

RA (2000)	19 57 05.02
DE (2000)	+39 49 36.09
Mag V	11.96
	-

Symbiotic Nova (1964)

Nebular emission spectrum
Nova Outburst

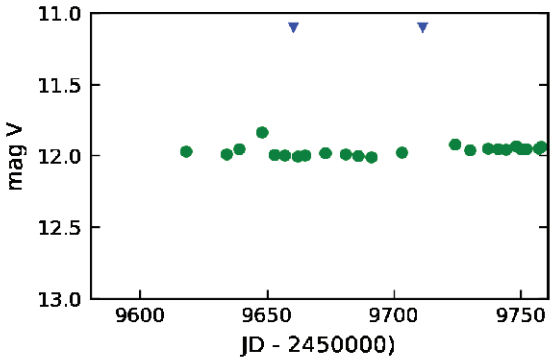

AAVSO V band lightcurve
ARAS Spectra: blue triangles

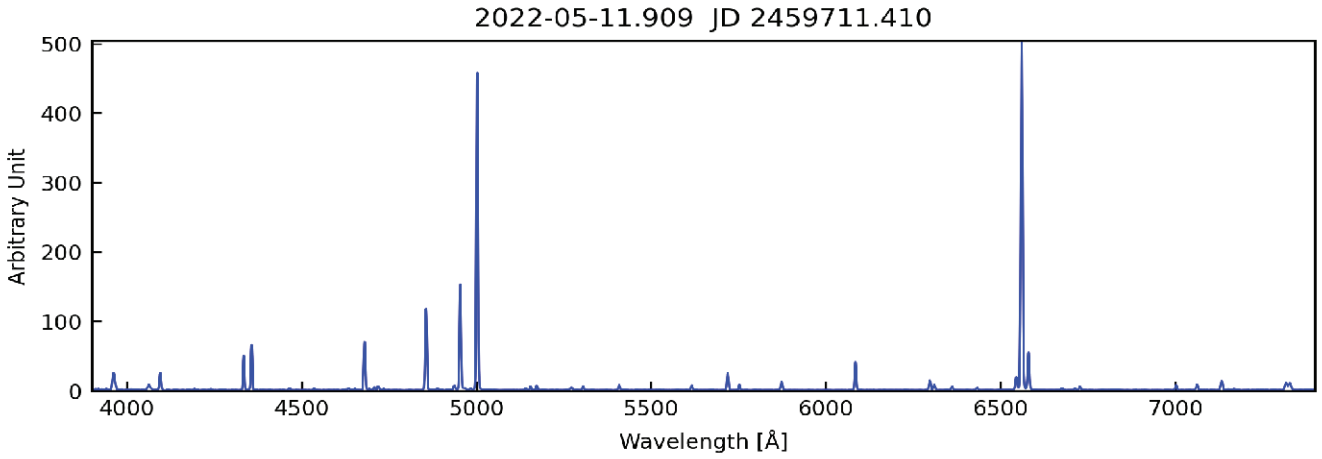

Observer: P. A. Dubovsky
Site: Kolonica Instrument: C14+LISA+Atik-460ex Resolution: 1037

V1261 Ori

RA (2000)	05 22 18.65
DE (2000)	-08 39 58.05
Mag V	no data
Orb. phase	0.97 - 0.26

Symbiotic in UV

Nebular emission spectrum
Quiescent State
No emission lines detected

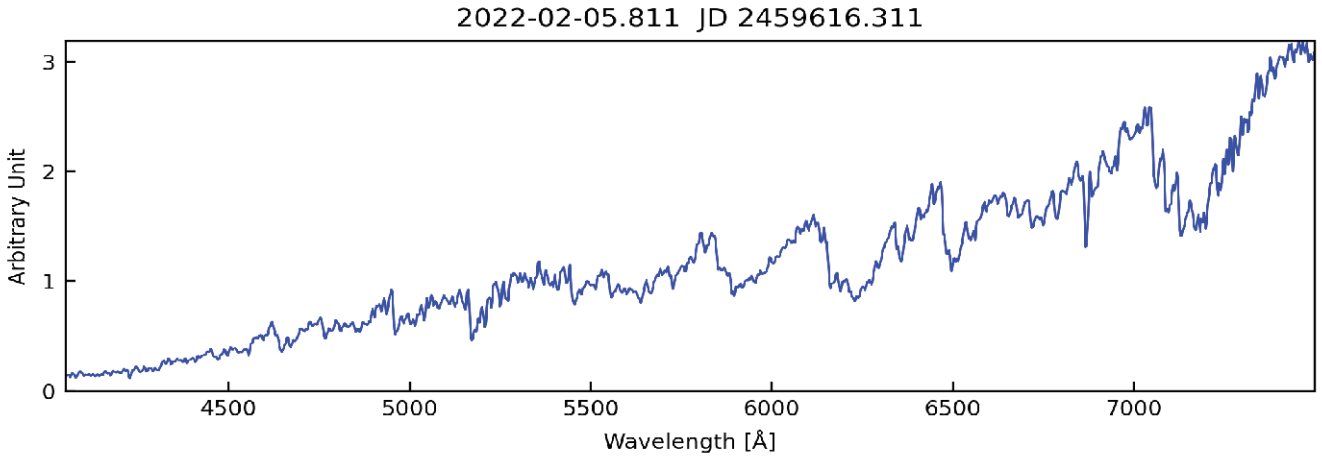

Observer: F. Boubault
Site: Saint-Jean-d'Illac Instrument: C8_LISA_ATIK414 Resolution: nan

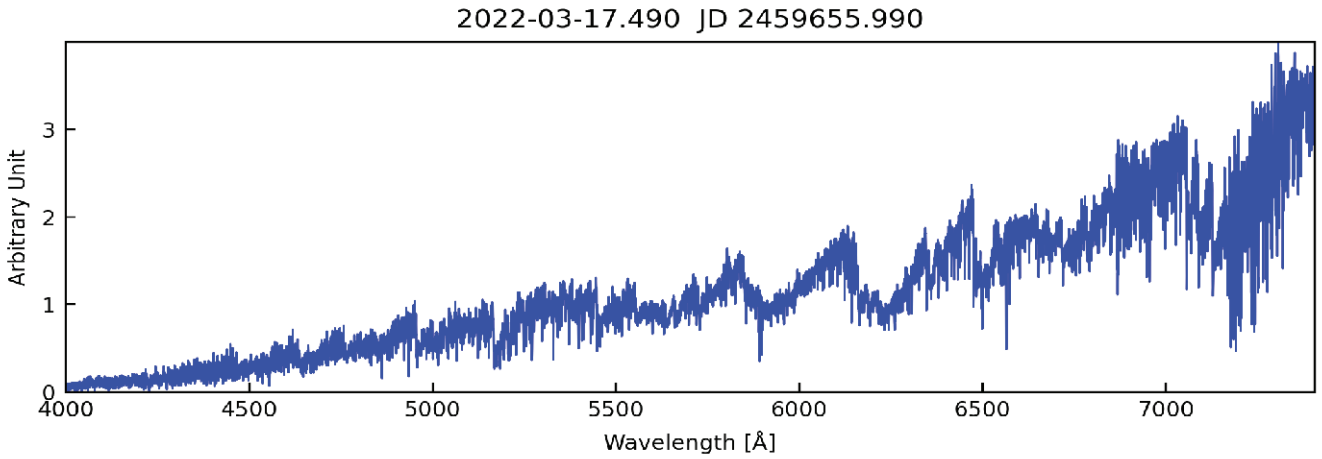

Observer: C. Eldridge
Site: Mardella Instrument: CDK1000-eShel-Atik-460ex Resolution: nan

V1413 Aql

RA (2000)	19 03 46.84
DE (2000)	+16 26 16.97
Mag V	12.31
	-

Classical Symbiotic Star

Nebular emission spectrum
Low ionization He II absent

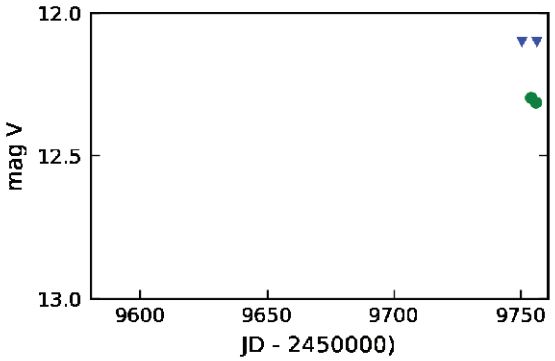

AAVSO V band lightcurve
ARAS Spectra: blue triangles

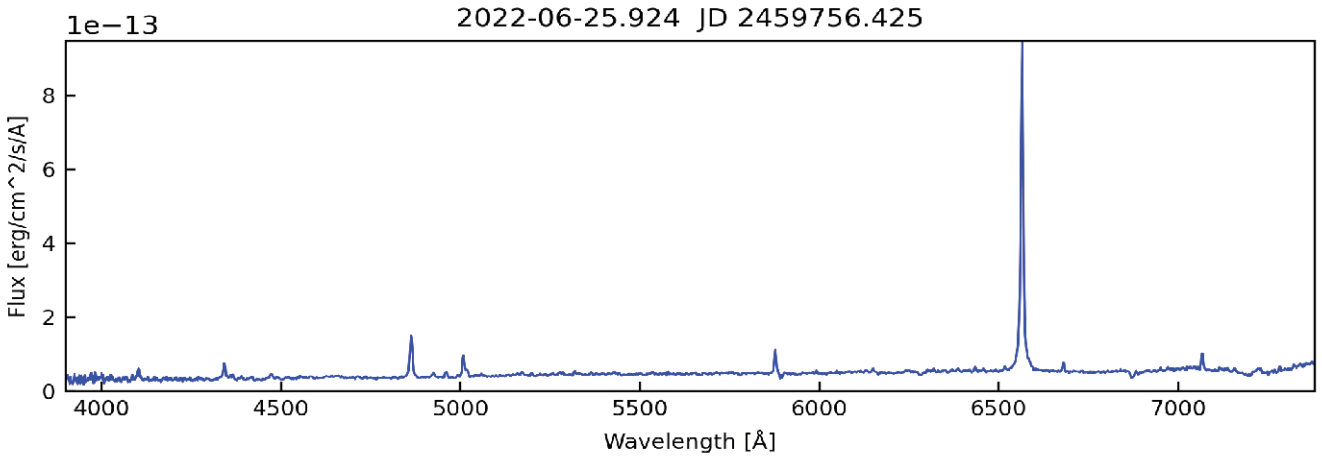

Observer: D. Boyd
Site: West Challow Observatory Instrument: C11 + LISA + SXVR-H694 Resolution: 1132

V399 Pav

RA (2000)	19 42 25.38
DE (2000)	-68 07 35.34
Mag V	no data
	-

Classical Symbiotic Star

Orbital Variations

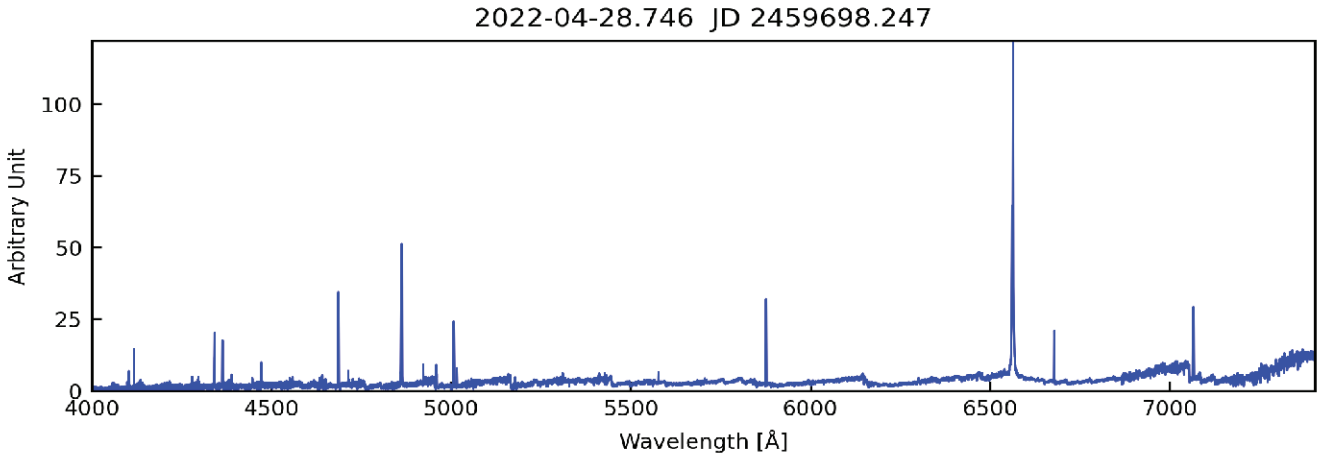

Observer: C. Eldridge
Site: Mardella Instrument: eShel on CDK-1000 Resolution: nan

V417 CMa

RA (2000)	06 59 11.30
DE (2000)	-29 02 05.15
Mag V	no data
	-

Low SNR

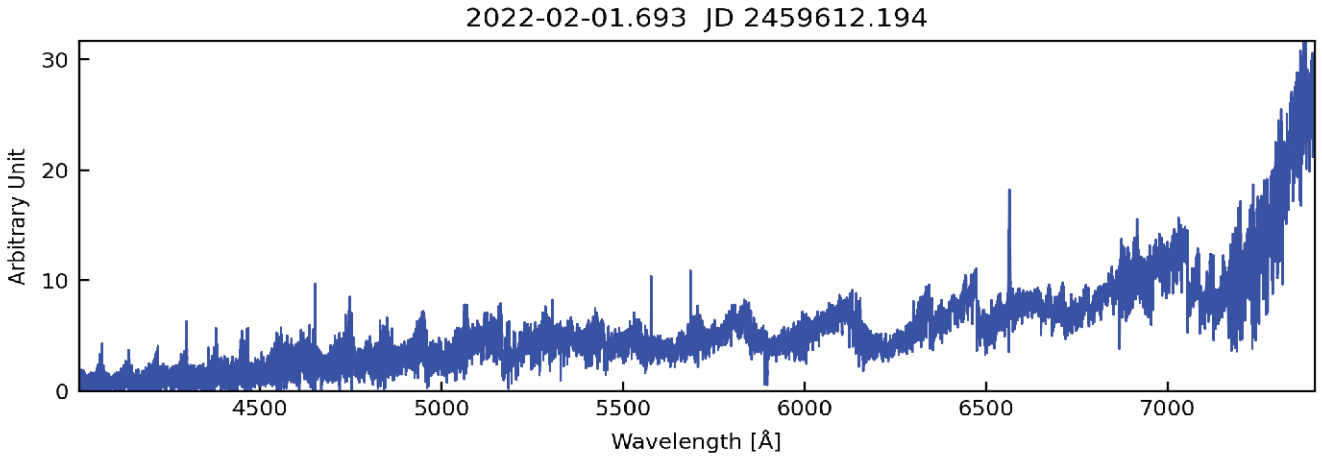

Observer: C. Eldridge
Site: Mardella Instrument: CDK1000-eShel-Atik-460ex Resolution: nan

V443 Her

RA (2000)	18 22 07.85
DE (2000)	+23 27 19.93
Mag V	11.44
	-

Classical Symbiotic Star

Quiescent State
Orbital Variations

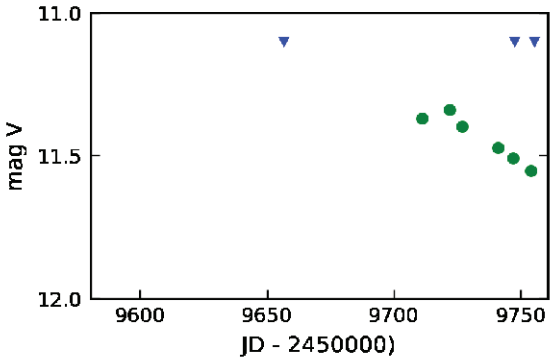

AAVSO V band lightcurve
ARAS Spectra: blue triangles

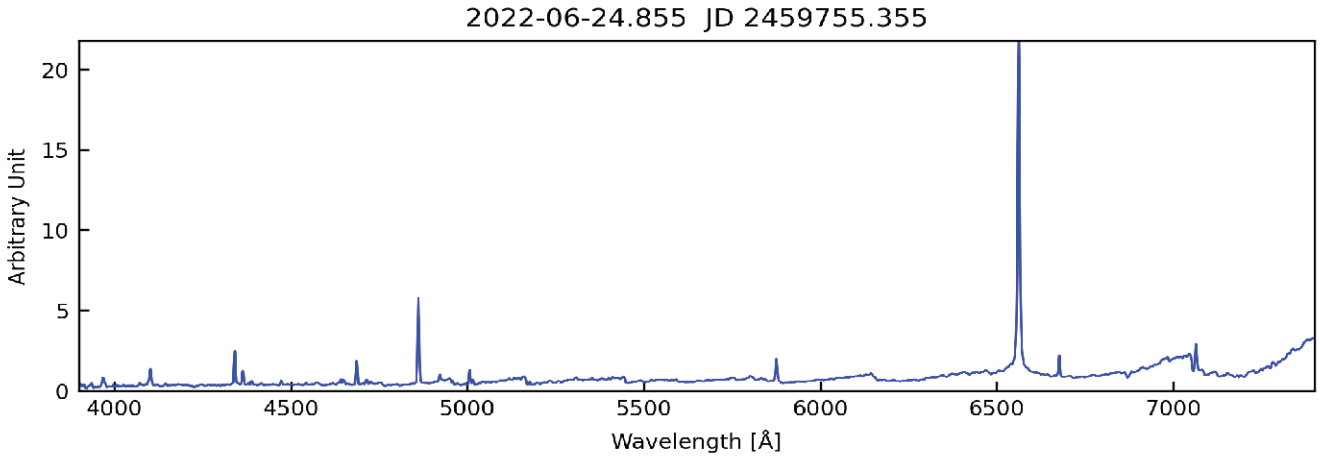

Observer: P. A. Dubovsky
Site: Kolonica Instrument: C14+LISA+Atil460ex Resolution: 1024

V471 Per

RA (2000)	01 58 49.66
DE (2000)	+52 53 48.46
Mag V	13.02
	-

Yellow Symbiotic Star

Quiescent State
Orbital Variations

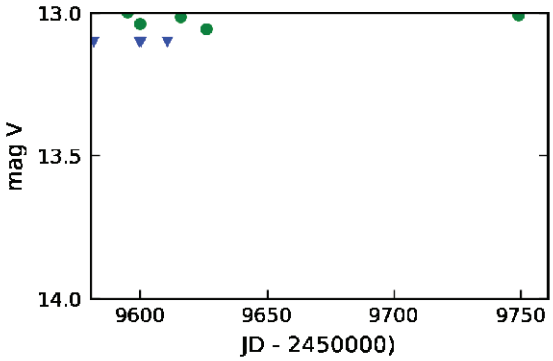

AAVSO V band lightcurve
ARAS Spectra: blue triangles

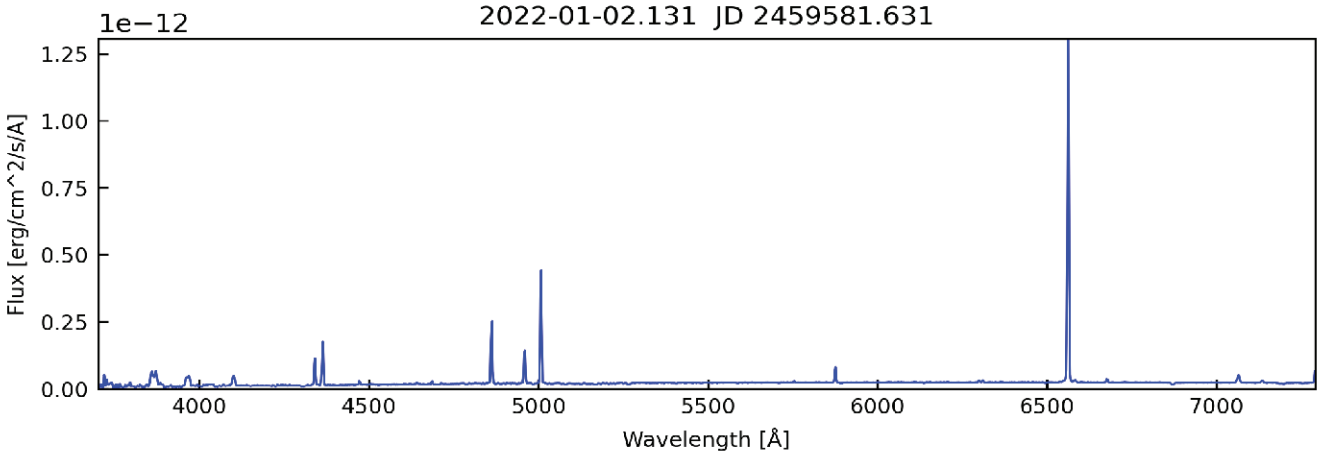

Observer: F. Sims
Site: Desert Celestial Observatory Instrument: CDK14 LISA Atik414ex Resolution: 995

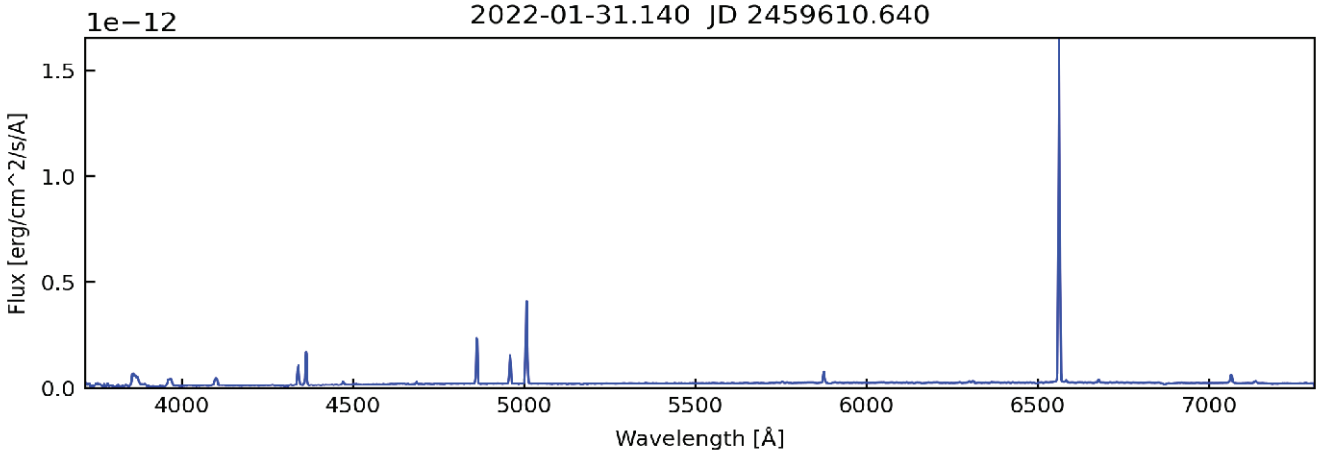

Observer: F. Sims
Site: Desert Celestial Observatory Instrument: CDK14 LISA Atik414ex Resolution: 1024

V503 Her

RA (2000)	17 36 40.46
DE (2000)	+23 18 11.67
Mag V	12.36
	-

Suspected Symbiotic Star

Quiescent State
No emission lines detected

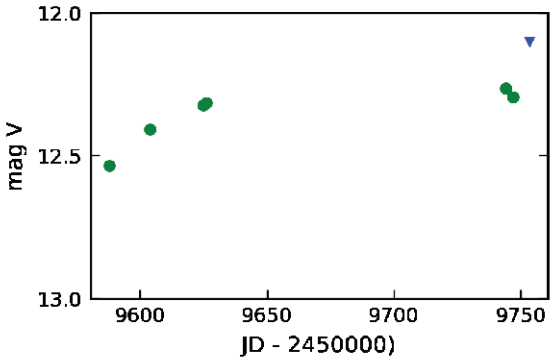

AAVSO V band lightcurve
ARAS Spectra: blue triangles

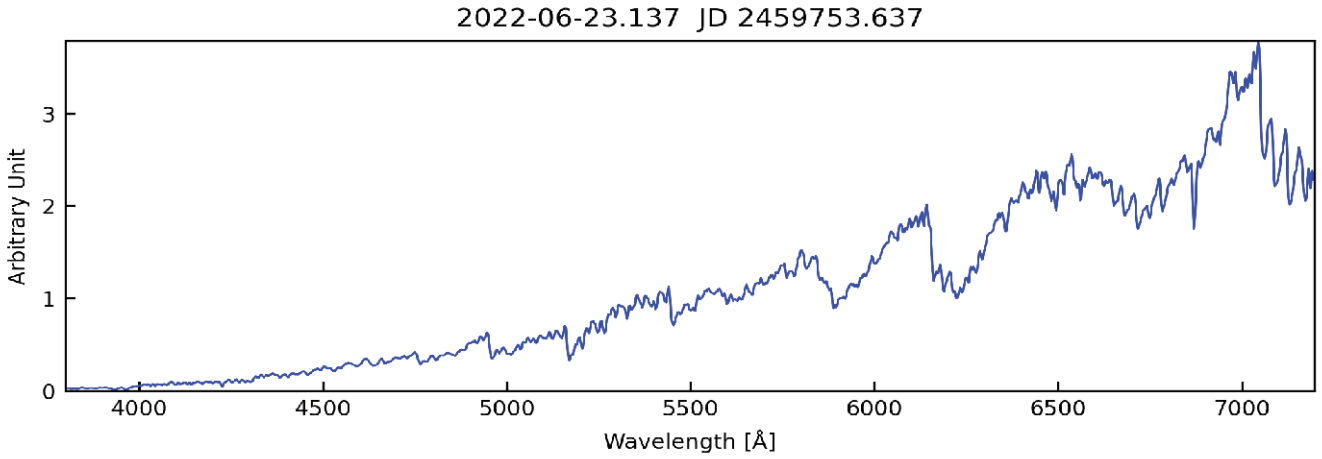

Observer: K. Shank
Site: Carrollton TX Instrument: C14E@F7.6+LISA+SX Tirus825M Pro Resolution: nan

V648 Car

RA (2000)	10 11 02.94
DE (2000)	-57 48 13.94
Mag V	no data
	-

Low ionisation symbiotic star

Weak He I 5876
Balmer lines in emission

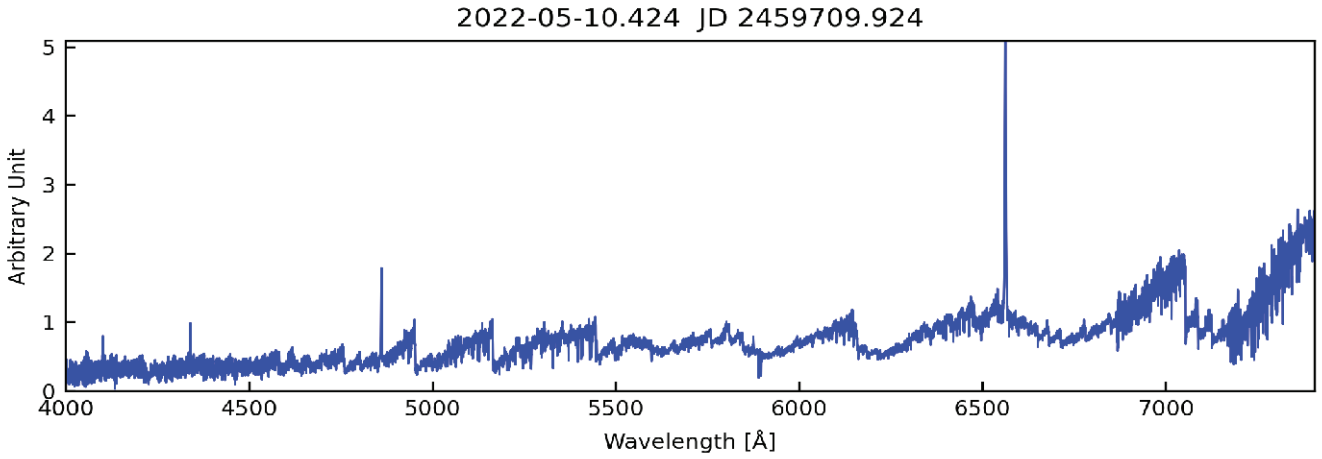

Observer: C. Eldridge
Site: Mardella Instrument: CDK1000-eShel-Atik-460ex Resolution: nan

V694 Mon

RA (2000)	07 25 51.28
DE (2000)	-07 44 08.08
Mag V	8.37
	-

Accretion Powered Symbiotic

Peculiar

Low State
H alpha in emission

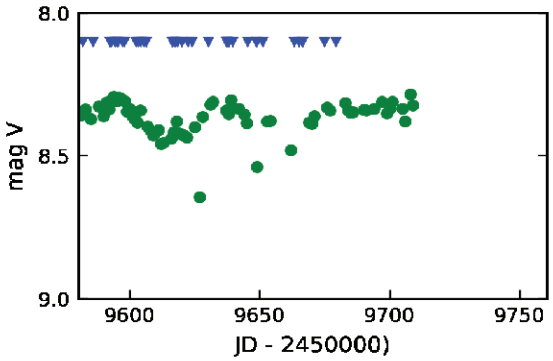

AAVSO V band lightcurve
ARAS Spectra: blue triangles

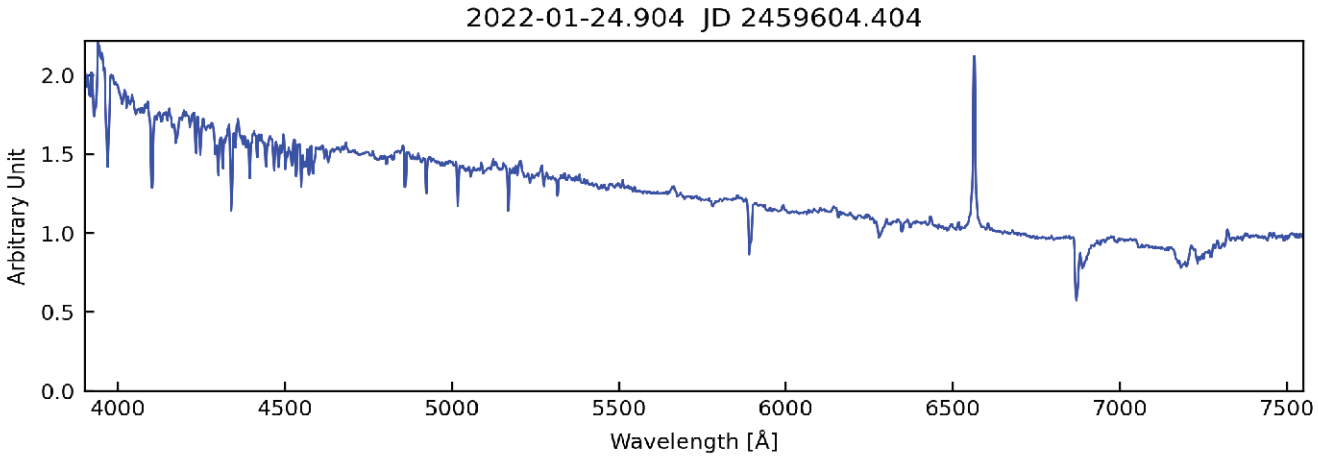

Observer: T. Medulka
Site: Kolonica Instrument: C14+LISA+Atik-460ex Resolution: 807

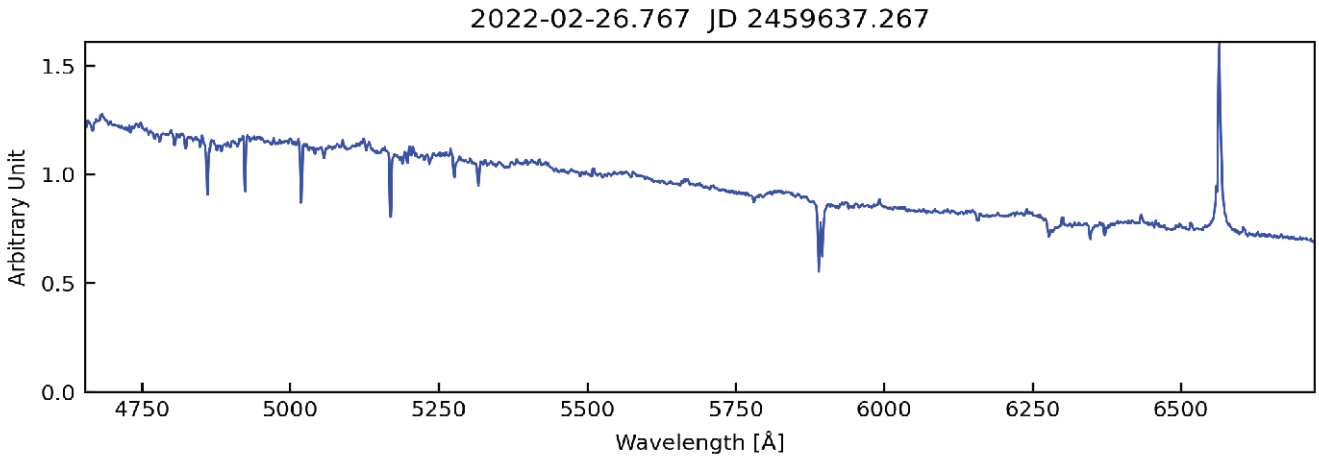

Observer: J. Michelet
Site: Claix Instrument: RC12-Uvex600-Atik460EX Resolution: nan

V917 Sco

RA (2000)	17 48 04.28
DE (2000)	-36 08 17.32
Mag V	no data
	-

Classical Symbiotic Star

Quiescent State
Orbital Variations

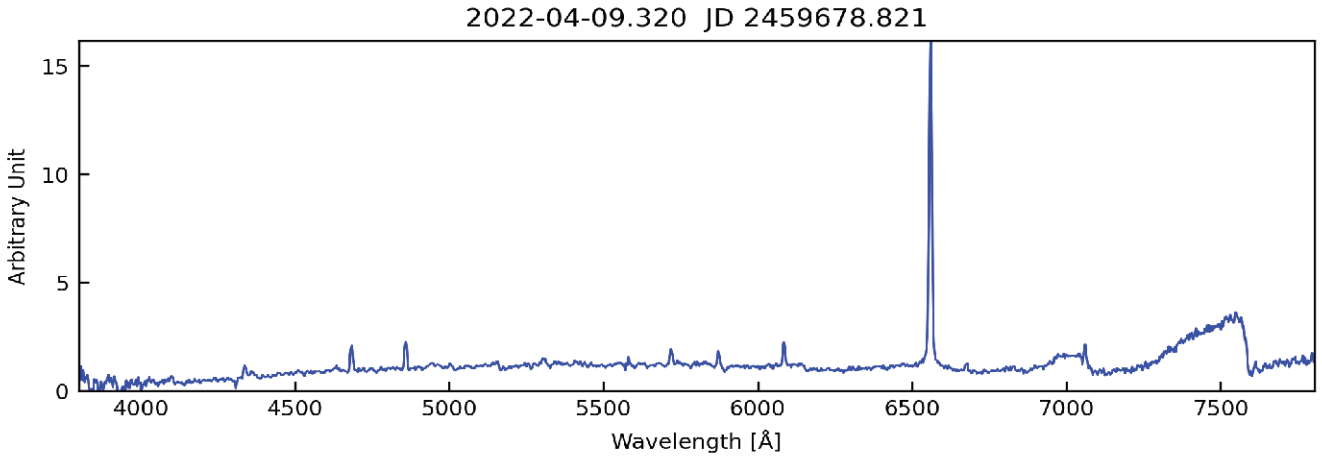

Observer: 2SPOT
Site: DSC Chile Instrument: RC12-Alpy-ATIK414Ex Resolution: 561

WRAY 15-1167

RA (2000)	14 03 18.64
DE (2000)	-58 09 34.92
Mag V	13.53
	-

Classical Symbiotic Star

Outburst

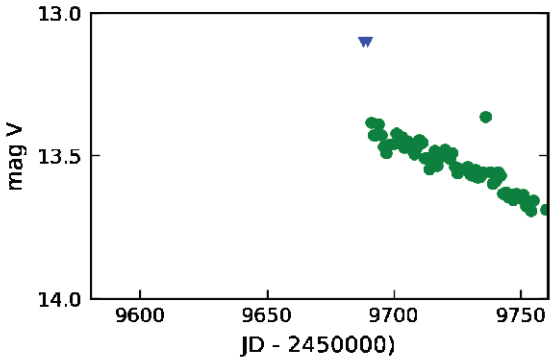

AAVSO V band lightcurve
ARAS Spectra: blue triangles

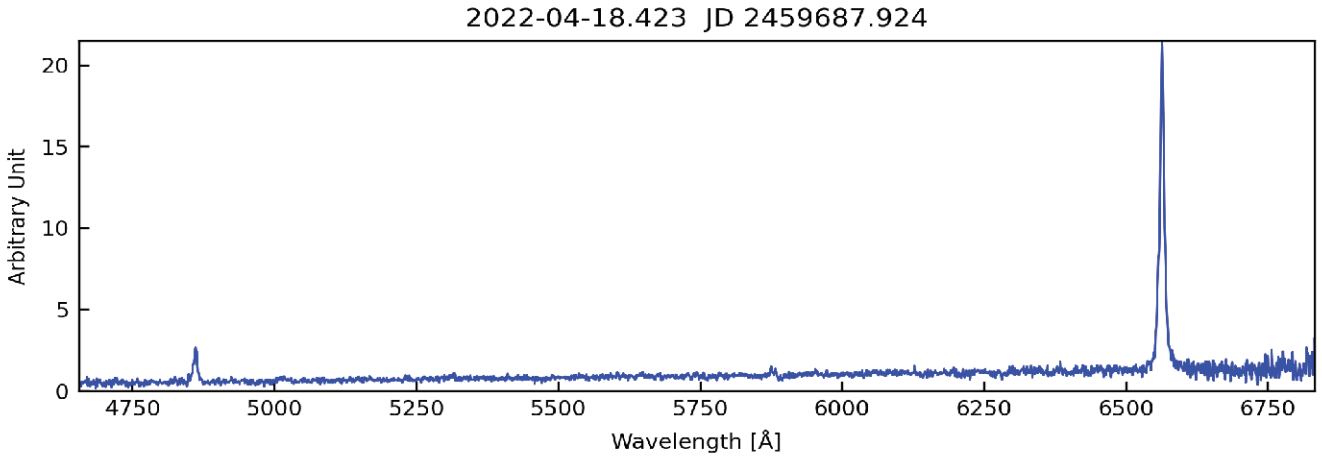

Observer: P. Velez
Site: iTelescope Facility, SSO, Australia Instrument: UVEX 600lines PW CDK 12.5 ASI183MM Resolution: 1371

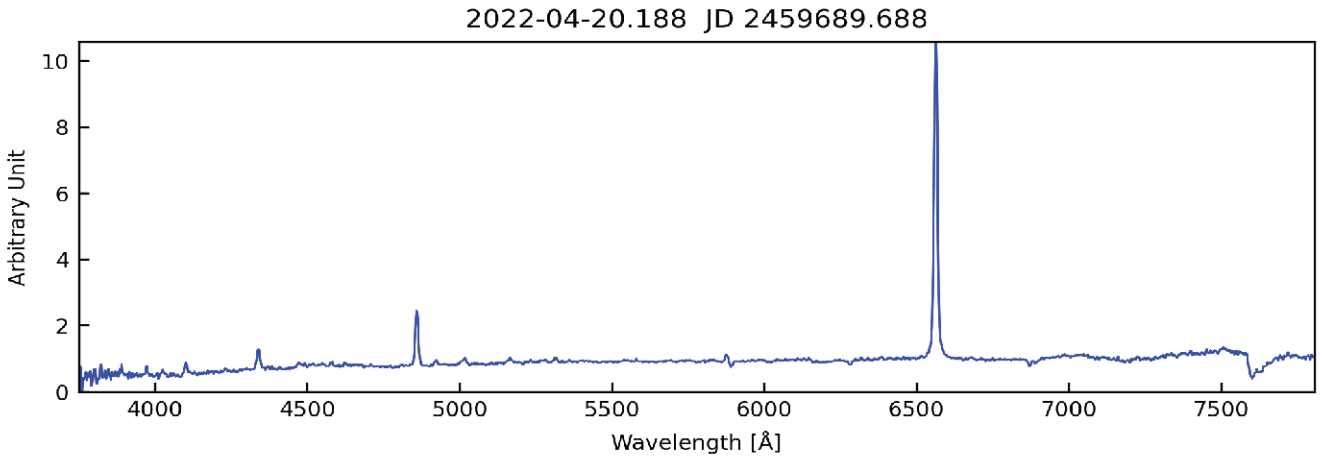

Observer: 2SPOT
Site: DSC Chile Instrument: RC12-Alpy-ATIK414Ex Resolution: 567

WY Vel

RA (2000)	09 21 59.13
DE (2000)	-52 33 51.65
Mag V	7.04
	-

Low ionization state
Rich metal lines emission spectrum

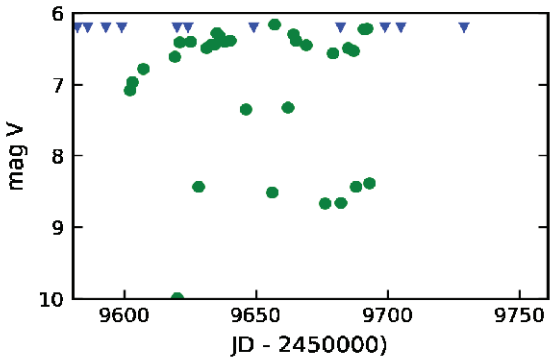

AAVSO V band lightcurve
ARAS Spectra: blue triangles

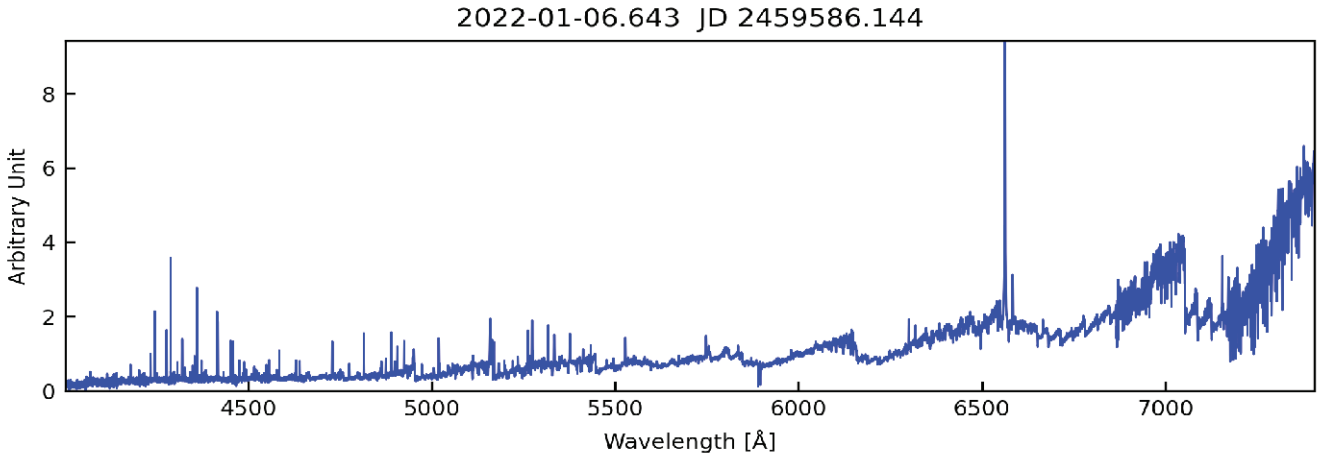

Observer: C. Eldridge
Site: Mardella Instrument: eShel on CDK-1000 Resolution: nan

YY Her

RA (2000)	18 14 34.19
DE (2000)	+20 59 21.19
Mag V	12.66
	-

Classicla Symbiotic Star

Quiescent State
Orbital Variations

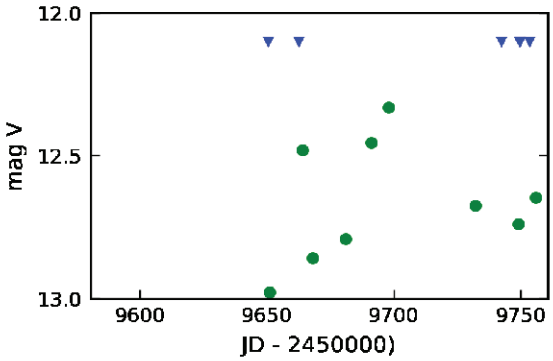

AAVSO V band lightcurve
ARAS Spectra: blue triangles

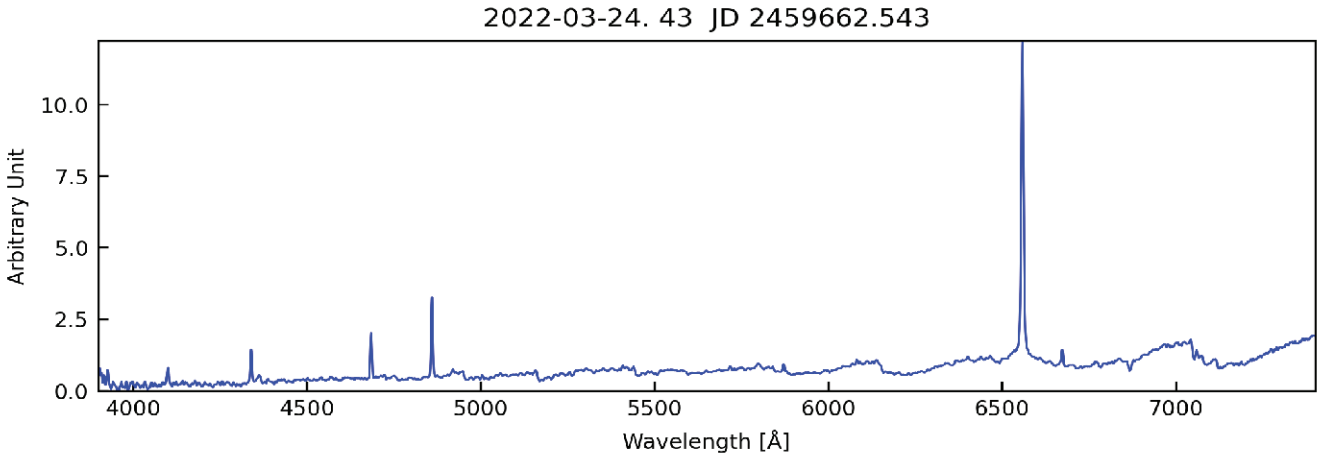

Observer: P. A. Dubovsky
Site: Kolonica Instrument: C14+LISA+Atik-460ex Resolution: 947

Z And

RA (2000)	23 33 39.96
DE (2000)	+48 49 05.97
Mag V	10.62
	-

Prototypical Symbiotic Star (in GCVS)

Quiescent State
Orbital Variations

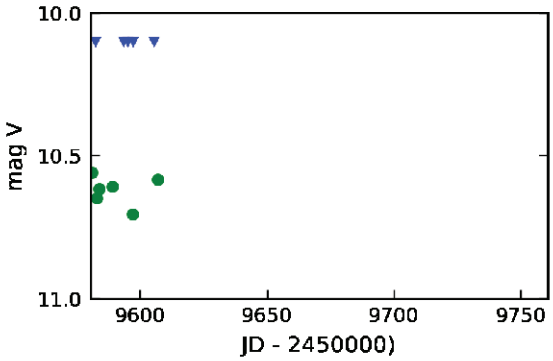

AAVSO V band lightcurve
ARAS Spectra: blue triangles

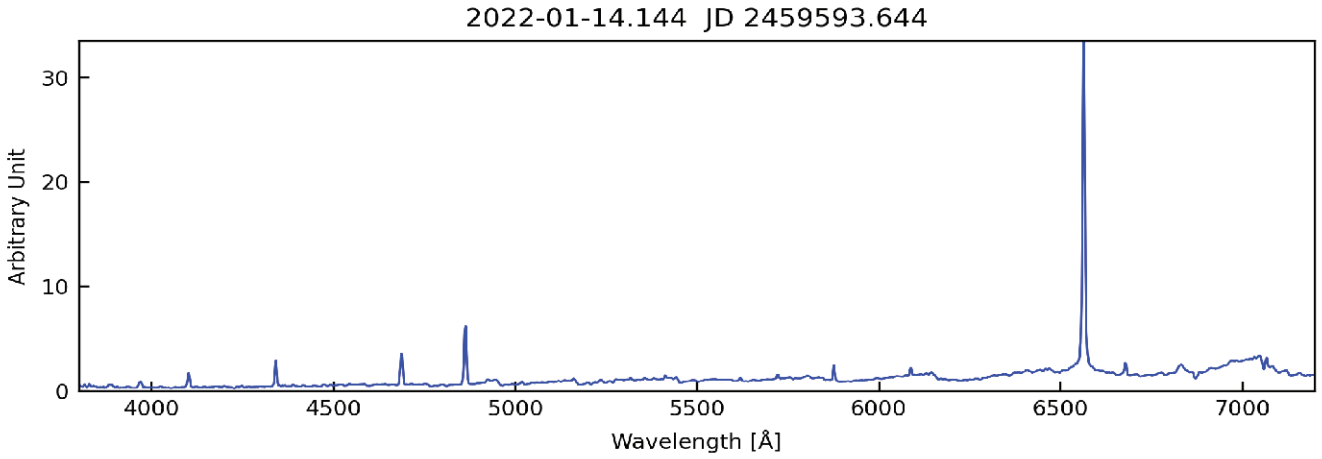

Observer: K. Shank
Site: Carrollton TX Instrument: C14E@F7.6+LISA+SX Tirus825M Pro Resolution: 0

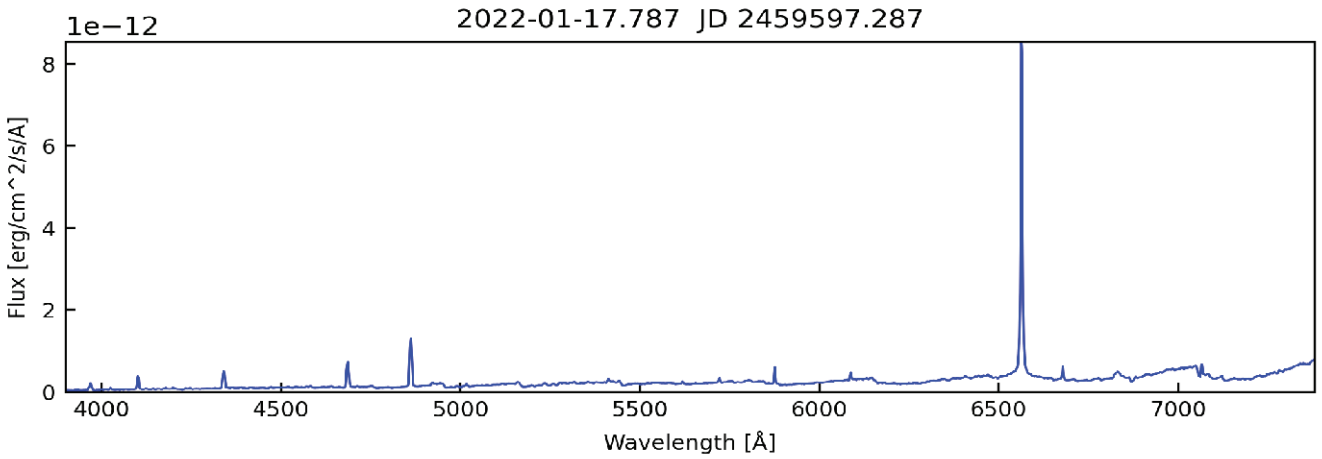

Observer: D. Boyd
Site: West Challow Observatory Instrument: C11 + LISA + SXVR-H694 Resolution: 1098

ZZ CMi

RA (2000)	07 24 14.00
DE (2000)	+08 53 51.80
Mag V	9.75
	-

Suspected Symbiotic Star

H alpha in emission

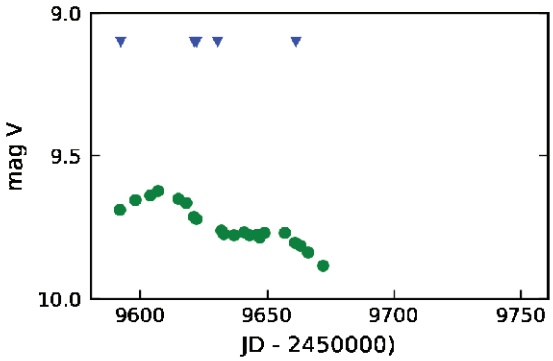

AAVSO V band lightcurve
ARAS Spectra: blue triangles

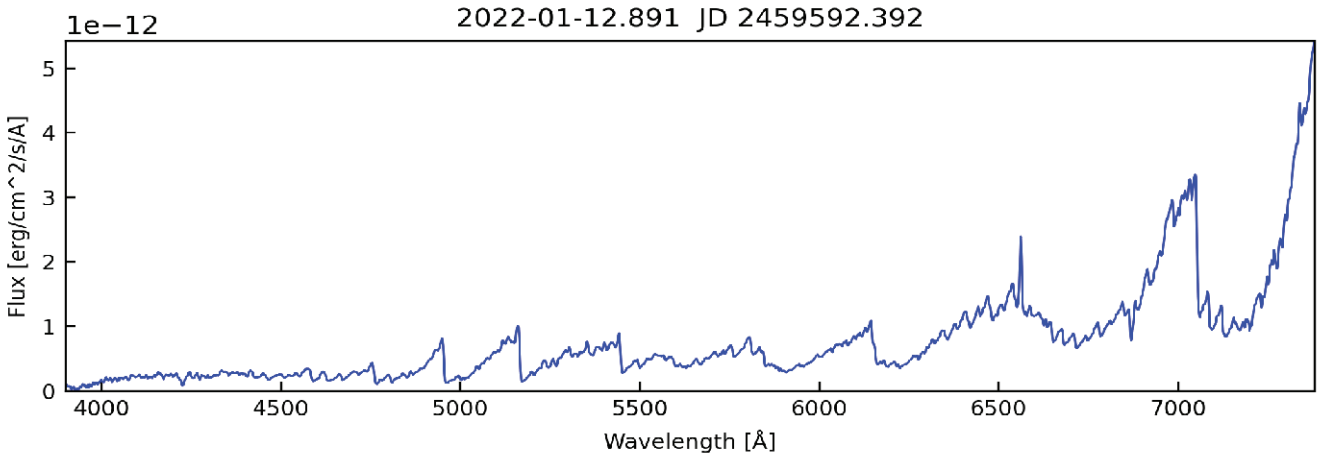

Observer: D. Boyd
Site: West Challow Observatory Instrument: C11 + LISA + SXVR-H694 Resolution: 1107

BX Mon: egress of eclipse

Thanks to a spectrum sent by Franck Boubault (2022-02-26) showing a peculiar aspect: almost pure red giant continuum, we launched a request for a monitoring of BX Mon. It appears clearly from photometry and spectroscopy that BX Mon was in the egress of a deep eclipse.

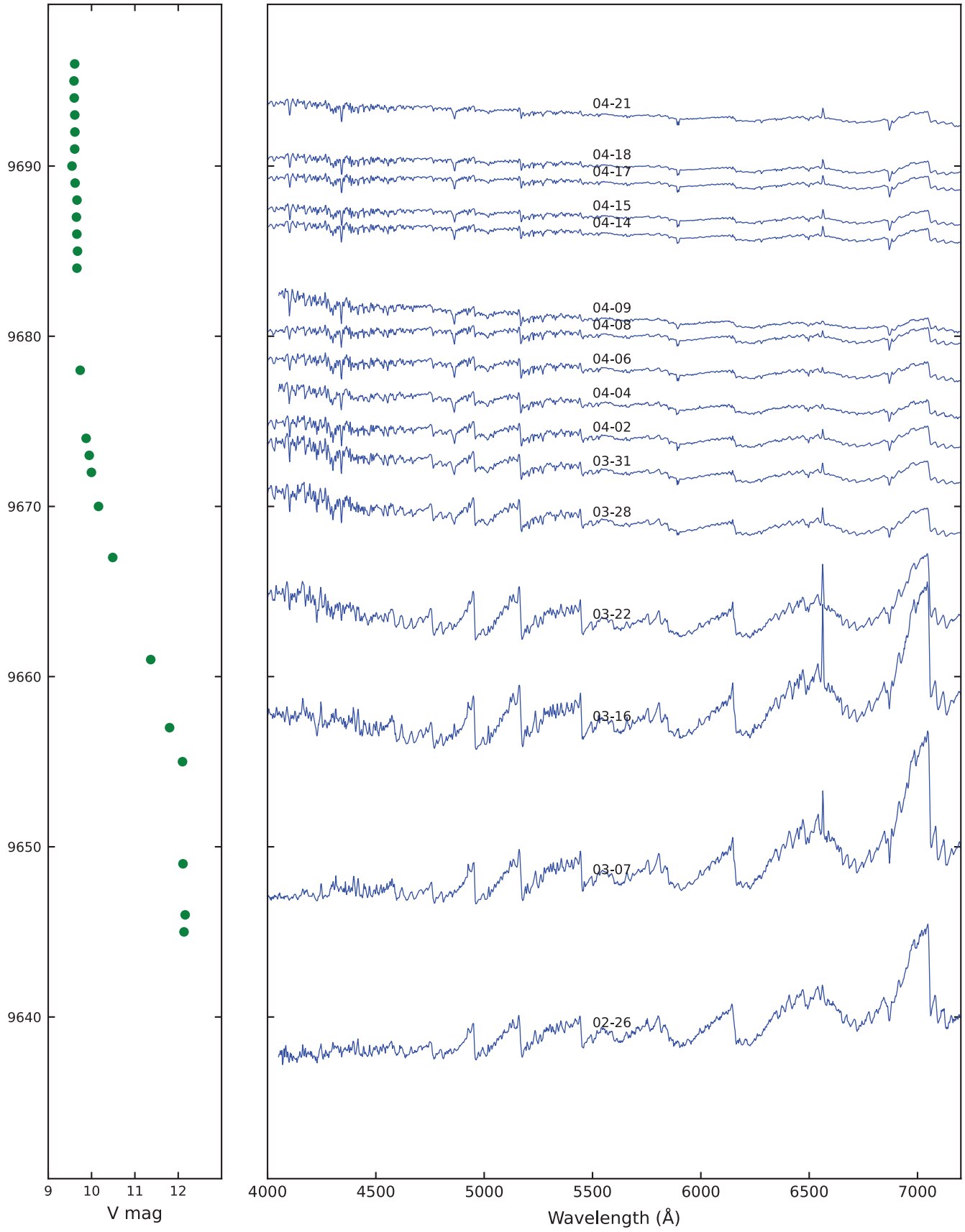

Fig. 1 - The egress of the eclipse with low resolution spectra (LISA R = 1000) secured by Franck Boubault (2), Forrest Sims (11) , David Boyd (1). Spectra normalized at λ = 5500 Å

BX Mon 2022 Eclispe egress

by Forrest Sims

BX Mon

Photometry

BX Mon is a Symbiotic Star that experienced an eclipse event in March/April of 2022. Simbad identifies the spectral type for BX Mon as M5/6IIIe. The recent quiescent V magnitude of BX Mon is about 9.6. The hot component of BX Mon was eclipsed by the red giant at approximately JD 2459645 (March 6, 2022). During this eclipse, the V magnitude decreased to about 12.2.

David Boyd has analyzed historical AAVSO photometry data and extracted V and B band photometry. Fig. 1 V band photometry which is more extensive, shows a rising trend between 2000 and 2022. There are 7 eclipse minima clear visible in the V band light curve which all result in a similar minimum magnitude of about 12.5, which is presumable the magnitude of the M5/6 III star.

The mean time interval between the deepest points of the minima of these eclipses is 1272 days with a std dev of 95 days. This gives a low precision estimate of the orbital period.

Peranso was used to perform a period analysis of the V and B band data after normalizing them to the same mean level and removing the rising trend over this period. Lomb-Scargle analysis gives a period of 1255 +/- 12 days. ANOVA (Analysis of Variance) gives 1259 +/- 33 days.

These results compare with the orbital period of 1256 +/- 16 days in Leibowitz & Formiggini (2011) based on an analysis of photometric data between 1983 to 2009, their section B of the light curve.

BX Mon V mag photometry from AAVSO database.

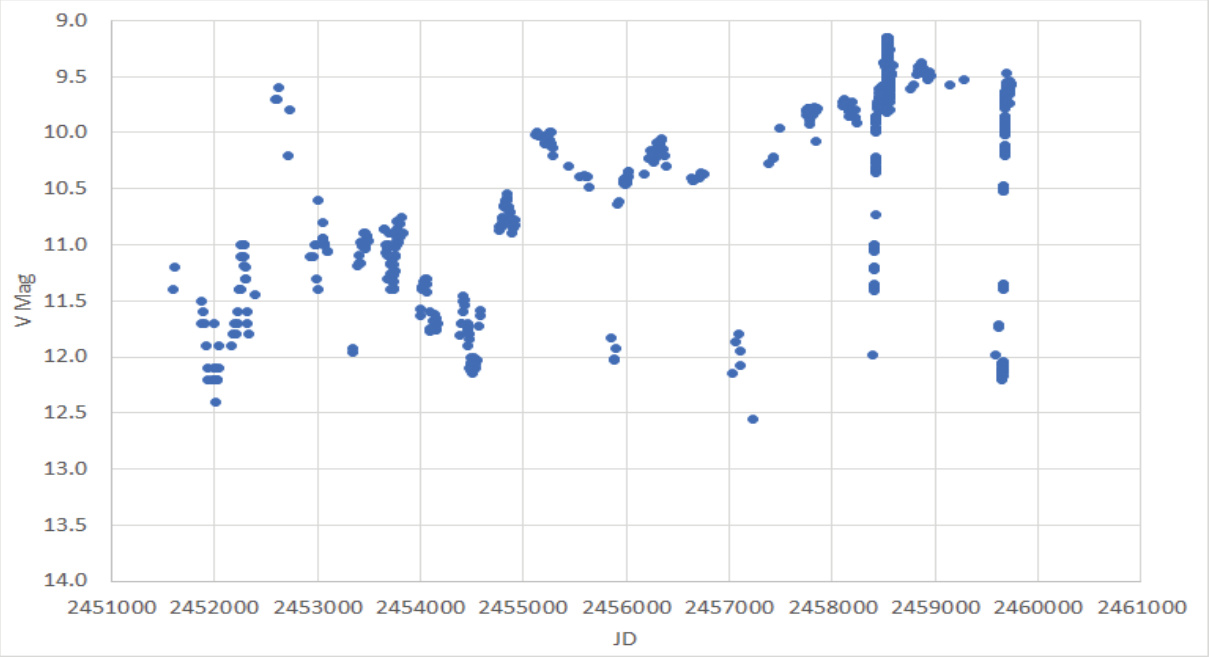

Figure 1. V magnitudes for BX Mon from AAVSO database.

AAVSO V mag photometry
Fig. 2 shows V mag photometry vs JD starting from the peak of the 2022 eclipse to the egress point.

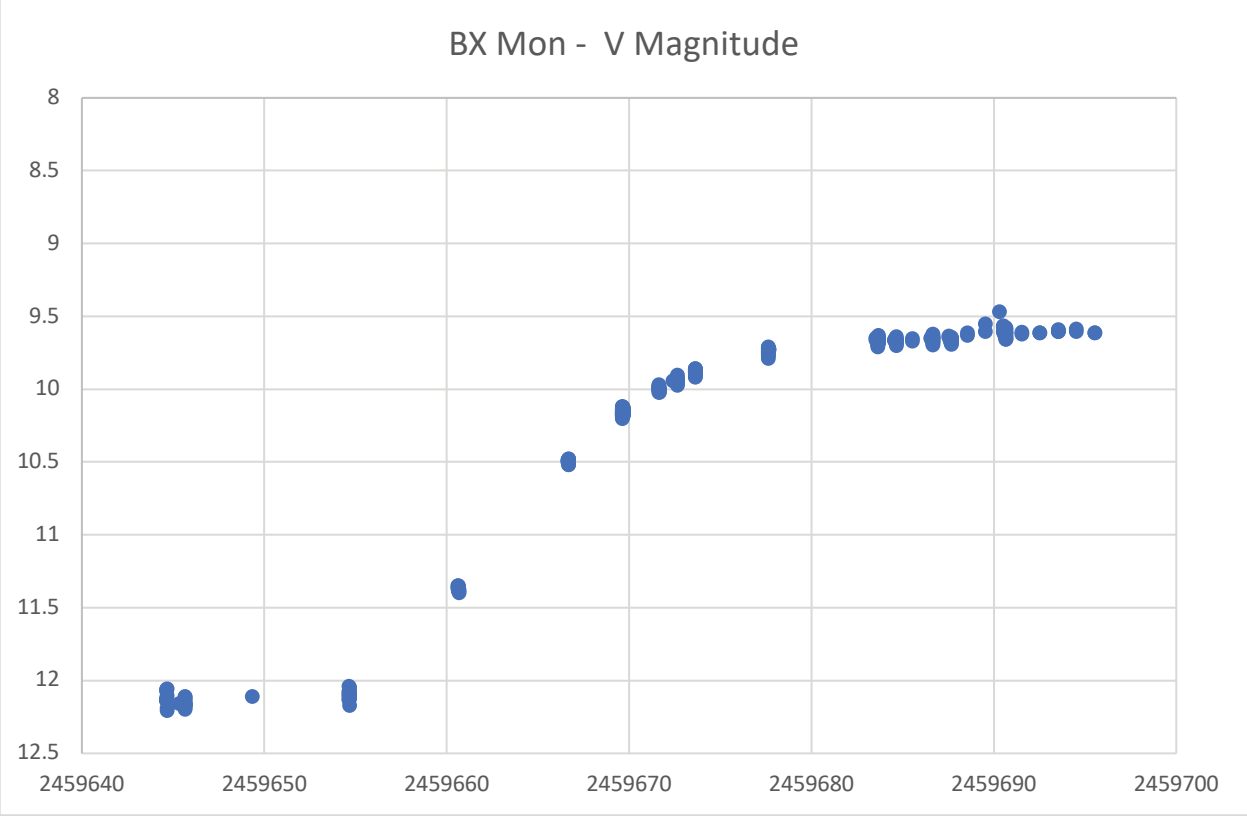

Figure 2. V magnitudes by Julian date for BX Mon from eclipse peak to the point of egress.

And Fig. 3 shows the same data but plotted by photometric phase using an Epoch of 2449580 and a Period of 1250 days. This period is based on the most recent two eclipse events.

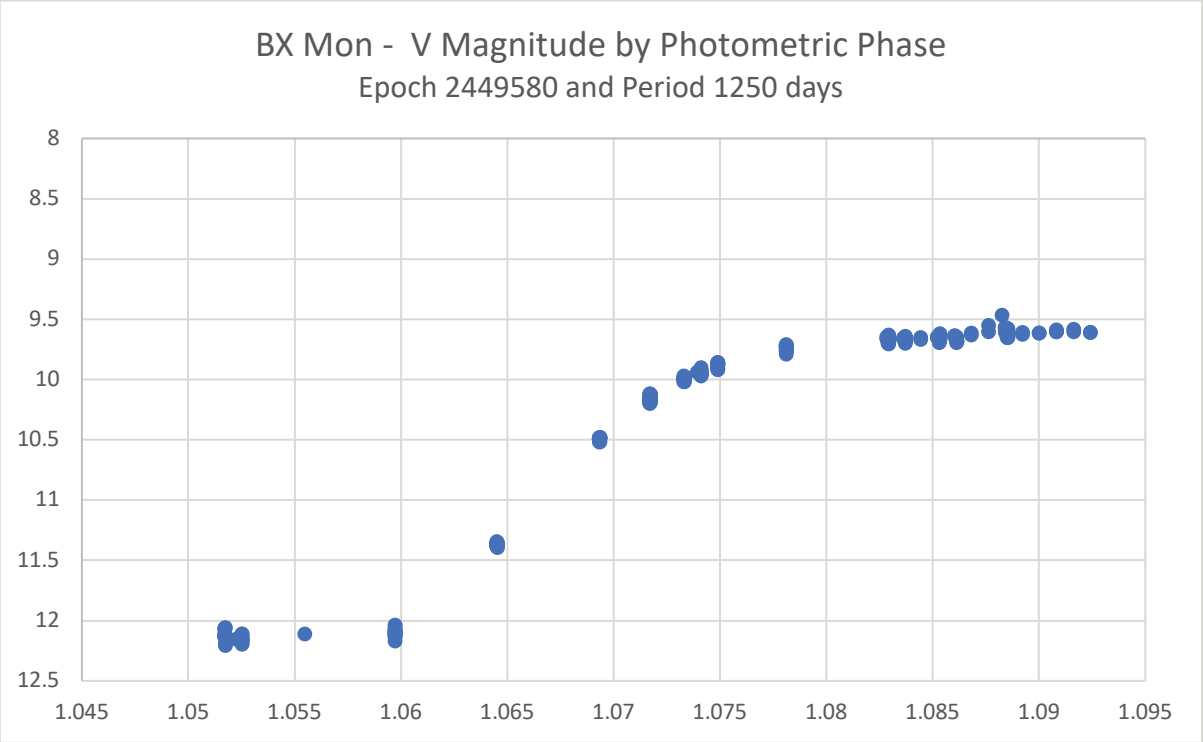

Figure 3. Photometric phase calculated based on Epoch of 2449580 and an Orbital Period of 1250 days.

Spectroscopy

The following plot Fig. 4 shows the changes in low resolution flux calibrated spectrum taken with a Shelyak LISA spectrograph as the eclipse progresses from March 7 to April 21, 2022.

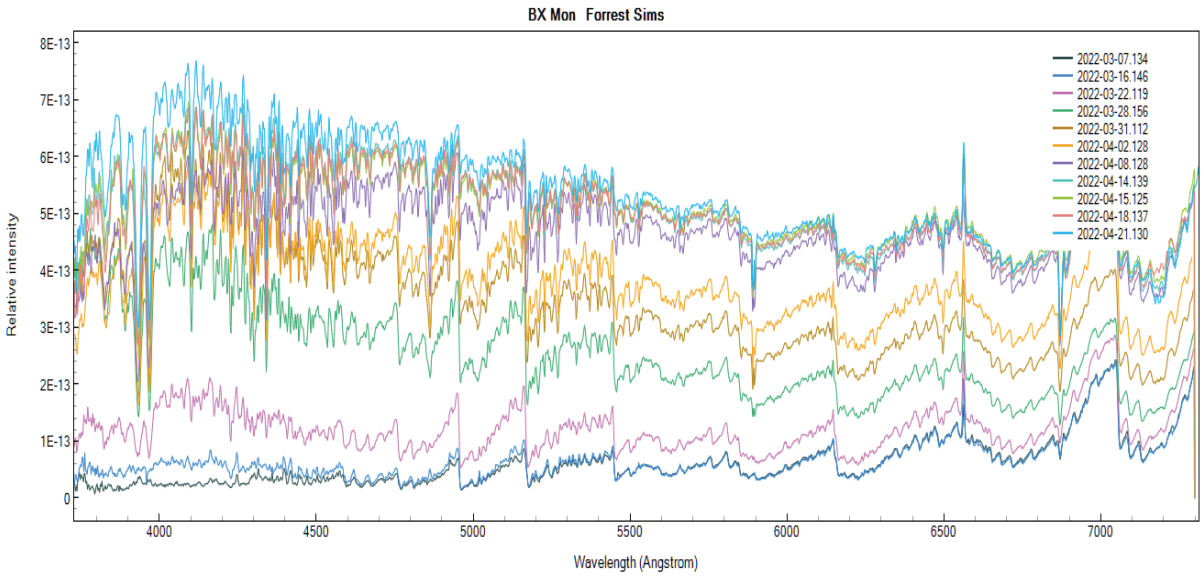

Figure 4. BX Mon – Eclipse Egress 2022. This plot shows the changes in the flux calibrated spectrum during the egress from March 6, 2022, to April 21, 2022, with the most recent spectrum at the top.

Next, we will look at some quantitative ways to examine the evolution of the eclipse by measuring changes in the spectrum. The next plot shows the changes in the Equivalent Width (EW) of the Halpha line during the eclipse.

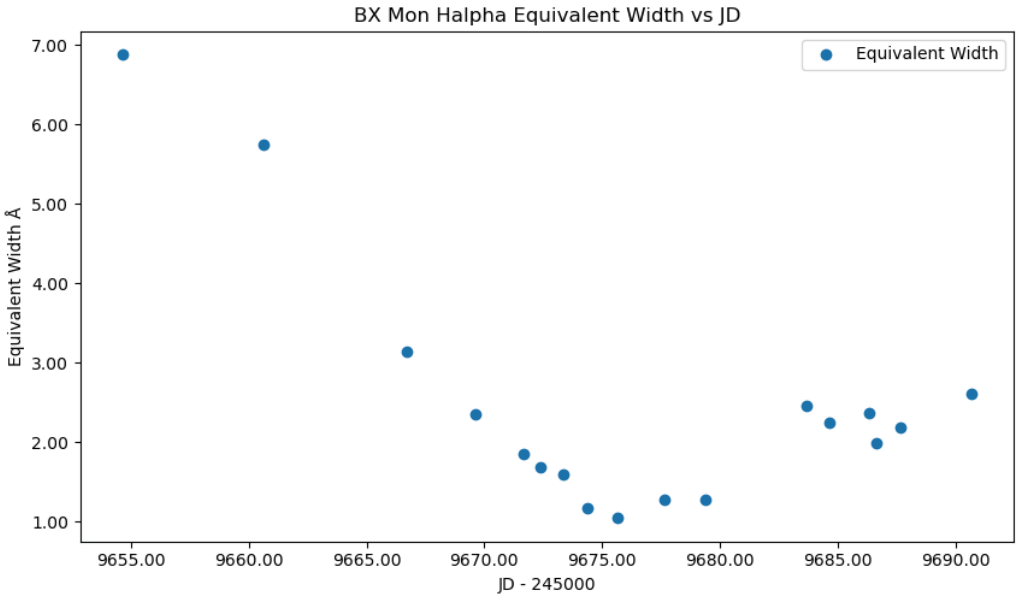

Figure 5. Equivalent Width of the Halpha line vs Julian Date during the eclipse egress.

Another parameter we can measure is the TiO Index for Titanium Oxide bands. The following graph depicts how the TiO1 Index is calculated. Three specific regions of the spectrum are identified for each band. The following plot uses the TiO1 Band as an example. Each of these regions represented by the red horizontal bar is 30 Å wide. The mean flux over each 30Å region is calculated. Then the TiO Index value is calculated using the following formula:

```
TiO = -2.5*math.log10((flambda2_mean_value)/ \
            ((flambda1_mean_value + (flambda3_mean_value -
flambda1_mean_value) \
                *((TiO_flambda2 - TiO_flambda1)/(TiO_flambda3 -
TiO_flambda1)))))
```

Figure 6. Python code snippet showing calculation of Tio Index.

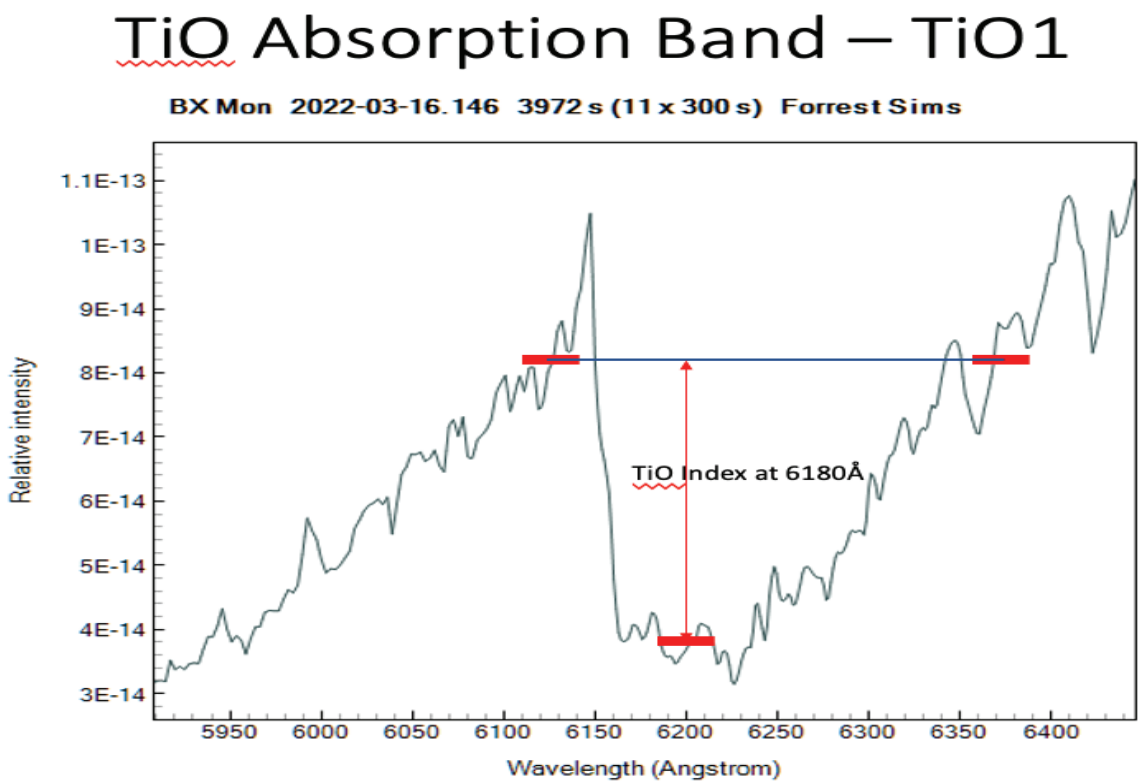

Figure 7. Input parameters for the calculation of TiO1 Index.

The following chart shows the 4 TiO Bands where we have calculated a TiO Index value.

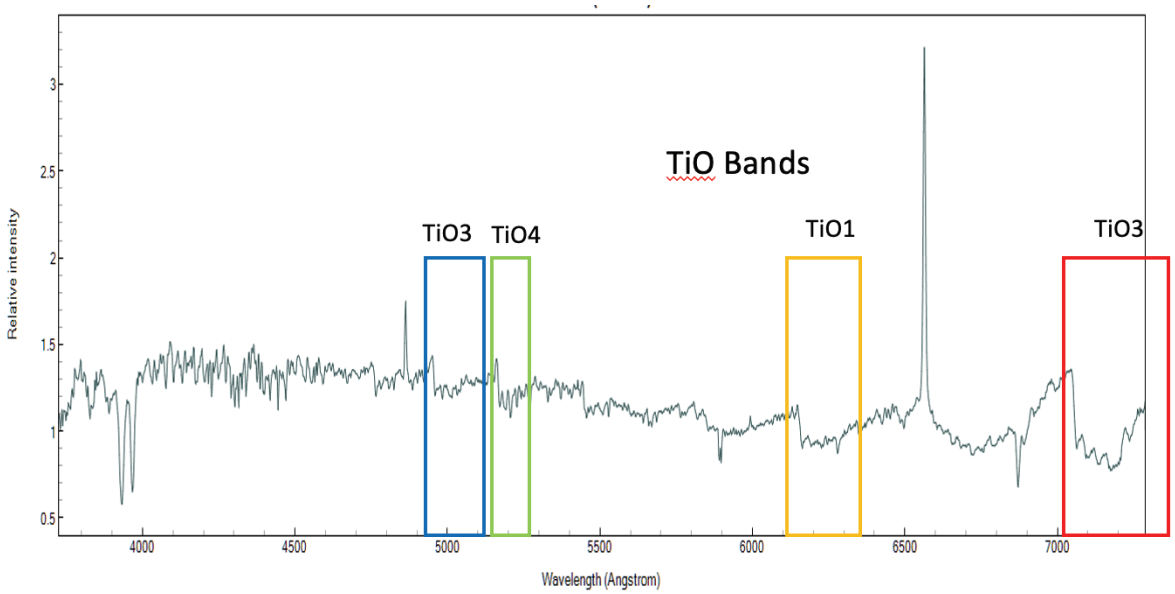

Figure 8. Graph showing the TiO Band regions used in analysis shown with a spectrum of BX Mon at eclipse

The Tio Bands wavelength regions for calculating TiO Index values are defined as follows:

Band TiO1	Wavelength Å	Interval
λ1	6125	6110 - 6140
Λ2	6180	6165 - 6195
Λ3	6370	6355 - 6385

Band TiO2	Wavelength Å	Interval
λ1	7025	7010 - 7040
Λ2	7100	6985 - 7115
Λ3	7400	7385 - 7415

Band TiO3	Wavelength Å	Interval
λ1	4940	4925 - 4955
Λ2	4983	4868 - 4998
Λ3	5140	5125 - 5155

Band TiO4	Wavelength Å	Interval
λ1	5154	5139 - 5169
Λ2	5190	5175 - 5205
Λ3	5280	5265 - 5295

Table 1. Specific wavelengths used to calculate TiO Band Index values.

The following TiO Index plots are for the four bands described above and only cover the date range for the March/April 2022 eclipse event. At the peak of the eclipse around JD2459645, the TiO Bands in the spectrum of the red giant are deepest (The Index value is at its highest level)

Note: the point at about JD 2459686 is a not good spectrum in this wavelength region but it is usable in other TiO Band regions

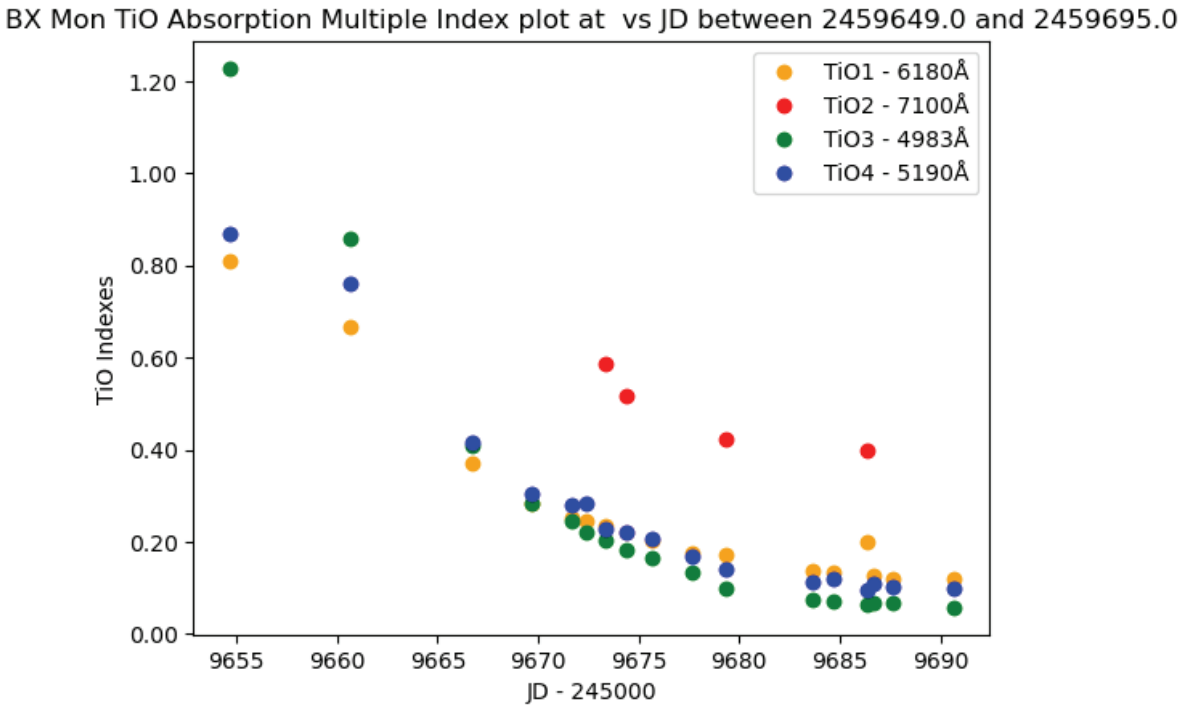

Figure 9. All 4 TiO Index values are plotted vs JD. Only 4 spectra in the ARAS database had data beyond 7400Å sufficient to calculate the TiO2 Band.

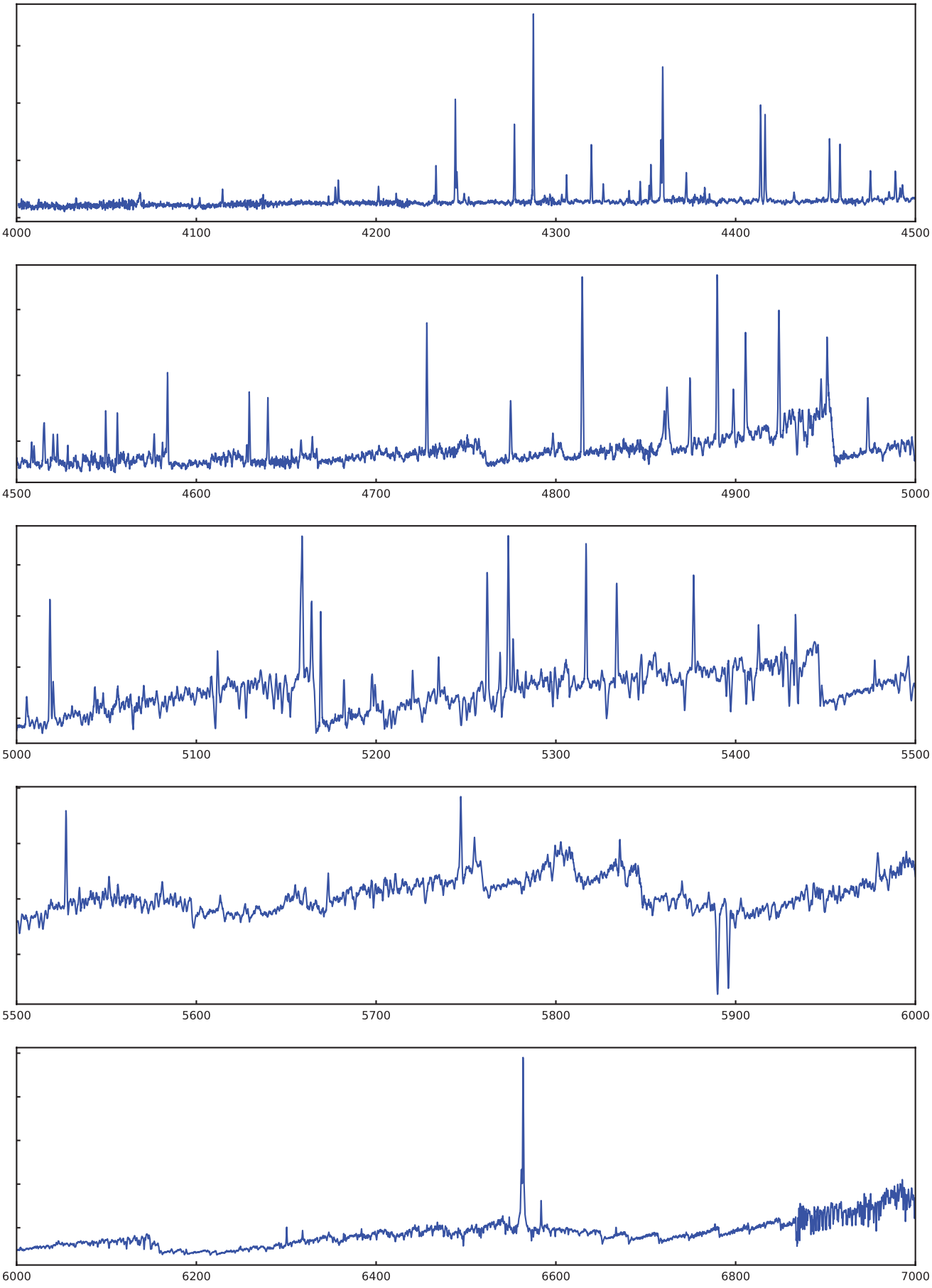

Fig 1. Colin Elridge 2022-02-09 R = 11000

THE INTERMEDIATE LUMINOSITY OPTICAL TRANSIENTS (ILOT) AND STELLAR MERGERS

Steve Shore

INTRODUCTION

Eruptive means transient but not all transients are eruptive. Many of those sources now being registered in robotic photometric surveys are quite ordinary, such as flare stars, protostars, and dwarf novae. Others are explosive, such as supernovae and classical novae. And then there are the "others", many of which are now classified only by their phenomenology and awaiting explanation. These include "supernova impostors", luminous blue variables, red novae, and other *intermediate luminosity optical transients* (also called ILOT). The designation "intermediate luminosity" a sort of catch-all for photometrists. It's like saying 'bigger than a mouse and smaller than an elephant" and only possible as an identifier for extragalactic sources. In the Galaxy, the combination of uncertain distances (even with Gaia, since these sources are, well, transients) and extinction (depending inextricably on the line of sight) render it almost impossible to specify the intrinsic properties of the source without spectroscopy. In extragalactic settings, since you know the source is in another galaxy whose distance you can somehow obtain, it's easier. Not unambiguous, just easier. There is always, still, the residual systematic uncertainty arising from internal dust in the parent galaxy and whatever might be along the line of sight within our system but, at least for the Galaxy, that's more under control.

So it's possible to distinguish three broad ranges. Those that are non-destructive and, thermonuclear or hydrodynamic in origin – novae, cataclysmic variables, symbiotics in outburst – are in the low end. They reach luminosities of about $\leq 10^5 L_\odot$ or so, depending on the individual systems, and either repeat or, at least, leave a system that eventually returns to some quiescent state. That may take weeks or centuries, and eruptions may happen once in a human lifetime or repeatedly, but there isn' usually an equivocal identification of the mechanism (although there are exceptions, ASSASSN-17hx being a possible example). The high end are supernovae, whose luminosities are orders of magnitude greater and whose energetics involve the destruction of the star by a combination of nuclear explosions and gravitational collapse, or *kilonovae*, that require the merger of neutron stars and are identified mainly through follow-up observations of gravitational wave sources. But in the range of $10^6 - 10^8 L_\odot$, there sits a zoo of other objects that share many of the same photometric and spectroscopic behaviours but with very different combinations.

In this instalment, I'll focus on the one intermediate luminosity transient that we know from Galactic sources, and that can be observed even with modest equipment at low resolution. the Luminous Red Novae. A few useful, detailed reviews [1] [2] [3] will help if you want to do a traceback on some of the literature.

But first, to set the stage for the event, I'll go over some modifications in the physical picture that are needed to understand what happens when a pair of cohabiting stars suddenly find themselves becoming a bit too cohabiting for comfort.

1. THE ROLE OF TIDES, THE ROCHE RADIUS, AND THE MERGER OF COMMON ENVELOPE SYSTEMS

The scenarios for many luminous transients now invoke binarity so it may be helpful to review a few things that make binary systems especially attractive to the massive star community.

Mechanical stability of a single star is governed by the balance between the internal pressure gradient and gravity. If a thermal pulsing drives changes in the pressure, these changes are (usually) not so large that its increase overwhelms the gravitational acceleration and you end up with a stable oscillator. Anything that increases the pressure gradient within the star drives the layer toward an imbalance but only in the largest amplitude variables does the energy carried in the outward propagat-

[1] https://ui.adsabs.harvard.edu/abs/2019A%26A...630A..75P/abstract
[2] https://ui.adsabs.harvard.edu/abs/2022arXiv220607070A/abstract
[3] https://ui.adsabs.harvard.edu/abs/2021A%26A...654A.157C/abstract

ing pressure wave produce a net outward acceleration. Outflow can also be driven by a too steep (for hydrostatic balance) pressure gradient in the outer parts of the stellar envelope because of the contribution of.radiation pressure. This is important for many of the objects you've been following. In the deep interior, radiation is important in supporting the mass but it's diffusively transported as if it were very viscous. The resulting structure is more inflated than without including this acceleration but not outflowing. In the atmosphere, instead, single lines, or bands, or specific continuous opacity sources can become such strong absorbers at the wavelengths of the local flux peak that they drive a wind. A combination of radiation and pulsation can be devastating for the star, the basic mechanism proposed in the outbursts of luminous blue variables such as S Dor and its massive cousins. These stages are predictable, the physical conditions under which they occur are tuned, and knowing the stellar structure at any stage signals its stability. In short, if you have a single massive star, whether at the moment we know the precise mechanism or not, you can predict if and when it will behave badly.

In a binary, things are much more prone to instability because there is an essential difference with a single star, the gravitational effect of the companion is never negligible. It's not simply that "two is greater than one". Stellar evolution in binaries is essentially qualitatively different.

The size of the critical surface for either component depends on the separation of the stars and the mass ratio. The scaling is only approximate but it's enough to say that the point at which at least a portion of the star unbinds is when the radius is a fair fraction of the separation of the stars. More important is that the critical surface depends on the mass ratio so is *larger for the more massive star*. This is another way of saying that the more massive star can sustain a greater tidal distortion. But if, in the course of its evolution, a star should extend to anywhere near this critical limit, matter will necessarily be forced outward by the imbalance of the internal pressure and the strongly reduced local gravitational acceleration. In other words, like the air in a balloon whose nozzle has been left open, the gas is literally forced outward. This happens at a low velocity, around the speed of sound for the envelope, and is nowhere near at escape velocity from the system, so that most gas must fall toward the companion.

This much you're used to from many sources, from Algol binaries, to symbiotics to cataclysmics.

the catch in the merger case is that as the WD spirals deeper into the giant, the mass interior to its orbit is decreasing so the Roche radius of the interior mass is also being reduced. This, along with the heating from drag, is presumed to accelerate the plunge and expels the envelope at a progressively increasing rate. Consequently, unlike the stable common envelopes of W Uma stars and other contact binaries on or near the main sequence, here we set up a double catastrophe. The environment is being heavily polluted by an expanding thick torus of gas, shaped in part by the orbital angular momentum it's carrying away from the system and by the enhanced wind from the giant due to the excess heating. Whatever subsequently happens when and if he WD reaches the core of the giant, this plunge cannot end quietly.

The merger idea is the latest twist on an old idea. In the 1970s, Paczynski proposed that a late occurring common envelope phase is responsible for producing the short period cataclysmic systems such as classical and dwarf novae. The puzzle was how to arrange for a star to become a massive white dwarf in a system with a period as short as hours. Others, Webbink and Soker among them, studied the idea of mergers producing planetary nebulae or some stellar remnant.

Mergers have also been implicated in more prosaic systems, the *blue stragglers* – so named because they are members of intermediate and old star clusters that appear to be main sequence stars but have luminosities above the turnoff point in the color-magnitude diagrams, beyond the point at which core hydrogen burning ends for single stars – and the FK Com stars – which are rapidly rotating, spotted and dynamo active giants that don't have binary companions. It has been argued that the *Great Eruption* of η Car in the 1840s was such an event; to be specific, one scenario is that a triple system underwent a merger with the 5 year binary, now imbedded deep within the detritus of the eruption, is actually the third member of the original system in orbit about whatever the central remnant is.

2. WHAT IS A MERGER AND WHAT DOES IT LOOKS LIKE?

The constituent stars in symbiotic binaries, the systems with which you are so familiar, cohabit an in an environment. The wind of the giant, that envelops the white dwarf and powers the accretion luminosity, has little effect on the overall orbital dynamics of the binary. While it transfers angular momentum both to the gainer and out of the system, the WD can move almost freely through it. There

may be a focusing because of the gravitational attraction of the WD and the angular momentum of the red giant but that's all. The gainer emits hard radiation because of the accretion, from the ubiquitous disk that forms around it and from shocks at the surface and from possible wakes that form because of the motion of the gainer through the environment. The ambient mass density is, however, so low that the WD is a mere obstacle. You see the same thing in the Solar system, how the Earth and its magnetosphere locally disturb the flow of the heliosphere but this has no effect on the orbital evolution of the planets.

2.1 In-spiral and engulfment

But now consider an different system, still consisting of the same components but at closer range or where the giant has literally engulfed the WD. This becomes more like the problem encountered with low Earth orbiting satellites. The environment can be dense enough that it exerts a drag on the satellite. This loss of orbital kinetic energy is critical. In a bond two body system, the orbital energy and angular momentum are directly proportional so a loss of kinetic energy induces a flow inward drift. There's nothing new here, we're discussed this before for accretion disks in which the combination of velocity shear and viscosity induces an inflow. In the satellite case, the body speeds up, increasing the drag and accelerating the infall with possible shock feedback on the ambient medium and heating of the plunging body. What this has to do with binary *stars* is that should one of the components of the binary produce a local medium that is sufficiently dense, the orbital motion of the WD will be impeded and the same fate awaits it as the Earth satellite: its orbit decays and eventually leads to a plunging encounter with the interior of the red giant.

The fundamental difference is the feedback on the environment. We're not talking about an artificial satellite of kg or even thousands of kg but an approximately solar mass degenerate star. This doesn't produce a simple localized shock, the whole envelope of the giant is affected. Sufficient heating and turbulence can be induced to lift off the outer layers of the giant with loss of the angular momentum and further acceleration of the plunge. But the theoretical details remain murky. The usual description is that the compact companion goes into a deep "plunge" state after a slower in-spiral that, at least in the models as so far computed, produces some sort of merger. It's the "some sort" that is vexing because once in the vicinity of the core the WD will be drastically altering the physical conditions under which nuclear processing occurs. Depending on the evolutionary state of the giant, the star may be experiencing shell burning, and the plunging WD will encounter that region in its journey. What happens is anyone's guess but two changes are certain: the gravitational influence of the WD will now be important and the envelope, which is convective, will not remain in thermal balance.

The shrinking of the Roche radius relative to the size of the giant requires a reaction from the envelope. The common envelope actually has "open funnels", the critical points on opposite sides of the stellar pair (indicated as L_2 and L_3 in the diagram) at which the local gravitational acceleration is balanced, in the co-rotating binary system, by the centrifugal acceleration. It's flung out of the binary, transporting mass and angular momentum away from the system. The material concentrates toward the orbital plane, although it isn't clear by how much, and expands outward, accumulating at large distance. This material can be so abundant that it turns self-shielding from the central system, and so locally dense that it changes state from atomic to molecular gas and even condenses dust. Unlike a normal stellar wind, this event is completely out of balance and as the underlying system expels progressively more mass the component stars move progressively closer. How the two stars accommodate to this bizarre state is not understood, the theoretical simulations only provide a scenario. What is certain is the final state cannot be established quietly: there must be an explosive ejection of matter. Again, one looks to η Car to have a sense of what that looks like: two axisymmetric, massive, dust-laden lobes of material that expand at high velocity perpendicular to the plane of the binary. What the final merger product looks like is also unknown.

3. SOME SPECTROSCOPIC EXPECTATIONS

I've argued that the circumsystem environment is heavily polluted by the gas expelled from the giant even before the merger. The column densities are expected to be quite large so in many ways this expanding torus looks like a very slow nova envelope. For the moment, assume the central object emits a pulse of UV at the moment of the merger. This is like the nova but, here, in a sort of inverse relation: the ejecta are long-lived, the central source is impulsive. So you would anticipate for a dense enough environment that the UV will be absorbed by the atoms and re-emitted optical and IR lines, the familiar fluorescence you know from novae and

symbiotics. The main differences here are the velocities and the amount of mass. In symbiotics, florescence is particularly evident in the appearance of the O VI Raman lines (6825, 7080Å) that require a substantial neutral hydrogen column for conversion. A few other cases, for instance O I fluoresced by Lyβ, are known from other sources. But one of the most striking features of red Novae is the prevalence of [[Ca II] 7991,7323Å emission. The Ca II forbidden lines are excited by absorption in Ca II 3933, 3964Å (the H and K lines), requiring low density to insure the upper levels are not collisionally de-excited. Other lines of Fe II and associated ions are also observed but this doublet is the outstanding anomaly. Otherwise, the spectra look much like very opaque nova ejecta. For the extragalactic sources, the problem has been the relatively low resolution, 50 - 100 km^{-1}, with which the spectra are acquired. It is possible, however, to get a clearer picture analyzing a Galactic system.

3.1 The Galactic example: V1309 Sco

Although there are a few sources that have been flagged as examples of this process, only one was observed *before* the outburst that is presumed to accompany the merger, V1309 Sco. The spectroscopic analysis it has many similarities to what we've discussed for novae, supernovae, and symbiotics so some of it will seem very familiar. But there are important differences that affect the spectral evolution and its interpretation.

The optical light curve of the event is unique. Photometry of the precursor state was obtained serendipitously [4].

The OGLE project happened to be robotically monitoring this field for gravitational microlensing events, one of which this was originally thought to be. Retrospective examination of the photometry, after the event, revealed a startling, truly unprecedented result. A decade before it went haywire, the source showed a contact binary light curve with a period of about 1.44 days. Perhaps eclipsing but certainly analogous to the W UMa type curves so well known from the literature. Yet sometime around 2006. The light curve changed and the period, which had been slowly decreasing, around 0.001 days/year, went into a rapid decline closer to 0.006 days/year, ending with a period less than 1.41 days before the light curve ascended more than 5 magnitudes and then dropped from the peak above $I \approx 9$ to below 17 mag, where it has remained since 2010. It appears that the outcome of this encounter is explosive. If we go by the one case at hand, V1309 Sco increased systematically in brightness for a few years before its disappearance behind a vast curtain of ejected matter, sufficient to completely obscure the system since 2008 behind a veil of dust and molecular gas. ALMA observations show an extended structure [5] but its geometry is not yet sufficiently resolved. Millimeter and optical/infrared spectroscopy shows the environment to be predominantly molecular. A very recent observation, the detection of a lithium overabundance in the star, provides another window into the interior at the time of the event. Lithium is produced by a very particular nuclear reaction:

$$^4He +^3 He \rightarrow^7 Li + \gamma$$

called the *Cameron-Fowler reaction*, that generates this primary isotope of Li in the absence of protons. It's the signature of high temperatures and deep mixing in giants but here it appears to also indicate nucleosynthesis during the explosion [6]. In one sense, this seems like an extreme nova ejection and much of the analysis we've discussed past columns would seem applicable. The analysis, should will look very familiar to you from V5668 Sgr, V1405 Cas, V339 Del, and other classical novae, may be of interest (it just appeared in A&A) [7].

3.2 Light echos, fluorescent waves, and reverberation as spectrophotometric time machines

Now to the complications. One was found after the outburst of V838 Mon. This star has become a poster child for the stellar astrophysics community, perhaps even more famous and certainly more remarkable than any of the static images produced by HST. The time evolution of the environment of this source is available [8]. This is a *light echo*.

You're all familiar with "heat lightning", although perhaps not by its American slang name: flashes that looks like lightning around you without a sound or rain. This is, actually, the same as V838 Mon, just a bit faster because the scale is more than a trifle smaller. Were the clouds at a few tenths of a parsec distant, you'd see the same thing.

When the outburst occurred, the resulting expanding light pulse scattered off anything that hap-

[4] https://www.aanda.org/articles/aa/pdf/2011/04/aa16221-10.pdf

[5] https://ui.adsabs.harvard.edu/abs/2018A%26A...617A.129K/abstract

[6] https://ui.adsabs.harvard.edu/abs/2022arXiv220706779K/abstract

[7] https://arxiv.org/pdf/2206.03191.pdf

[8] https://hubblesite.org/contents/media/videos/2004/10/419-Video.html?keyword=Novae

pened to intervene along the line of sight. If this were continuum, all you would see is a broadband brightening. But this is the light from the source at the moment of its brightest presentation and records not only the continuum but the complete spectrum. That includes the UV and infrared. So if the surrounding medium is gas rich, not just dusty, the UV will fluoresce optical and infrared lines *precisely as in the case of illumination of nova ejecta by the underlying WD*. Now comes the part that makes the interpretation more difficult but is accessible to your observations. The time of arrival at some distance, say D, is the light travel time, D/c. But that is relative to the source, not *you*. if you imagine drawing a circle around the source that presents the same time of arrival at D (See Fig. 2a), it takes more time for the signal from $-D$ to reach you than $+D$, twice as long.

So you see the effect delayed, or put differently, you see the emission from that circle from an earlier time. Since the source changes during that time but it may be unresolved, you're spectrophotometrically mixing epochs in each observation. In fact, you're simultaneously seeing the "current" state of the source *and* its past, which may have actually been brighter! If the scattering medium is somehow separated by some distance from the source, there will be an initial delay in the first pulse and you may not see the reaction of the medium at all to the first light because it is from so small a region along your line of sight, as I'm showing in the figure.

This isn't only an issue for mergers, it's true for *any* luminous transient and that includes supernovae and even luminous blue variables. For instance, Tycho[9], which was observed in 1572, produced a sufficiently bright echo that the type of supernova could be identified based on its observation only a few years ago (that is, more than 400 years later), see for instance [10] [11] [12]. Although you won't be able to perform such high spatial resolution observations, the effects of the echo will nonetheless "corrupt" your spectra.

That's for a passive echo, the "heat lightning" example. But there's as an *active, fluorescing* effect that depends on the state of the surrounding gas. Consider what happens if a UV pulse hits a thick ring of low ionization gas. The photons will be absorbed and scattered as they pass through the medium, and if there isn't sufficient flux to ionize the line of sight the peripheral ions will be exposed to a degraded radiation field over a long, diffusive time. In other words, you see different depths being excited over an interval of time. This will smear out the response of the whole region. More important, since the pulse has a possibly short duration, the forward portion of the environment (call this the +D part) is decaying even while the rearward (-D) is rising. If the pulse is ionizing, this shows up as distinct behaviors for individual ions from the environment. I hope this is making sense. Yes, I know this is complicated, but if you have a time series – the importance of which we've repeatedly discussed – you can unravel the effects and perform an archaeology of the state of the system before it underwent merger.

The effect on the surroundings will also differ with spectral interval. In the infrared, heating of imbedded (or newly formed) dust produces an active response in delayed thermal emission. This also depends on the luminosity of the event but not as directly on its spectral energy distribution. Emission in the so-called polycyclic aromatic hydrocarbon (PAH) bands in the near infrared is more sensitive to the UV component of the radiation so the 3-8μ interval can vary differently from the longer wavelengths. With the extended sensitivity of a few of the new spectrographs, e.g. StarEx, you start to get some of the emission detectable, especially for scattered light.

It's important to note that had we chosen to discuss active galactic nuclei instead of red novae, the same idea of using an impulse to trace structure would have been called *reverberation mapping*. Because the circumnuclear environment is so large, thousands of AU to parsecs, a variation of the central engine – anything in the immediate vicinity of the central black hole – produces a light pulse that excites and ionizes the surroundings. Because the matter is stored in, and follows the dynamics of, an circulating accretion disk, the line profile actually traces out the environment. In the opposite sense to the matter surrounding a merger, the highest velocity circulation is in the innermost portions of the disk, even if we are not in strictly freely orbiting (so-called Keplerian) conditions. Thus, emission line wings are thought to form there. The cores are from the more extended regions. The ionization is also highest near the center. So a combination of profile and ionization changes trace out the dynamics of the disk, a technique that's been employed for some time.

So let's turn back to V1309 Sco. At first, immediately after the maximum and in the early opti-

[9] In the usual bad habit, it's the supernova, not the astronomer!
[10] https://iopscience.iop.org/article/10.1086/587158/fulltext/72553.text.html
[11] https://arxiv.org/pdf/0810.5106.pdf
[12] https://articles.adsabs.harvard.edu/pdf/2013IAUS..281..335U

cal decline, primarily absorption lines were observed against the central source. These took the form of an Fe-curtain but not the same as in novae: this one remained static in strength but shifted at about -100 km s^{-1}. The remarkable feature of the spectra was the *absorption* line at [O I] 6300Å. Recall that forbidden lines are not impossible, just highly unlikely and intrinsically very weak. This doublet is a ground state multiplet, it will always absorb unless in recombination or otherwise pumped. The same holds for the [Ca II] lines. The other, permitted resonance lines are from neutral atoms, the Na I D doublet and K I 7699Å. Both showed strong absorption at the same velocity as [O I]. Strikingly, a few months into the outburst, [O I] turned over into emission, as did [Ca II], the absorption disappeared and many Fe II and [Fe II] transitions appeared as some of the curtain turned over from absorption. This sequence is a consequence of the echo, first showing absorption because it had not yet diffused in enough of the surrounding torus to ionize and excite the emission in a sufficiently large solid angle. But in time, the emission from the forward and backside sections of the torus emerged in emission.

3.3 CK Vul 1670: another Galactic case

The nature of the nova of 1670, known now as CK Vul, is still controversial but the direction of evidence points to an analogous red Nova event. The remarkable feature of this historical outburst is the wealth of archival quality visual estimates of its brightness. The eye is a lousy detector in an absolute sense but rather good in a relative sense. The nova light curve was reconstructed in a remarkable effort [13], I urge you to read, at least the first section on the archival work, I don't know anything that so clearly illustrates how our observations will leave a permanent contribution for the future (consider that you're in the line of decent from Cassini and Hevelius and Tycho and Kepler)! Although the remnant, compact but resolved now, looks something like a planetary nebula, its spectrum is like that expected for an old nova. For this event, the reconstruction shows the characteristic variation of a Red Nova over a two year interval, two maxima in the visible (take a look at the reviews cited at the star of this column). Newton had yet to turn his prism towards sunlight so we have no spectroscopic record of what happened but we know what's there now.

[13] https://articles.adsabs.harvard.edu/pdf/1985ApJ...294..271S

4. CODA

I'll stop here, hoping you're not saturated or dazed. The study of such phenomenologically complex events requires everything we've discussed over the years, from density and thermal spectroscopic diagnostics to using line profiles and their changes to understand the dynamics and energetics of such events. In the next few years, there will certainly be more of these discovered. More to the point, in some nearby galaxies (e.g., NGC 300), these and related transients can reach maxima that put them in the range of your observations. Galactic candidates will likely turn up in the products of all-sky surveys, from the Vera Rubin telescope project (formerly known as the Large Synoptic Survey Telescope) to the numerous optical robotic projects planned for the near term. You're spectroscopists and understand well the contribution and limitations of photometry, your involvement will become progressively more vital in understanding these temporary guests. In the next column, we'll see that many of the ideas discussed here also apply to the class of stars called luminous blue variables or *LBV*s.

I also want to take a moment to thank my colleague and dear friend Elena Mason, of the Trieste Observatory - INAF, for a decade of collaboration, arguments, and excitement trying to understand the cosmos and without whom everything I've discussed here would have been for naught.

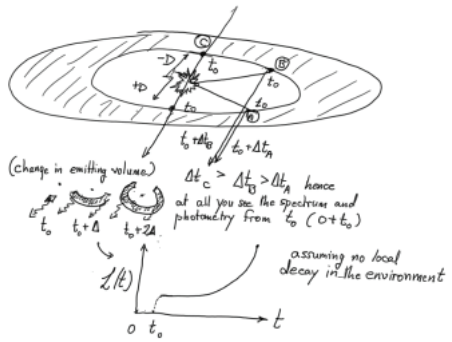

(a) Example of how a light echo develops in time for a circum-system ring. The pulse causes the atoms (e.g., [O I]) to fluoresce at the same time but the light travel time depends on the angle relative to the observer. The bottom curve shows the time development, the partial rings show that portion seen in fluorescence by a distant observer at different times.

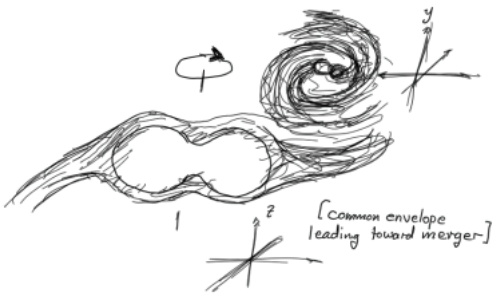

(b) The merger event, a cartoon showing the formation of a common envelope engulfing the two components and the mass lost through the outer parts of the critical tidal surface. This is the partof the event responsible for the formation of the ring shown in Fig.1(a)

Figure 1

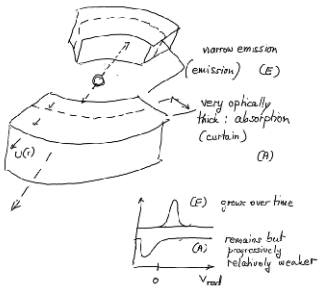

(a) Profile decomposition for the fluorescence showing that an absorption is produced along the line of sight from the approaching ring and an emission from the receding portion.

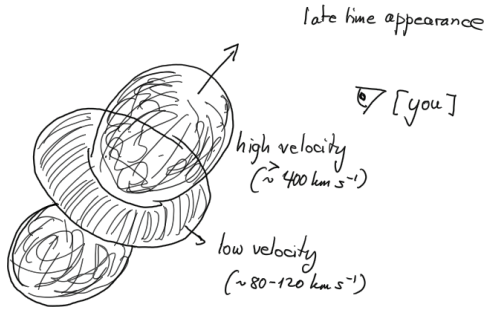

(b) Cartoon of the post-merger structure of the event, with lobes expanding off of the orbital plane that do not diectly collide with the slower moving pre-merger ring. The resemblence to eta Carina isn't a coincidence.

Figure 2

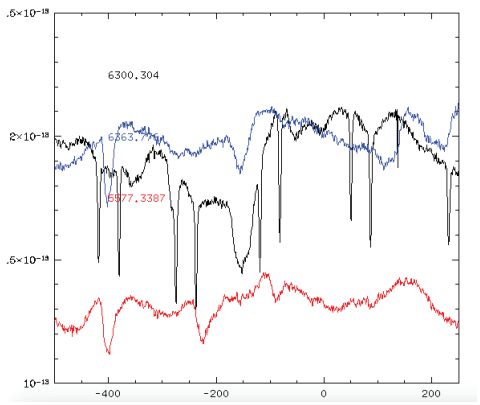

(a) day 15

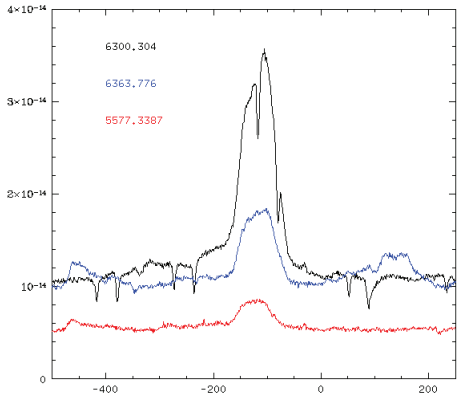

(b) day 35

Figure 3: V1309 Sco [O I]$\lambda\lambda$ 5577, 6300,6363 Å (UVES)

How this all fits together:

First, the phenomenology - v_{rad} vs. excitation condition (ioniz. state, etc.)

First, the phenomenology - v_{rad} vs. excitation condition (ioniz. state, etc.)

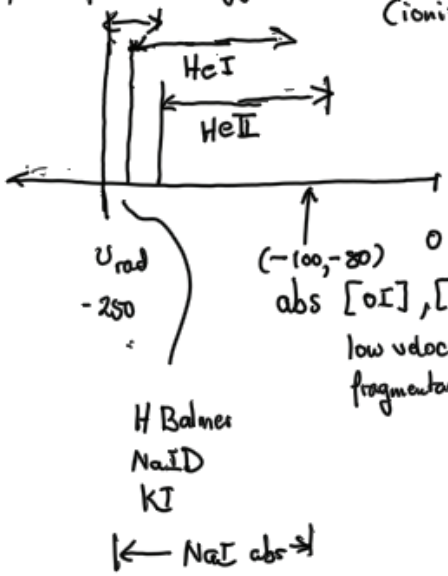

assume two components

[OI] abs, ~100 km s^{-1} always present (same for Balmer etc.)

this doesn't change in total optical depth, confined in velocity (as 6364/6300 velocity dependent) as for NaI D2:D1

emission lines: Balmer only lines always in emission but likely with some self-abs;

transition from abs/PCyg to emission: this is the merger-debris so:

l.o.s.

[CaII] also weaker, likely still there (there also is nothing on any of the sufficiently excited state lines)

[NB: I think it's easy to understand the PCyg formation stage for the fast ejecta and the disappearing abs.]

An emission line from the Earth's atmosphere

Paolo Berardi

The faint glow emitted by the Earth's atmosphere is probably overwhelmed by light pollution for many of us who live and observe in urban or suburban areas. However, spectroscopy is capable of detecting the presence because the source mainly emits specific wavelengths of radiation.

I happened to see it during a long observing session dedicated to Nova Persei 2020. The Lhires III spectrograph was centered on a small region around the h-alpha line, also including the forbidden oxygen lines at 6300 and 6363 A.
The spectrograph is equipped with the photometric slit, so you can see the vertical background line through the narrow (31 microns) and large (300 microns) part. I think it's a little more obvious in the large slit. Also, notice how the line gradually fades over time.

Airglow is different from auroras, the high-latitude phenomenon where solar energy and small particles travel down the magnetic field lines at the north and south poles into Earth's atmosphere. In addition to the spatial extent, auroras are highly structured while airglow is relatively uniform (sometimes waves and patches can form and change over minutes due to particular weather conditions).
As reported in the literature, airglow systematic decreases during the course of the night, confirming the progressive consumption of energy stored during day. That's what you see in the two-dimensional spectra shown above. They span from 18:35 (just before astronomical dusk) to 21:33 local time (UTC+1).

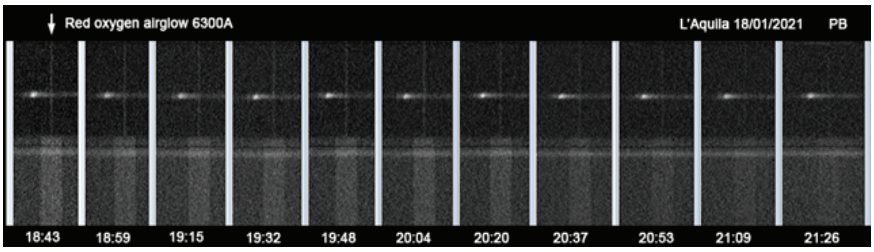

The broad line in the narrow slit is [O I] 6300 from the nova. The same atom, which is also present in the Earth's atmosphere, produces the night-sky emission line.
The oxygen line comes from a layer in the thermosphere at about 270 Km. During the daytime, the solar UV light breaks O2 oxygen molecules apart (photodissociation). The individual atoms initiate complex chemical reactions lasting beyond the sunset. The radiative lifetime of the excited oxygen atom is very long (~110 seconds) but the probability of a collision in upper atmosphere is relatively low, so a significant fraction of excited atoms have time to radiate their energy (collisions are the other reason for excited state deactivation).
This sort of chemical energy storage is also available at night and the related radiating process is called "chemiluminescence". This is the airglow phenomenon, stronger in daytimebut overwhelmed by scattered sunlight.

In the following three frames (see below), the oxygen line is somewhat more pronounced, maybe for some non-uniformity of airglow (the telescope movement relative to the sky, due to the sidereal tracking, should be taken into account).

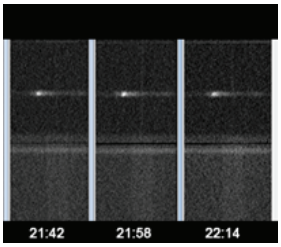

The airglow spectrum includes a lot of emission lines/bands at various wavelengths and also a continuum. That source of light is being investigated by astronomers, especially in large and remote observatories where it represents an important fraction of the sky-background light that affects astronomical observations. You can find more information in the references links below.

References

Ch. Leinert et al. - The 1997 reference of diffuse night sky brightness - https://ui.adsabs.harvard.edu/abs/1998A%26AS..127....1L/abstract
F. Patat - Where the shadows lie - The dark skies of Chile - http://www.eso.org/~fpatat/science/skybright/zenit/zenit_paper.htm
S. Noll et al. - An atmospheric radiation model for Cerro Paranal - https://www.aanda.org/articles/aa/pdf/2012/07/aa19040-12.pdf

PlotSpectra
a data visualization utility for amateur astronomical spectroscopy

Tim Lester

PlotSpectra will read and display the one dimensional FIT files produced by the excellent data reduction programs available to the amateur community. It's main goal is to provide an intuitive and efficient tool for the visualization of astronomical spectra. Plots suitable for posting to forums can be generated in PlotSpectra with very little effort. In addition to this core functionality there are tools to facilitate the comparison of different spectra, the measurement of spectral features and spectral line identification and labeling.

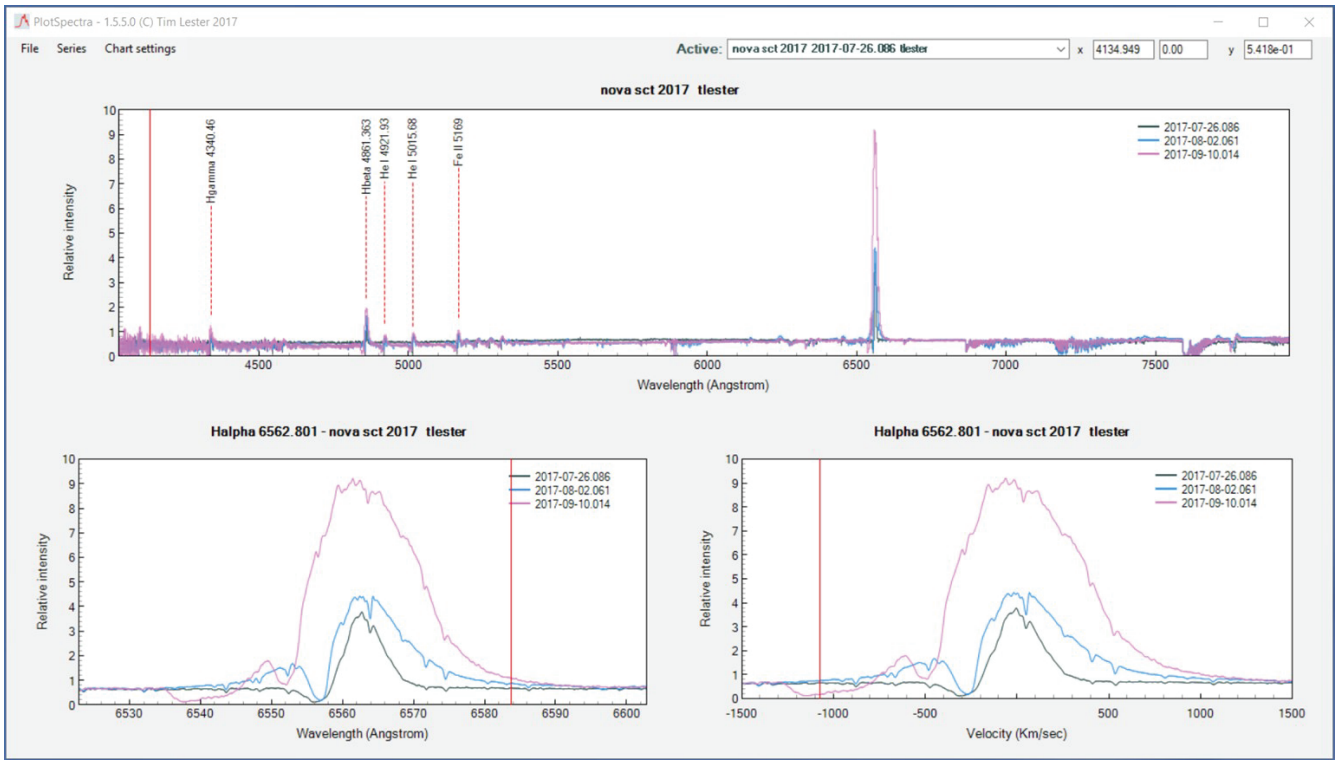

Main features:

- Three plot areas. A main intensity vs wavelength plot as well as expanded sub plots for wavelength and velocity.
- The data and headers from multiple FIT files can be loaded into a series set with control over which series are displayed and which one is active.
- Intelligent auto labeling of the series and chart title using data from the FIT headers.
- Individual series can be shifted by wavelength, velocity or intensity multiplier.
- Full control of plot formatting including a primary and secondary intensity axis, stacked plots and multi-region velocity plots.
- An intelligent auto scaling option and aesthetic auto tick mark increments and labeling.
- Full control of spectral line annotation from a choice list of lines that can be user modified.
- Ability to normalize all displayed series to the active series over a selected region.
- Continuum normalization using a penalized cubic spline fitted to selected regions.
- Series alignment on a selected feature using either a wavelength or velocity shift.
- A signal to noise estimator that can be used when two sets of data are available.
- Measurement of standard spectral line parameters with polynomial or penalized cubic spline fitting options for the continuum.
- The ability to save a .png image of each plot area. Useful for uploading to forums.

- The ability to produce publication worthy plots by printing to Microsoft's "print to PDF" device.

Feature guide

Opening FIT files
One or more FIT files may be opened from the PlotSpectra "File" menu or PlotSpectra may be added to the "send to" list on Windows right click context menu. The latter can be enabled in settings. The FIT files are loaded into a set of chart series that may be controlled using the "Series" menu.

Basic controls:

- The cursor is active when the mouse is in a plot region and the numbers at the top right of the main plot screen show the x position, the width of any selected region and the intensity of the active series at that position.
- Regions are selected using the left mouse button and dragging. The selected region is indicated with a grey background.
- The drop down list labeled "Active" is used to select the current active series if more than one has been loaded. Actions occur on this series only unless indicated otherwise.
- Double clicking on the main plot will center the two sub plots on that wavelength.
- The mouse wheel controls the intensity scale of the main plot. The Ctrl key plus mouse wheel will offset the intensity axis. Auto scaling is disabled after the mouse wheel is used.
- The mouse wheel controls the wavelength and velocity scale of the two sub plots.
- Right clicking in a plot area brings up a context menu listing the actions available.

Series control
The "Series" menu on the main screen provides several items for the control of which series are visible and their sort order as well as a settings item which brings up a window for more detailed control.

Series setup window:

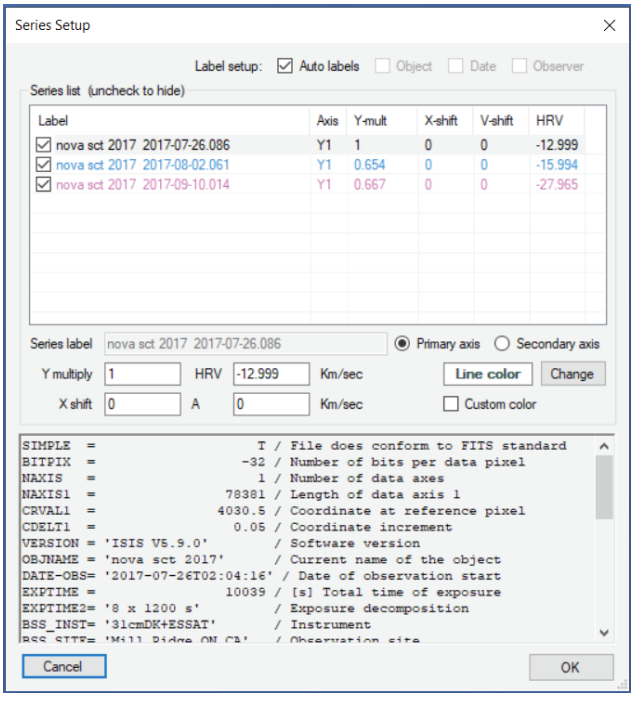

- Allows control over series labeling. Auto labels will attempt to differentiate the series in a sensible way using data from the FIT headers.
- Shows a list of the currently loaded FIT files (series). The check box controls which are visible in the plot areas.
- Provides control over which axis (primary or secondary) the series is plotted on and the line color. Series colors are auto assigned from one of three per-defined color palettes that are selected in settings.
- The text boxes allow an intensity multiplier as well as wavelength and velocity shifts to be applied to a series. If series have been aligned in the main plot area then the shifts applied will be indicated in these boxes.
- A text box for entering a heliocentric radial velocity correction is also provided. If the FIT header

indicates one has been applied to the data this box will be auto filled with the offset.

- The scrollable text box at the bottom shows the FIT header for the selected series.

Chart control

Chart control windows for each plot area can be opened using the "Chart settings" menu or via the right click context menu of each plot area.

Chart setup windows:

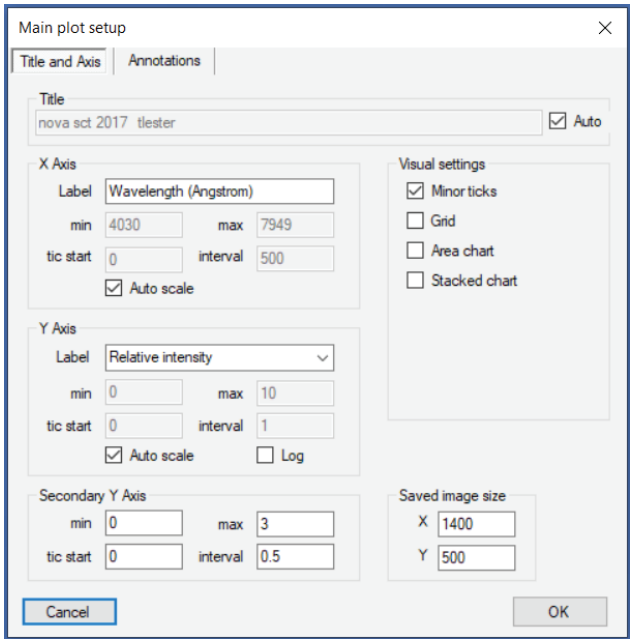

- These screens provide control over the chart tile, axis labels, axis ranges and tick marks of the plot area. The default is for auto titles and auto scaling of axis using information from the FIT headers of all the currently displayed series.
- The auto scaling of the intensity axis is dynamic. It will adjust according to what is currently displayed.
- Grid display can be enabled or disabled. The default for this is set in PlotSpectra settings.
- If there are several series a stacked chart may be enabled for the main plot or the velocity plot with control over series spacing and series label offset.
- The "Saved image size" boxes specify how many x/y pixels to use for saved .png plot images. These numbers will be remembered.

Center wavelength control for the sub plots

The center wavelength of these plot areas can be set to a spectral line by selecting an entry in the "Plot center choices" list. This list is the same as the Choice list on the annotations tab. The spectral line name and wavelength will be added to the title of the plot. Note that the center wavelength of these plot areas are tied together provided the velocity plot is not set up as a multi-region plot (see below).

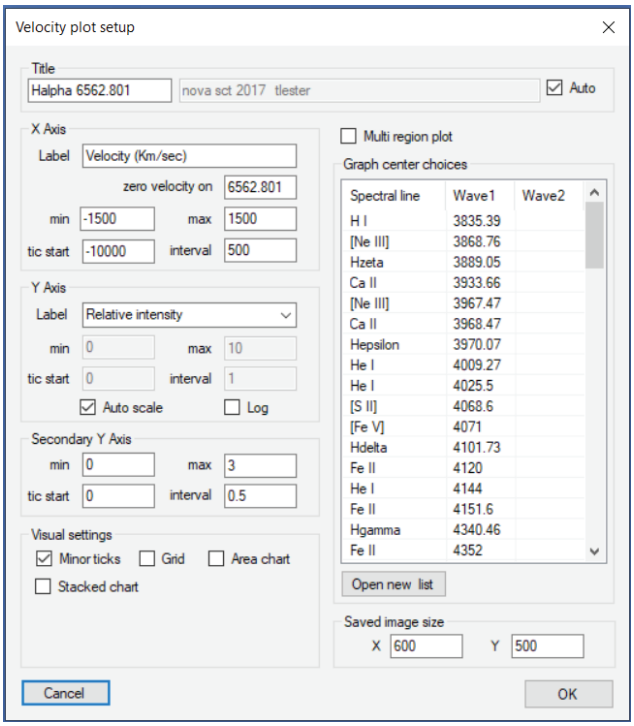

Multi-region plots

The velocity plot can be set to overlay multiple regions of the spectrum. This is done by checking the "Muli region plot" control and then checking off several lines on the choice list (for example Hgamma, Hbeta and Halpha). Note that when in multi region mode this plot does not respond to double clicks on the main plot.

Spectral line labeling

Two methods for specifying spectral line labels on the main plot are provided. One control window is on the annotation tab of the main chart setup window. The other control window is accessed from the "Edit annotations" item on the right click context menu. These two controls are complimentary.

Main plot setup window – Annotations tab:

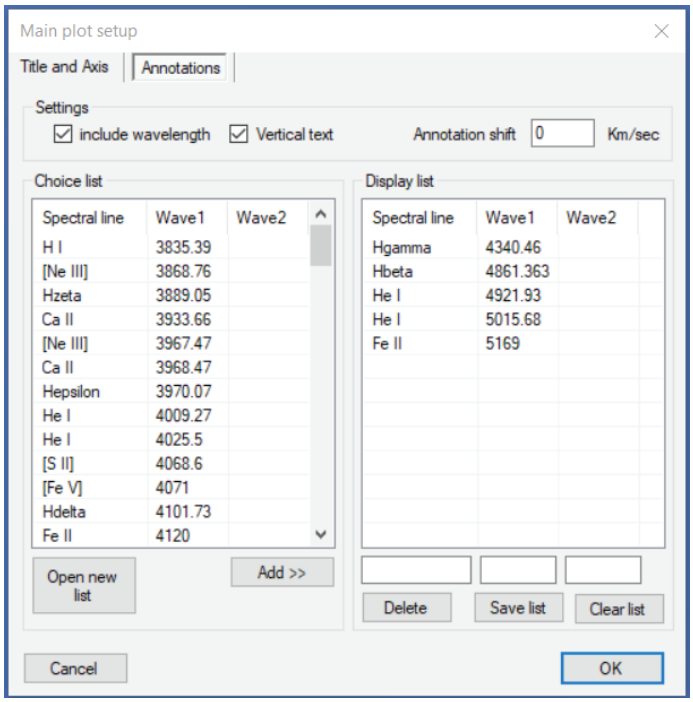

- This screen shows a list of pre-defined lines to choose from and a list of the line labels to be displayed.
- The Display list is populated by double clicking on entries in the Choice list or by using shift/crtl to select several items and clicking the Add>> button.
- The label name and wavelength of an entry on the Display list may be modified by the user using the text boxes below the list, however, this does not add a new entry to the choice list.
- Plotspectra provides a default set of lines for the Choice list that nay be modified by the user. The list is a simple .csv file (spectral_lines.csv) that can be accessed from Settings.
- A different Choice list (.csv file) may be loaded at any time using the "Open new list" button. This is not persistent and will be reset using the default spectral_lines.csv file each time PlotSpectra starts.
- Once set up the display list can be saved (as a .csv file).
- If desired the annotations may be shifted by a given velocity to better match the positions in the spectra. If this feature is used it is best not to display the wavelength as part of the label.

Right Click – Edit annotation window:

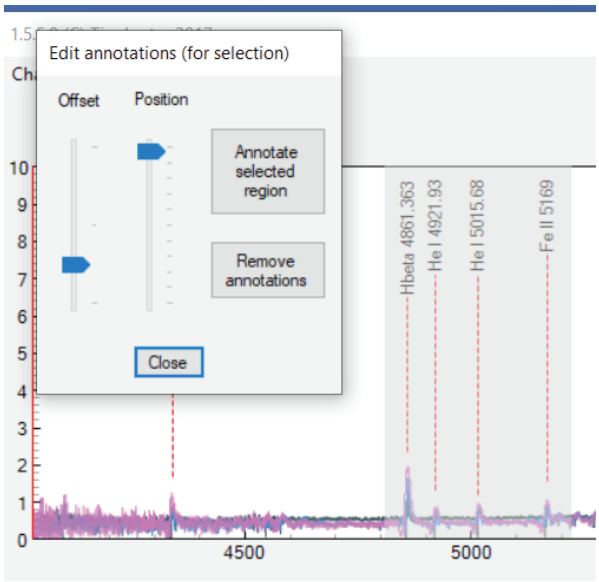

- Selecting "Edit annotations" from the right click context menu of the main plot area will bring up another control window for annotations.
- Labels can be added to (or removed from) a selected region of the plot. All entries in the current "Choice list" within the selected range will be added. Unwanted labels can be removed by selecting a small range around the unwanted lines and then using the "remove annotations" button. The Display list on the Annotations tab will be updated.
- The leader line offset and the vertical position of the labels in the selected area can be adjusted with the sliders. Red or black leader lines can be chosen in Settings.

Main plot context menu items:

Normalize

- **To active series**. This will normalize all currently visible series to the active series by scaling the intensity in order to equalize the average values over the selected wavelength range. The required multipliers are recorded for each series and can be seen in the "y multiply" box on the series setup window.
- **Continuum.** This will open a control window for penalized cubic spline fitting of the continuum. This is a special form of cubic spline that has a stiffness parameter that determines how closely the curve follows the individual data points. Upon opening this control the entire active series is selected for fitting. Regions around emission or absorption lines can be removed from the fitting using the "Delete selected range" button. The normalize button will divide the spectrum by the resulting fitted continuum. If "Apply to all visible series" is checked then a continuum for each series will be computed using the same fitting regions and each will be dived by its respective continuum. The resulting spectra are added as new series and identified with (norm cont) in the series label.

Align selection

- **Wavelength shift.** This will perform a simple alignment of all the visible series to the active series. It is accomplished by measuring the 50% intensity values of the emission or absorption edges within the selected region. The baseline is determined from the end points of the selected region. The wavelength shifts that are applied can be seen in the series setup window and can be set back to 0 if needed.
- **RV shift.** This operates the same as above, however, the spectrum is shifted by an applied velocity instead.

Selected line position

This will center the cursor on an emission or absorption line within the selected region. It uses the same method as in "Align selection" to determine the center value. The cursor position text box contains the measured position.

Signal/noise

For this to operate two and only two spectra must be open in PlotSpectra. These spectra should have been processed from two different exposures or two equal groups of exposures for the particular object. The routine divides the spectrum from one group by the other. In the absence of noise this would result in a spectrum with a constant value of 1. Measuring the standard deviation over a wavelength interval after the division enables the S/N versus wavelength to be estimated which is the resulting plot. This is added as a new series identified with (S/N) in the series label.

Detailed spectral line measurements

This feature is accessed from the sub plot context menu item "Measure". The window that opens provides the controls for setting a reference, fitting the continuum and performing the measurement on a selected region. While this window is open the velocity plot will show an added mirror image spectrum in red.

PlotSpectra
a data visualization utility for amateur astronomical spectroscopy

Tim Lester

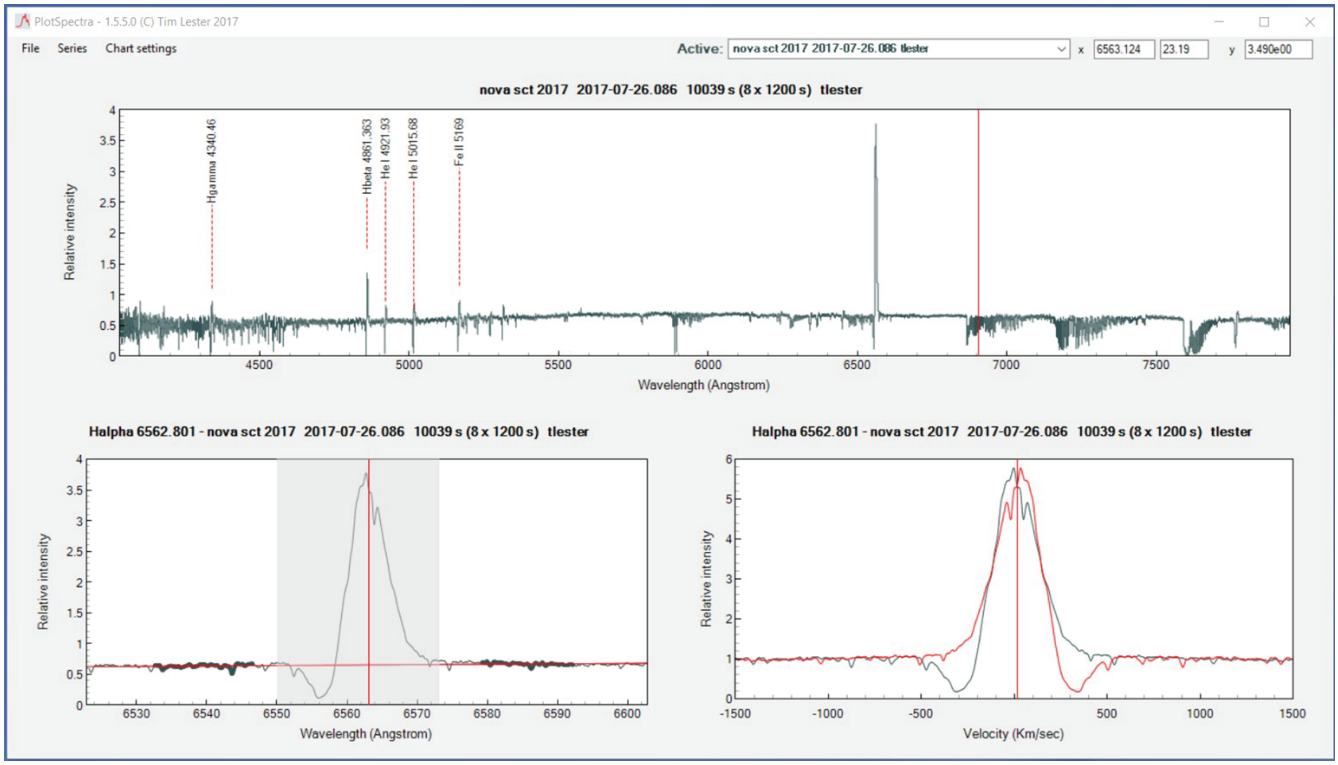

Reference section

- If the center of the subplots have already been set to a spectral line then the reference section will show the name of this line and its wavelength. Otherwise the center wavelength indicated will be the last double click position on the main plot or the center wavelength manually entered on the sub plot setup window.
- The "Set reference" button will bring up the sub plot settings window to allow centering of the plot on a line or a manually entered value.

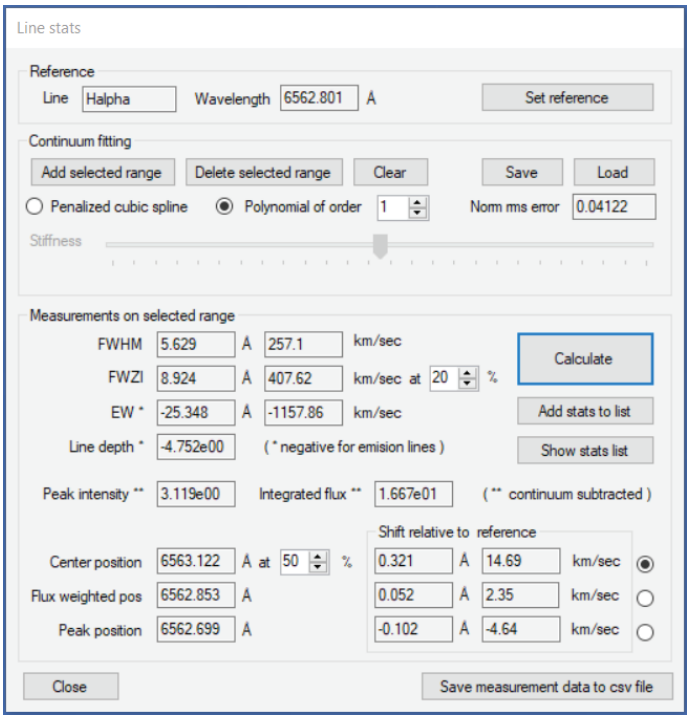

Continuum fitting section

- These controls are used to set up the baseline for the spectral line measurement. Either penalized cubic spline or polynomial fitting can be chosen. The default is polynomial fitting of order one i.e. linear. If penalized cubic spline fitting is chosen its stiffness slider becomes active.
- The spectral regions over which to fit the continuum are set up by selecting areas on the sub plot and using the "Add selected range" or "Delete selected range" buttons. These selected regions are shown in bold and the fitted line is shown in red. The "Nom rms error" box indicates the accuracy of the fit.
- The "Save" and "Load" buttons allow the fitting parameters to be saved and later recalled so that

a different spectrum can be measured with the same fitted regions and fitting method.

Measurements on selected range section

- First select a range on the sub plot that encompasses the spectral line to be measured and then click the "Calculate" button. The calculations will use the line generated by continuum fitting as the baseline inside this region. The velocity plot shows the result after dividing by this continuum.
- In addition to FWHM the width at a user defined height FWZI is calculated. The height is specified as a percentage of the peak height after subtracting the fitted continuum.
- Equivalent width EW and Line depth are negative for emission lines.
- Line depth is expressed as the fractional value of the line peak relative to the continuum while Peak intensity is the difference in intensity units.
- The values for "Peak intensity" and "Integrated flux" are calculated after subtracting the fitted continuum and are positive for emission lines.
- Three line center positions are reported. Center position is the mid position at the percentage line height entered in the scroll box. The flux weighted position is the mid point that balances calculated flux. The Peak position that is reported is the Center position at 98 percent of line height (or depth).
- The boxes to the right of the three positions display the shifts relative to the reference. The radio buttons control the red mirrored spectrum on the velocity plot and change the mirroring to occur around the associated calculated line position. This can be used as a visual aid for judging the measurement results.
- The "Save measurement data to csv file" button at the bottom right will save all the measurement results as well as curve fitting parameters and the data points for the portion of the spectrum and continuum that are currently displayed in the sub plot.
- The "Add stats to list" button under Calculate will add all the measurement results to a table so that measurements of several lines (or the same line on several spectra) can be accumulated. The "Show stats list" button will display this table. The table may be saved or copied to the clipboard for pasting into a spreadsheet. This table will persist only for the current PlotSpectra session.

Download PlotSpectra
https://1drv.ms/f/s!AvXqhKI5kEGRjEhdaQ6jaj8AHx_L

Additionnal Lines Lists in .cvs format:
http://www.astronomie-amateur.fr/Lines/Identification_SySt.html

Eruptive stars spectroscopy
ARAS DataBase

ARAS Spectral Database: Submitting and using spectra

ARAS Spectral Database:
https://aras-database.github.io/database/index.html

The ARAS Spectral Database is the result of the commitment of many observers who voluntarily make a substantial investment of their time and money to carefully acquire, process and share their spectra.

Submitting data to the database

While a basic validation check of submitted spectra is carried out prior to adding them to the database, it is primarily the responsibility of those submitting data to verify the quality of their spectra.

Detailed instructions on how to process and submit spectra to the database are given here:
Link to instructions (*in construction*)

Conditions for use of the data are described below. By submitting data to the database, observers acknowledge and accept these conditions of use. Ownership of data in the database remains with the observer.

Conditions for use of data from the database

This is an open database and in order that we can maintain this status, we expect those who make use of spectra from the database to abide by the following conditions:

1. The ARAS Spectral Database must be acknowledged in all publications which make use of spectra from the database by reference to the following publication:
http://articles.adsabs.harvard.edu/pdf/2019CoSka..49..217

2. Reference to the database should use the following link:
https://aras-database.github.io/database/index.html

3. The names of observers whose spectra are used in the analysis must be included in the Acknowledgements section of the publication.

4. If the publication includes, or is linked to, a table of observations, it is strongly encouraged that this should include the names of the observers.

5. It is the responsibility of the lead author to consider including observers as co-authors if they believe their observations have made a substantial contribution to the analysis.

6. Authors are strongly recommended to inform the ARAS Team via the following email address prior to any publication using spectra from the database to confirm the Acknowledgement is compliant with the conditions of use: francoismathieu.teyssier@gmail.com

François Teyssier (FR), David Boyd (UK), Forrest Sims (US)

Eruptive stars spectroscopy
Cataclysmics, Symbiotics, Novae

Spectroscopic monitoring of eruptive stars (e.g. symbiotic binaries, classical novae) by amateurs around the world, in both the northern and southern hemispheres, is a fundamental activity of the ARAS (Astronomical Ring for Amateur Spectroscopy) initiative. The group of volunteers demonstrates what can be accomplished with a network of independent, very small telescopes (from 20 to 60 cm), furnished with spectrographs of different resolution, from 500 to 15000, and covering the range from 3600 to 9000 Å. The observing program concentrates on bright symbiotic stars (67, to date) and novae (41, to date). The main features of the ARAS activity are rapid response to alerts, long term monitoring and high cadence. A part of the program involves collaborations based on requests from professional teams (e.g. CH Cyg, AG Dra, R Aqr, SU Lyn, T CrB) for long term monitoring or specific events.

Your observations, taken with higher cadence than usually followed in the literature will be key to understanding this in a broad range of systems.

S. Shore, 2015

Your dedication, interest, and persistence are continuing gifts to the community, to future generations who may eventually be able to understand these phenomena because of the precision and care of your contributions. You may think it's just one spectrum, or one datum, but without the history any inferences are tentative at best and misleading at worst.

S. Shore, 2020

… the presented results showed also the importance of professional/amateur collaborations. ARAS Group is a perfect example that such collaboration can be very successful and can bring important results. Thanks to amateur photometric and spectroscopic data, we are now able to monitor the evolution of symbiotic systems on timescales which were not previously available.

R. Gàlis& al., 2019

We are grateful to all of the amateur astronomers that contributed their observations to this paper. In particular, we are thankful to members of the ARAS group for their wonderful work.

K. Ilkwiecz & al., 2015

High cadence of both photometric and spectroscopic observations as provided by AAVSO and ARAS databases allows a detailed mapping of usually fast events of outbursts

A. Skopal, 2019

Submit your spectra:

Please :
- respect the procedure
- check your spectra BEFORE sending them

Resolution should be at least R = 500
1. reduce your data in accordance with standard procédures
(notably offset, dark, flat,
correction of atmospheric and instrumental response)
2. the header must be compliant with BeSS file format
3. name your file as: _novadel2013_yyyymmdd_hhh_Observer
   Example: _chcyg_20130802_886_toto.fit
4. send you spectra to francoismathieu dot teyssier (at) gmail com (dot) com
for inclusion in the ARAS database and a copy to arasdatabase@gmail.com for double check by David Boyd and Forrest Sims.

The Letter is prepared by François Teyssier (FR), David Boyd (UK), Forrest Sims (US)

Download previous issues of the Eruptive Stars Information Letter:
http://www.astrosurf.com/aras/novae/InformationLetter/InformationLetter.html
The letter in the SAO/NASA Astrophysics Data System
https://ui.adsabs.harvard.edu/abs/2019ESIL...43...19T/abstract
ARAS database:
https://aras-database.github.io/database/index.html